

BEST FIT VOID FILLING SEGMENTATION BASED ALGORITHM IN OPTICAL BURST SWITCHING NETWORKS

A.K Rauniyar¹, A.S Mandloi²

¹Department of Electronics and Communication, Advanced College of Engineering and Management,
Kupondole, Lalitpur, Nepal

Email Address: amitu931@gmail.com

²Department of Electronics and Communication, Sardar Vallabhbhai National Institute of Technology, Surat,
India

Email Address: asm@eced.svnit.ac.in

Abstract

Optical Burst Switching (OBS) is considered to be a promising paradigm for bearing IP traffic in Wavelength Division Multiplexing (WDM) optical networks. Scheduling of data burst in data channels in an optimal way is one of a key problem in Optical Burst Switched networks. The main concerns in this paper is to schedule the incoming bursts in proper data channel such that more burst can be scheduled so burst loss will be less. There are different algorithms exists to schedule data burst on data channels. Non-preemptive Delay-First Minimum Overlap Channel with Void Filling (NP-DFMOC-VF) and Non-preemptive Segment-First Minimum Overlap Channel with Void Filling (NP-SFMOC-VF) are best among other existing segmentation based void filling algorithms. Though it gives less burst loss but not existing the channel utilization efficiently. In this paper we propose a new approach, which will give less burst loss and also utilize existing channels in efficient way. Also analyze the performance of this proposed scheduling algorithm and compare it with the existing void filling algorithms. It is shown that the proposed algorithm gives some better performances compared to the existing algorithms.

Keywords: *OBS, Scheduling Algorithm, Void Filling Algorithm, NP-DFMOC-VF, NP-SFMOC-VF, Channel Utilization.*

1. Introduction

Optical burst switching (OBS) [1] is emerging as the switching technology for next generation optical networks. Advantages of optical packet switching and circuit switching are combined in OBS and overcoming their limitations. Data (or payload) is separated from control packet. A control packet is sent before the payload to reserve the resources on the path to the destination of payload. When a control packet arrives at an intermediate node a wavelength scheduling algorithm [2] is used by the scheduler to schedule the data burst on an outgoing wavelength channel. The required information to schedule a data burst is arrival time and duration of data burst, which are obtained from control packet. On the other hand, scheduler keeps availability of time slots on every wave length channel and schedule a data burst in a channel depending upon the scheduling algorithm it uses. Different scheduling algorithms have been proposed in literature to schedule payload/ data burst. They differ in burst loss and complexity. Depending upon the channel selection strategy, they can be classified as Horizon and Void filling algorithm. Horizon algorithm considers the channels which have no scheduled data burst at or after current time t and the channels are called Horizon channels. Void filling algorithms consider the channels which have unused duration in between two scheduled data bursts. These are called Void channels. The example of non segmentation Horizon algorithms are FFUC, LAUC and non segmentation Void algorithms are FFUC-VF [3], LAUC-VF [4,5,6,7] and Min-EV [8]. The example of segmentation Horizon algorithms are Non preemptive Minimum

Overlap Channel (NP-MOC) [9], Non-preemptive Delay-First Minimum Overlap Channel (NP-DFMOC) [9] and Non-preemptive Segment-First Minimum Overlap Channel (NP-SFMOC) [9]. And the example of non segmentation void filling algorithms are Non preemptive Minimum Overlap Channel with Void Filling (NP-MOC-VF) [9], Non-preemptive Delay-First Minimum Overlap Channel with Void Filling (NP-DFMOC-VF) [9] and Non-preemptive Segment First Minimum Overlap Channel with Void Filling (NP-SFMOC-VF) [9]. Horizon algorithms are easy to implement and burst loss ratio is high, where as burst loss ratio is lower in Void filling algorithms but complex switching are required to implement. All, LAUC-VF, Min-EV, NPMOC-VF, NP-DFMOC and NP-SFMOC-VF consider one side of a void. There may be a possibility, in which a smaller data burst will be scheduled in a larger void where as a bigger data burst will be dropped. This will lead to higher burst blocking and lower channel utilization. In this chapter we propose a new channel scheduling algorithm which attempts to make efficient utilization of existing void within a channel. Thus, giving rise to higher channel utilization and lower blocking probability. Rest of the paper is organized as follows. Literature Review of the existing void filling algorithms are explained in Section 2. Methodology of the proposed best fit void filling algorithm is explained in scheme with Section 3. We compare our proposed scheme algorithm with NP-DFMOC-VF and NP-SFMOC-VF. Comparison and simulation results are presented in Section 4. Finally, some conclusions are drawn in Section 5.

2. Literature Review

In the following subsection a brief description of existing NP-DFMOC-VF and NP-SFMOC-VF void filling algorithms is presented.

2.1 Non-preemptive Delay First Minimum Overlap Channel with Void Filling (NP-DFMOC-VF)

The NP-DFMOC-VF calculates the delay until the first void on every channel and then selects the channel with minimum delay. If a channel is available, the unscheduled burst is scheduled on the free channel with minimum gap. If all channels are busy and the starting time of the first void is greater than or equal to the sum of the end time, E_a , of the unscheduled burst and MAX_DELAY , then the entire unscheduled burst is dropped. Otherwise, the unscheduled burst is delayed until the start of the first void on the selected channel, where the non-overlapping burst segments of the unscheduled burst are scheduled, while the overlapping burst segments are dropped. In case the start of the first void is greater than the sum of the start time, S_a , of the unscheduled burst and MAX_DELAY , then the unscheduled burst is delayed for MAX_DELAY and the non-overlapping burst segments of the unscheduled burst are scheduled, while the overlapping burst segments are dropped. For example, consider Fig. 1. By applying the NP-DFMOC-VF algorithm, the data channel D1 has the minimum delay, thus the unscheduled burst is scheduled on D1 after delaying the burst using FDLs. In this case, the overlapping segments of the burst are dropped though there is availability of channels D2 and D3 as shown in figure.

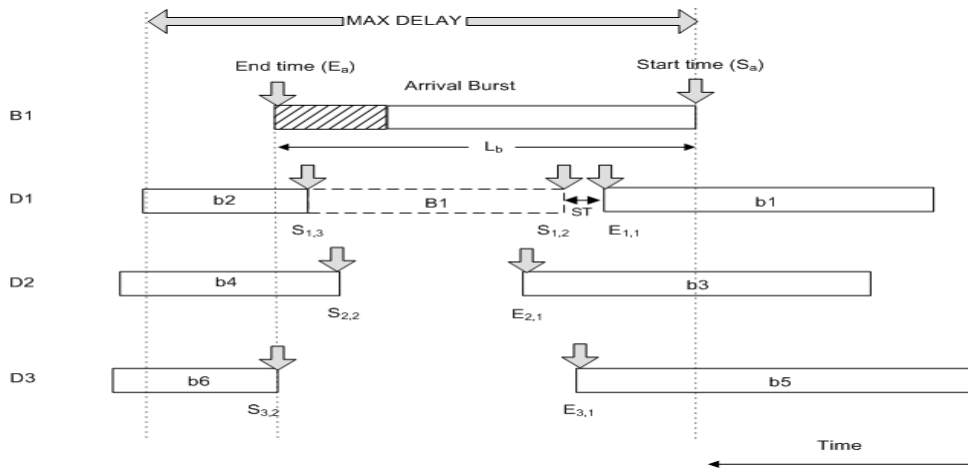


Fig 1 Illustration of NP-DFMOC-VF algorithm

Though there is presence of channels (D2 and D3) they can be only used for arrival of new bursts, the overlapping segments of the burst B1 are dropped and thus cannot be rescheduled which is the limitations of this algorithm. Hence to overcome this effect we move further to the next algorithms as discussed below.

2.2 Non-preemptive Segmented First Minimum Overlap Channel with Void Filling (NP-SFMOC-VF)

The NP-SFMOC-VF algorithm calculates the loss on every channel and then selects the channel with minimum loss. If a channel is available, the unscheduled burst is scheduled on the free channel with minimum gap. If all channels are busy and the starting time of the first void is greater than or equal to the sum of the end time, E_a , of the unscheduled burst and MAX_DELAY , then the entire unscheduled burst is dropped. If the starting time of the first void is greater than or equal to the end time, E_a , of the unscheduled burst, the NP-DFMOC-VF algorithm is employed.

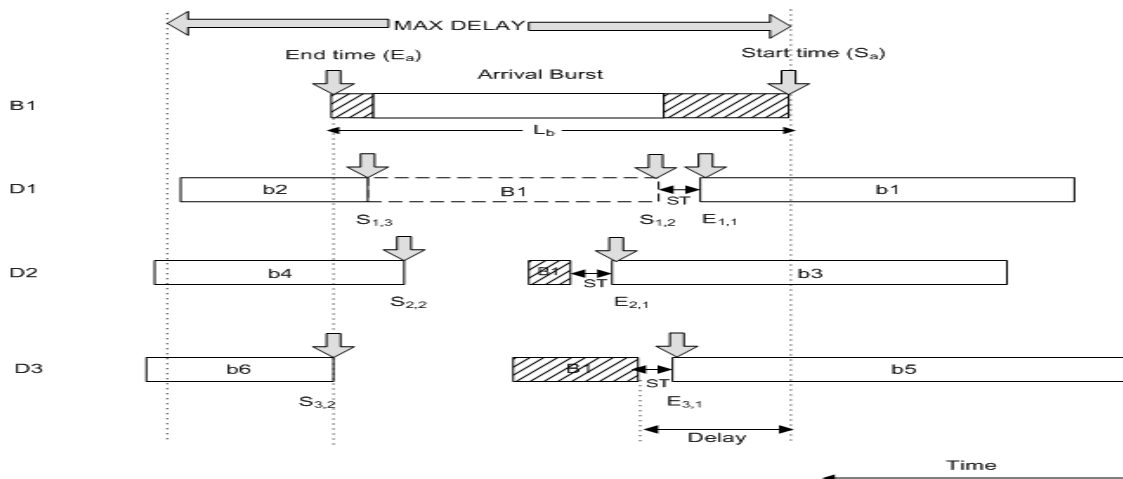


Fig 2 Illustration of NP-SFMOC-VF algorithm

Otherwise, the unscheduled burst is segmented (if necessary) and the non-overlapping burst segments are scheduled on the selected channel, while the overlapping burst segments are re-scheduled. For the rescheduled burst segments, the algorithm calculates the delay required until the start of the next void on every channel and selects the channel with minimum delay. The re-scheduled burst segments are delayed until the start of the first void on the selected channel. The non-overlapping burst segments of the re scheduled burst are scheduled, while the overlapping burst segments are dropped. In case the start of the next void is greater than the sum of the start time, S_a , of the unscheduled burst and

MAX_DELAY , the re-scheduled burst segments are delayed for MAX_DELAY and the non-overlapping burst segments of the rescheduled burst are scheduled, while the overlapping burst segments are dropped. For example, in Fig. 2, we observe that the data channel D1 has the minimum loss, thus the unscheduled burst is scheduled on D1, and the unscheduled burst B1 has both head overlapping and tail overlapping on which head overlapping re-scheduled burst segments are scheduled on D3 (as it incurs the minimum delay) and tail overlapping re-scheduled burst segments are scheduled on D2.

Though there is no loss of data bursts as shown in figure but for head overlapping and tail overlapping portion separate channels D3 and D2 respectively has been used which in turns to be expensive in terms of cost and looks un-effective as well. Thus the limitations of existing algorithms are both algorithms consider only one side of void. Next we propose a new channel scheduling algorithms which considers both end of a void in scheduling and also utilizes void efficiency and blocking probability of data burst is minimum.

3. Methodology

In this section we propose a new scheduling algorithm called Best Fit Void Filling (BFVF), which attempts to maximize the channel utilization and minimize the burst loss. Our propose algorithm first selects all possible void channels, on which the data burst can be scheduled. Then selects one of the possible void channel such that the void utilization factor is maximum. We calculate the void utilization factor as:

$$\text{Utilization} = (a * 100) / x$$

Where 'a' is the data burst length and 'x' is the void length.

In figure 3, for first case, void utilization factor for B1 on channel D1, D2 and D3 are $(E_a - S_a) / ((S_{1,2}) - (E_{1,1}))$, $(E_a - S_a) / ((S_{2,2}) - (E_{2,1}))$, $(E_a - S_a) / ((S_{3,3}) - (E_{1,1}))$ respectively. If void utilization factor exceeds over 100 percent then the factor having close to 100 percent is considered. Here according to figure, using void utilization factor, it selects the channel D3 for the first case to schedule the portion of data burst B1. Since it cannot schedule all the portion of data burst B1 the overlapping portion of data bursts segments is reschedule. For that the remaining channel is D1 and D2 since channel D3 is already been used. For reschedule data burst segments that is for second case we again calculate the void utilization factor for remaining portion of data burst B1 which have to be rescheduled and calculated as $(E_a - R_a) / ((S_{1,2}) - (E_{1,1}))$, $(E_a - R_a) / ((S_{2,2}) - (E_{1,1}))$ where R_a is the start time for reschedule burst segment. In case, the void is greater than MAX_DELAY , the unscheduled burst is delayed for MAX_DELAY and the non overlapping burst segments of unscheduled burst is scheduled, while the overlapping burst segments are dropped. In this case, according to formula the data channel D2 is selected since its channel utilization factor for remaining reschedule burst segment is better than channel D1.

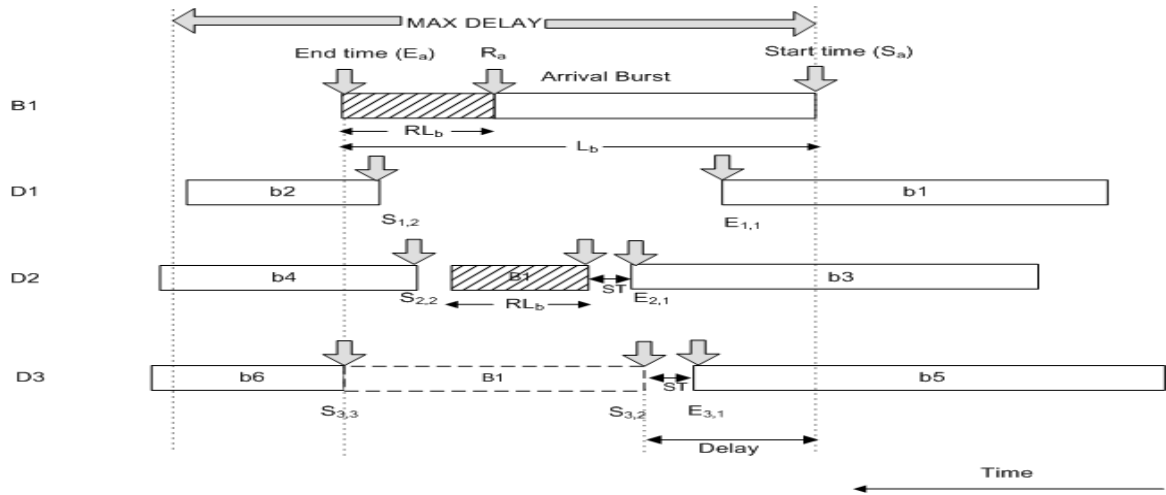


Fig 3 Illustration of BFVF segmented based algorithm

Hence, the reschedule data burst segment is scheduled on channel D2. And the data channel D1 which is free can be completely used for new arrival data burst. Thus the channel utilization is higher and burst loss ratio is lower in our propose scheme than in NP-DFMOC-VF and NP-SFMOC-VF algorithms. We work out an example to show void utilization on our proposed algorithm. We assume the following numerical values. For first case,

- $(S_{1,2}) - (E_{1,1}) = (220-140) = 80 \mu\text{s}$
- $(S_{2,2}) - (E_{2,1}) = (210-160) = 50 \mu\text{s}$
- $(S_{3,3}) - (E_{3,1}) = (230-145) = 85 \mu\text{s}$
- Length of data burst B1 (L_b) = $(E_a - S_a) = 110 \mu\text{s}$
- Switching time (ST) = $10 \mu\text{s}$
- Maximum Delay = $250 \mu\text{s}$

Using channel utilization factor formula,

For D1, channel utilization = $(110 \times 100) / 80 = 137.5\%$

For D2, channel utilization = $(110 \times 100) / 50 = 220\%$

For D3, channel utilization = $(110 \times 100) / 85 = 129.4\%$

Here, we select the channel D3 since channel utilization of channel D3 is close to 100 percent as compare to channel D1 and D2. Note if the channel utilization had been less than 100 percent we go for channel utilization less than 100 percent instead of more than 100 percent.

For second case, (for RL_b)

Length of remaining data burst segment of B1, (RL_b)

- $RL_b = (E_a - R_a) = 230 - 195 = 35 \mu\text{s}$

Remaining channel D1 and D2

- $(S_{1,2}) - (E_{1,1}) = (220-140) = 80 \mu\text{s}$
- $(S_{2,2}) - (E_{2,1}) = (210-160) = 50 \mu\text{s}$
- Switching time (ST) = $10 \mu\text{s}$

Using channel utilization factor formula for RL_b ,

For D1, channel utilization = $(35*100)/80 = 43\%$

For D2, channel utilization = $(35*100)/50 = 70\%$

In this case, channel D2 is selected for reschedule the remaining data burst of B1 i.e. for RL_b . Also, the free channel D1 can be used for new arrival of data bursts. This shows that void utilization is higher in our proposed algorithm.

Table 1 Input data for channel scheduling of different algorithms

	CASE I (NPDFMOC-VF)			CASE II (NPSFMOC-VF)			CASE III (BFVF SEGMENTED)		
	B1	B2	B3	B1	B2	B3	B1	B2	B3
$L_b = Ea - Sa$ (μs)	90-40=50	137-62=75	102-52=50	135-45=90	140-40=100	129-75=54	230-120=110	275-150=125	270-210=60
	$(S_{i,j}) - (E_{i,j}) \mu s$			$(S_{i,j}) - (E_{i,j}) \mu s$			$(S_{i,j}) - (E_{i,j}) \mu s$		
D1	106-66=40			110-66=44			255-165=90		
D2	128-50=78			138-80=58			235-180=55		
D3	130-62=68			130-62=68			240-200=40		
D4	135-70=65			135-75=60			220-140=80		
D5	140-75=65			120-85=35			210-160=50		
D6	110-72=38			110-70=40			230-145=85		
D7				130-50=80			255-210=45		
D8				135-90=45			250-215=35		
D9				140-85=55			252-220=32		
ST (μs)	10			10			10		
W	6			9			9		
Maximum Delay (μs)	127			200			255		

Table 2 Output data for channel scheduling of different algorithms

	CASE I			CASE II			CASE III		
	NPDF MOC -VF	NPSF MOC -VF	BFVF Segme nted Based	NPDF MOC -VF	NPSF MOC -VF	BFVF Segme nted Based	NPDF MOC -VF	NPSF MOC -VF	BFVF Segme nted Based
Delay for non overlap ping burst B1	20 μ s	20 μ s	40 μ s	27 μ s	27 μ s	25 μ s	30 μ s	30 μ s	55 μ s
Delay for non overlap ping burst B2	10 μ s	10 μ s	10 μ s	36 μ s	45 μ s	32 μ s	5 μ s	25 μ s	5 μ s
Delay for non overlap ping burst B3	24 μ s	30 μ s	33 μ s	15 μ s	25 μ s	15 μ s	0 μ s	10 μ s	0 μ s
Number of channel Used	3	6	4	3	9	6	3	9	6
Total packet loss	30 μ s	0 μ s	0 μ s	10 μ s	0 μ s	0 μ s	115 μ s	0 μ s	2 μ s

4. Simulation and Results

We compare the performance of our proposed BFVF segmented based algorithm with that of NP-DFMOC-VF and NP-SFMOC-VF algorithm through simulation. For simulation proposed and to be more précised we take three cases for channel scheduling.

In each case we take three bursts B1, B2 and B3 which have to be scheduled by using different algorithms. W is the maximum number of outgoing data channels. According to given input data of table 1, we obtained an output as table 2 which is shown below. Considering a table II and its cases I, II and III we can see that in case I delay is more in our proposed algorithm as compare to NP-DFMOC-VF and NP-SFMOC-VF but in case II delay is less in our proposed algorithm than NP-DFMOC-VF and NP-SFMOC-VF where as in case III in our proposed algorithm delay is more for data burst B1 and less for data burst B2 and B3 as compare to NP-DFMOC VF and NP-SFMOC-VF.

Hence we can say that delay does not depend on type of algorithm we used but it depends on how the data bursts are schedule on the channels. Also from simulation of figure 4, 5 and 6 this can be seen.

Again considering table 2, this time we consider total packet loss for different algorithms versus number of channel used for different algorithms. According to table we simulate the result for this as shown in figure 7, 8 and 9. We can see that packet loss for our proposed algorithm is zero for case I and II and in case III packet losses are very low and number of channel used is also less comparing to NPSFMOC-VF algorithm. In NPDMOC-VF algorithm, though the number of channel used is less than NPSFMOC-VF and our proposed algorithm but the packet losses are very high in NPDMOC-VF then NPSFMOC-VF and our proposed algorithm.

Also from figure 1, 2 and 3 we draw a table and conclude the comparison of burst loss and channel utilization as follows.

Table 3 Comparisons of different algorithm in terms of Burst Loss and Channel Utilization

Algorithm	Burst Loss	Channel Utilization
NPDMOC-VF	High	High
NPSFMOC-VF	Low	Low
BFVF Segmented	Low	High

5. Conclusion

In this paper we discuss performance of horizon and void filling scheduling algorithm. It is found that the void filling scheduling algorithm performs better than the horizon scheduling algorithms. However, there are limitations to the existing void filling scheduling algorithms. This limitation is mainly due to that; the existing schemes consider either the start time of the new data burst or end time of the previously scheduled data burst or start time of previously scheduled data burst and the end time of the new data burst. They do not take into account the data burst length and void length. We proposed an algorithm called BFVF Segmented based algorithm, which takes the arrival data burst length and void length into account in scheduling. Proposed scheme calculates the void utilization factor, and schedule the new data burst into a void channel having maximum void utilization factor.

The proposed scheme is compared with NPDMOC-VF and BFVF Segmented. It is found that the proposed scheme perform better in term of channel utilization, packet loss and number of channel used.

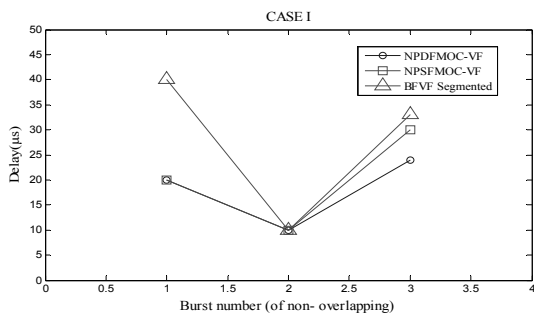


Fig 4 Delay vs. non overlapping burst for case I

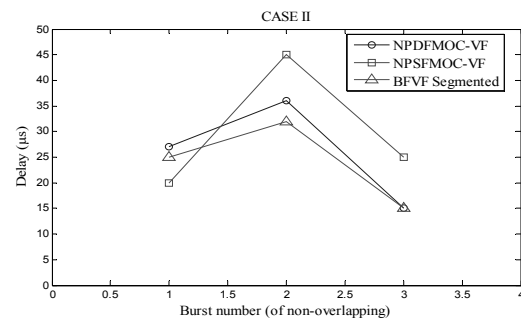


Fig 5 Delay vs. non overlapping burst for case II

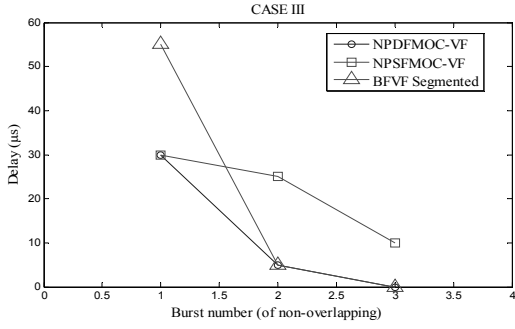


Fig 6 Delay vs. non overlapping burst for case III

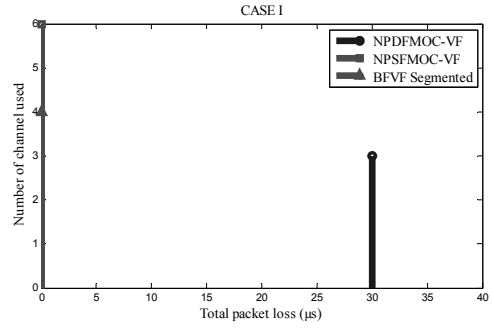


Fig 7 Number of channel used vs. Total packet loss for case I

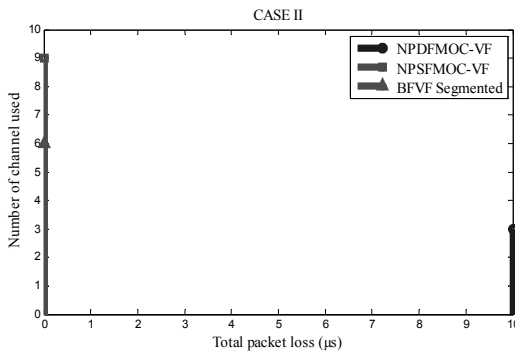


Fig 8 Number of channel used vs. Total packet loss for case II

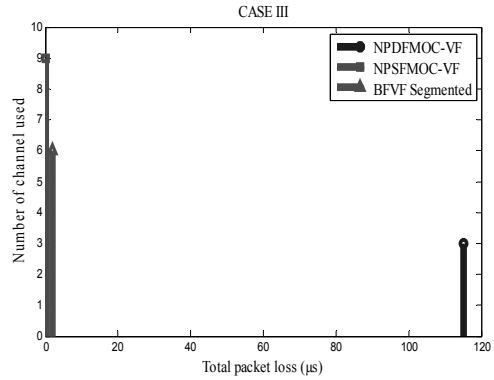


Fig 9 Number of channel used vs. Total packet loss for case III

References

1. K. Koduru, "New Contention Resolution Techniques for Optical Burst Switching," Master's thesis, Louisiana State University, May 2005.
2. K. Dozer, C. Gauger, J. Spath, and S. Bodamer, "Evaluation of Reservation Mechanisms for Optical Burst Switching," AEU International Journal of Electronics and Communications, vol. 55, no. 1, January 2001.
3. M. Ljolje, R. Inkret, and B. Mikac, "A Comparative Analysis of Data Scheduling Algorithms in Optical Burst Switching Networks," in Proceeding of Optical Network Design and Modeling, 2005, 2005, pp. 493 – 500.
4. Y. Xiong, M. Vandenhoute, and H. C. Cankaya, "Control Architecture in Optical Burst Switched WDM Networks," IEEE JSAC, vol. 18, no. 10, pp. 1838 – 1851, October 2000.
5. M. Yoo, C. Qiao, and S. Dixit, "QoS Performance of Optical Burst Switching in IP-Over-WDM Networks," IEEE Journal on Selected Areas in Communications, vol. 18, no. 10, October 2000.
6. W. M. Golab and R. Boutaba, "Resource Allocation in User-Controlled Circuit-Switched Optical Networks," LNCS Spinger-Verlag, vol. 16, no. 12, pp. 2081 – 2094, December 1998.
7. M. Yang, S. Q. Zheng, and D. Verchere, "A QoS Supporting Scheduling Algorithm for Optical Burst Switching DWDM Networks," In Proceeding of GLOBECOM 01, 2001, pp. 86 – 91.
8. J. Xu, C. Qiao, J. Li, and G. Xu, "Efficient Channel Scheduling Algorithms in Optical Burst Switching Networks," in Proceeding of IEEE INFOCOM, 2003, vol. 3, 2003, pp. 2268 – 2278
9. V.M Vokkarane and J.P Jue. "Segmentation-based non preemptive scheduling algorithms for optical burst-switched networks." In Proceedings, First Inter-national Workshop on Optical Burst Switching (WOBS), co-located with opti-Comm 2003, October 2003.

IMPROVEMENT OF COMPLEXITY AND PERFORMANCE OF LEAST SQUARE BASED CHANNEL ESTIMATION IN MIMO SYSTEM

Anand Kumar Sah¹, Arun Kumar Timalina²

¹Department of Electronics and Computer Engineering

Western Region Campus, Institute of Engineering, Tribhuvan University

Lamachaur, Pokhara, Nepal

²Department of Electronics and Computer Engineering

Central Campus, Institute of Engineering, Tribhuvan University

Pulchowk, Nepal

Abstract

Multiple-input multiple-output (MIMO) systems play a vital role in fourth generation wireless systems to provide advanced data rate. In this paper, a better performance and reduced complexity channel estimation method is proposed for MIMO systems based on matrix factorization. This technique is applied on training based least squares (LS) channel estimation using STBC for performance improvement. Simulation results indicate that the proposed method not only alleviates the performance of MIMO channel estimation but also significantly reduces the complexity caused by matrix inversion. The performance evaluations are validated through computer simulations using MATLAB in terms of bit error rate (BER) for modified LS with LS and MMSE channel estimation techniques. Simulation results show that the BER performance and complexity of the proposed method clearly outperforms the conventional LS channel estimation method.

Keywords: MIMO, STBC, LS, MMSE, Matrix Factorization

1. Introduction

Wireless communication systems continue to strive for ever higher data rates. To cater to both higher transmission rates and higher spectral efficiencies in order to increase the performance of communication systems, the wireless industry is already looking ahead and embracing multiple-input multiple-output (MIMO) systems [1, 2]. Using multiple transmit as well as receive antennas, a MIMO system exploits spatial diversity, higher data rate, greater coverage and improved link robustness without increasing total transmission power or bandwidth. However, MIMO relies upon the knowledge of channel state information (CSI) at the receiver for data detection and decoding. It has been proved that when the channel is Rayleigh fading and perfectly known to the receiver, the performance of a MIMO system grows linearly with the number of transmit or receive antennas, whichever is less [3]. Therefore, an accurate and robust estimation of wireless channel is of crucial importance for coherent demodulation in MIMO system.

A considerable number of channel estimation methods have already been studied by different researchers for MIMO systems. In certain channel estimation methods, training symbols that are transmitted over the channels are investigated at the receiver to render accurate CSI [4]. Compared with blind and semi blind channel estimations, training based estimations generally require a small data record. Hence, they are not limited to slowly time-varying channels and entail less complexity. One of the most efficient training based methods is the

least squares (LS) method, for which the channel coefficients are treated as deterministic but unknown constants [5]. When the full or partial information of the channel correlation is known, a better channel estimation can be achieved by minimum mean square error (MMSE) method [5]. The fundamental difference between these two techniques is that the channel coefficients are treated as deterministic but unknown constants in the former, and as random variables of a stochastic process in the latter. The MMSE estimation has better performance than LS estimation at the cost of higher complexity as it additionally exploits prior knowledge of the channel coefficients. But practically this kind of information is sometimes not known beforehand, which makes MMSE-based technique infeasible.

OFDM is becoming widely applied in wireless communications systems due to its high rate transmission capability with high bandwidth efficiency and its robustness with regard to multipath fading and delay [1]. It has been used in digital audio broadcasting (DAB) systems, digital video broadcasting (DVB) systems, digital subscriber line (DSL) standards, and wireless LAN standards such as the American IEEE® Std. 802.11™ (WiFi) and its European equivalent HIPRLAN/2. It has also been proposed for wireless broadband access standards such as IEEE Std. 802.16™ (WiMAX) and as the core technique for the fourth-generation (4G) wireless mobile communications.

There are two main problems in designing channel estimators for wireless OFDM systems. The first problem is the arrangement of pilot information, where pilot means the reference signal used by both transmitters and receivers. The second problem is the design of an estimator with both low complexity and good channel tracking ability. The two problems are interconnected. In general, the fading channel of OFDM systems can be viewed as a two-dimensional (2D) signal (time and frequency). The optimal channel estimator in terms of mean-square error is based on 2D Wiener filter interpolation. Unfortunately, such a 2D estimator structure is too complex for practical implementation. The combination of high data rates and low bit error rates in OFDM systems necessitates the use of estimators that have both low complexity and high accuracy, where the two constraints work against each other and a good trade-off is needed. The one-dimensional (1D) channel estimations are usually adopted in OFDM systems to accomplish the trade-off between complexity and accuracy [1–4]. The two basic 1D channel estimations are block-type pilot channel estimation and comb-type pilot channel estimation, in which the pilots are inserted in the frequency direction and in the time direction, respectively. The estimations for the block-type pilot arrangement can be based on least square (LS), minimum mean-square error (MMSE), and modified MMSE.

2. Problem Definition

The complexity of channel estimation mainly increases due to matrix inversion. To reduce the complexity of MIMO detection, several matrix factorization techniques have been applied on MIMO systems recently. Orthogonal matrix triangularization is a matrix factorization technique that reduces a full rank matrix into simpler form. Some other matrix factorizations like lower upper (LU) decomposition, singular value decomposition (SVD) can also be used to avoid explicit matrix inversions. But orthogonal matrix triangularization is preferable over other methods as it guarantees numerical stability by minimizing errors caused by machine roundoffs [6]. Matrix factorization is used to conduct large matrix calculations in alternate ways, and applied for system complexity reduction. The decoding algorithm for layered space-time codes based on matrix triangularization is

presented in [7]. The authors in [8] proposed a low-complexity maximum-likelihood decoding approach based on matrix factorization for signal detection in MIMO systems. In [9], a combined detection algorithm based on matrix triangularization is proposed to reduce the complexity of the MIMO detection algorithm. Reduced complexity hardware architecture for MIMO symbol detector using matrix factorization is proposed in [13] which support two MIMO schemes of space-frequency block codes and space division multiplexing of the codes. However, in all works matrix factorizations decrease complexity, but performance improvement is not justified. In this paper, a channel estimation method is proposed for MIMO system by employing orthogonal matrix triangularization on LS estimation which minimizes the computational complexity and at the same time improves the performance. The coding scheme of MIMO considered in this paper is space-time block coding (STBC) which is an attractive approach for improving quality in wireless links.

3. MIMO System and Model

Digital communication using multiple-input–multiple-output (MIMO), sometimes called a “volume-to-volume” wireless link, has recently emerged as one of the most significant technical breakthroughs in modern communications. MIMO systems can be defined simply. Given an arbitrary wireless communication system, we consider a link for which the transmitting end as well as the receiving end is equipped with multiple antenna elements. The idea behind MIMO is that the signals on the transmit (TX) antennas at one end and the receive (RX) antennas at the other end are “combined” in such a way that the quality or the data rate (bits/sec) of the communication for each MIMO user will be improved. Such an advantage can be used to increase both the network’s quality of service and the operator’s revenues significantly. A compressed digital source in the form of a binary data stream is fed to a simplified transmitting block encompassing the functions of error control coding and (possibly joined with) mapping to complex modulation symbols. The latter produces several separate symbol streams. Each is then mapped onto one of the multiple TX antennas. After upward frequency conversion, filtering and amplification, the signals are launched into the wireless channel. At the receiver, the signals are captured by possibly multiple antennas and demodulation and de-mapping operations are performed to recover the message.

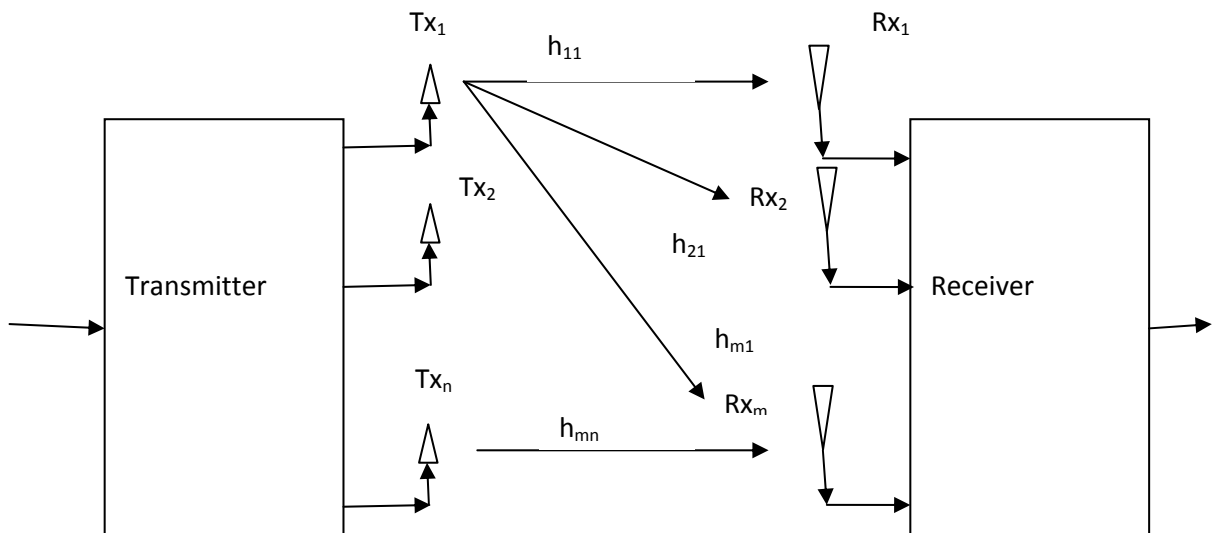


Fig 3.1 MIMO system with N transmit and M receive antenna

In a single user MIMO model with N transmit and M receive antennas, the MIMO system equation is given by

$$\begin{bmatrix} r_1 \\ r_2 \\ \vdots \\ r_m \end{bmatrix} = \begin{bmatrix} h_{11} & h_{12} & \dots & h_{1n} \\ h_{21} & h_{22} & \dots & h_{2n} \\ \dots & \dots & \dots & \dots \\ h_{m1} & h_{m2} & \dots & h_{mn} \end{bmatrix} \begin{bmatrix} s_1 \\ s_2 \\ \vdots \\ s_n \end{bmatrix} + \begin{bmatrix} n_1 \\ n_2 \\ \vdots \\ n_m \end{bmatrix} \quad (3.1)$$

Or in matrix form: $r = Hs + n$ (3.2)

where H is the channel matrix of size $M \times N$, r is the $M \times 1$ received signal vector, s is the $N \times 1$ transmitted signal vector, and n is an $M \times 1$ additive white Gaussian noise vector with zero mean and variance σ^2 . The channel matrix H is the factor by which the signal is amplified and is also known as the channel coefficient. The element h_{ij} in the channel matrix H represents the complex gain between transmitter antenna j and receiver antenna i .

The MIMO system model is shown in Fig 3.2.

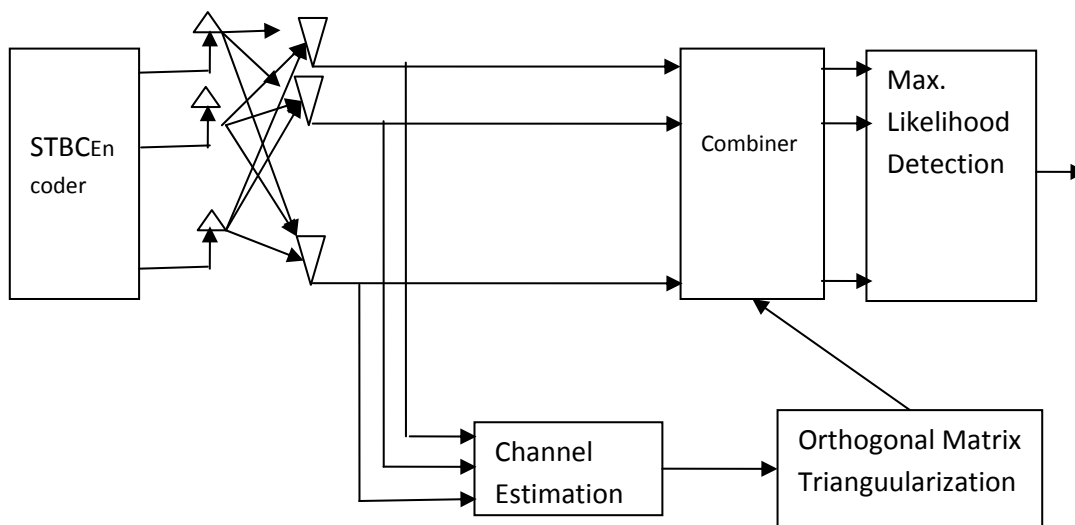


Fig 3.2 MIMO System Model

Data symbols $S_1; S_2; S_3; \dots; S_L$ are encoded by S that is the transmission matrix of an STBC, where $[S]_{ij}$, $i = 1; 2; \dots; N_t$ and $j = 1; 2; \dots; T$ represent element of the linear combination of symbols and their complex conjugates, which are transmitted simultaneously from the i -th transmit antenna in the j -th symbol periods [17]. S is independent identically distributed (i.i.d) Gaussian random signals with zero mean and variance matrix given by

$$E\{S_n S_m H\} = \begin{cases} \sigma^2, & n = m \\ 0, & n \neq m \end{cases} \quad (3.3)$$

Where $E\{\cdot\}$ implies the expectation and σ^2 is the power accompanying one symbol. The input-output relation of the system can be written as

$$Y = HS + W \quad (3.4)$$

Where S is the $N_r \times T$ transmit matrix, Y is the $N_r \times T$ received matrix and W is an $N_r \times T$ i.i.d. Gaussian random noise matrix with zero mean. The MIMO channel response is described by $N_r \times N_t$ matrix H. A general entry of the channel matrix H is denoted by $\{h_{ij}\}$. This represents the complex gain of the channel between the j -th transmitter and the i -th receiver and can be written as

$$H = \begin{bmatrix} h_{11} & \cdots & h_{1n} \\ \vdots & \ddots & \vdots \\ h_{m1} & \cdots & h_{mn} \end{bmatrix} \quad (3.5)$$

Where

$$\begin{aligned} h_{ij} &= \alpha + j\beta = \sqrt{\alpha^2 + \beta^2} \cdot \exp(j \arctan(\beta/\alpha)) \\ &= |h_{ij}| \cdot \text{EXP}(j\Phi_{ij}) \end{aligned} \quad (3.6)$$

In a rich scattering environment with no line-of-sight (LOS), α and β are independent and normal distributed random variables, then channel gains $\{h_{ij}\}$ are usually Rayleigh distributed.

The signals are transmitted over channel. The combined signal \bar{r}_n at the receiver is

$$\bar{r}_n = [c \sum_{i=1}^n \sum_{j=1}^m |h_{ij}| |h_{ij}|] + S_n + W_n = c \|H\|_F^2 S_n + W_n, n = 1, 2, \dots, L \quad (3.7)$$

where W_n is the noise term after combining. At the receiver the maximum likelihood (ML) decoder is used to detect the transmitted symbol. The ML decoder can be simplified using the orthogonality of S. The received symbol, hence, can be determined by

$$\hat{S}_n = \arg \min | \bar{r}_n - c \|H\|_F^2 S |^2 \quad (3.8)$$

This is a low complexity orthogonal system model that can be considered highly attractive for practical applications.

4. Channel Estimation Techniques

Basically, methods of channel estimation can be classified according to four dimensions [17].

- From the view of estimation theory, there are
 - Least Square (LS) Estimation
 - Minimum Mean Square Error (MMSE) Estimation
- According to the processing domain, estimation can be done in

- Time Domain
- Frequency Domain
- Due to the different pilot-symbol arrangements, there are
 - Estimator with Block-Type Pilot (Training Based)
 - Estimator with Comb-Type Pilot (Pilot Symbol Aided Modulation)
- With different estimation iteration, there are:
 - Iterative Methods
 - Direct Methods

4.1 LS Estimation Technique

The knowledge of CSI is required at the receiver to recover the transmitted signals properly in MIMO systems. In training based channel estimation, the training symbols that are known to the receiver are multiplexed along with the data stream and examined in the receiver to estimate the channel. In practice, training based LS estimation is more frequently used due to its acceptable performance. But this estimation involves matrix inversions, which result in high computational complexity and hence undesirable for hardware implementation. The orthogonal matrix Triangularization is a very convenient technique to avoid matrix inversion and is preferable because of its clever implementation in highly parallel array architecture.

In a $N_t \times N_r$ MIMO system, totally $(N_t N_r)$ channels are needed to be estimated between transmitters and receivers. The received training symbols can be expressed as

$$y = Hx + n \quad (4.1)$$

where x is the transmitted training signal, y is the received signal and n is the noise response. The channel response H is assumed to be random and quasi-static within two transmission blocks. The LS approach solves the estimation equation (4.1) by minimizing the cost function as,

$$J(H) = (y - Hx)^H (y - Hx) \quad (4.2)$$

The gradient of equation (4.2) is given below,

$$\frac{\partial}{\partial H} J(H) = -2x^H y + 2x^H x \quad (4.3)$$

Minimizing the gradient to zero yields the LS estimation \hat{H} of the channel response obtained by

$$\hat{H} = (x^H x)^{-1} x^H y \quad (4.4)$$

4.2 MMSE Technique

Improved performance compared to ZF can be obtained by attempting to minimize both interference and noise at the same time. This is done by the Minimum Mean Squared Error (MMSE) detection scheme, which is a trade off between noise inflation and interference suppression. The weight matrix for MMSE detection is given by:

$$W^H = H^H (\rho^2 I_m + H H^H)^{-1} \quad (4.5)$$

Where I_M and I_N are the $M \times M$ and $N \times N$ identity matrices respectively.

4.3 Proposed Channel Estimation Technique

The inversion of $x^H x$ in equation (4.4) has a high complexity and will significantly increase when the size of x increases, which is dependent on the number of transmit antennas. To avoid complexity because of matrix inversion, orthogonal matrix triangularization is applied on x . The matrix triangularization can be calculated via Householder transformation, or Givens rotation. The Givens rotation is a recursive method that requires a larger number of floating point operations as compared to the Householder transformation method [19]. In this work, Householder transformation is chosen to minimize the required operations. In the Householder approach, a series of reflection matrix is applied to the matrix, x , column by column to annihilate the lower triangular elements. The reflection transformations are orthonormal matrices that can be written as

$$A = (I + \beta v v^H) \quad (4.6)$$

where v is the Householder vector and $\beta = -2 / \|v\|_2$. For the matrix x , to annihilate the lower elements of the k -th column the A_k 's are constructed as follows:

- i. Let v equal the k -th column of x
- ii. Update v by $v = x + \|x\|_2 \Upsilon$, where $\Upsilon = [1; 0; \dots; 0]^T$
- iii. Determine β by $\beta = -2 / \|v\|_2$
- iv. A_k 's are calculated according to equation (4.6).

The A_k 's formed from the above steps are pre-multiplied by x sequentially as follows

$$A_n, \dots, A_1 x = \begin{bmatrix} R \\ 0 \end{bmatrix} \quad (4.7)$$

where, R is a $n \times n$ upper triangular matrix, 0 is a null matrix, and the sequence of reflection matrices form the complex transpose of the orthogonal matrix Q^H , i.e., $Q^H = A_n, \dots, A_1$ and $I = Q^H Q$.

Thus, equation (4.7) can be written as

$$x = Q \begin{bmatrix} R \\ 0 \end{bmatrix} \quad (4.8)$$

The error function for estimation in equation (4.4) can be expressed as

$$\varepsilon = y - \hat{H}x; \text{ if } \varepsilon = 0; \text{ then } y = \hat{H}x \quad (4.9)$$

By combining equations (4.6) and (4.7) the received signal stands

$$y = \hat{H}x = \hat{H}Q \begin{bmatrix} R \\ 0 \end{bmatrix} \quad (4.10)$$

The Hermitian of $Q \begin{bmatrix} R \\ 0 \end{bmatrix}$ is multiplied to both sides of equation (4.10) to derive the proposed channel estimation

$$\hat{H}_{OMT} = y Q^H \begin{bmatrix} R \\ 0 \end{bmatrix} H \quad (4.11)$$

As R is an upper triangular matrix, \hat{H}_{OMT} can be solved through back-substitution. The proposed estimation is a numerically stable low complexity solution to channel estimation of MIMO systems.

5. Result and Discussion

This section presents comparisons between Block error rates (BER) for the different channel estimation schemes. The results presented here are obtained from simulations performed in MATLAB. The channel is considered to be Rayleigh and the modulation scheme to be BPSK for simplicity in simulation. The block error rate is calculated by performing 10^6 trials at each SNR point. The block error rate is calculated for each SNR value. Performing 10^6 trials at each SNR value refers to sending same block of data 10^6 times from transmitter towards receiver for that SNR value. If the transmitted block of data don't match with the detected data at the receiver then an error occurs. I calculate the total number of error that has occurred during 10^6 trials. The block error rate is then calculated for a SNR value as total number of error divided by total number of trials. As an example if total number of error is 5×10^5 for 10^6 trials at a SNR value then the block error rate for this SNR value is

$$\text{Block error rate} = 500000 / 1000000 = 1/2$$

A new realization of channel was chosen in each trial and for each SNR value.

The simulation results shown in this section are limited to 4 by 4 and 2 by 2 transmit and receive antenna MIMO system only. The BER performance of the different channel estimation techniques and Alamouti STBC can be analysed under varying number of antennas.

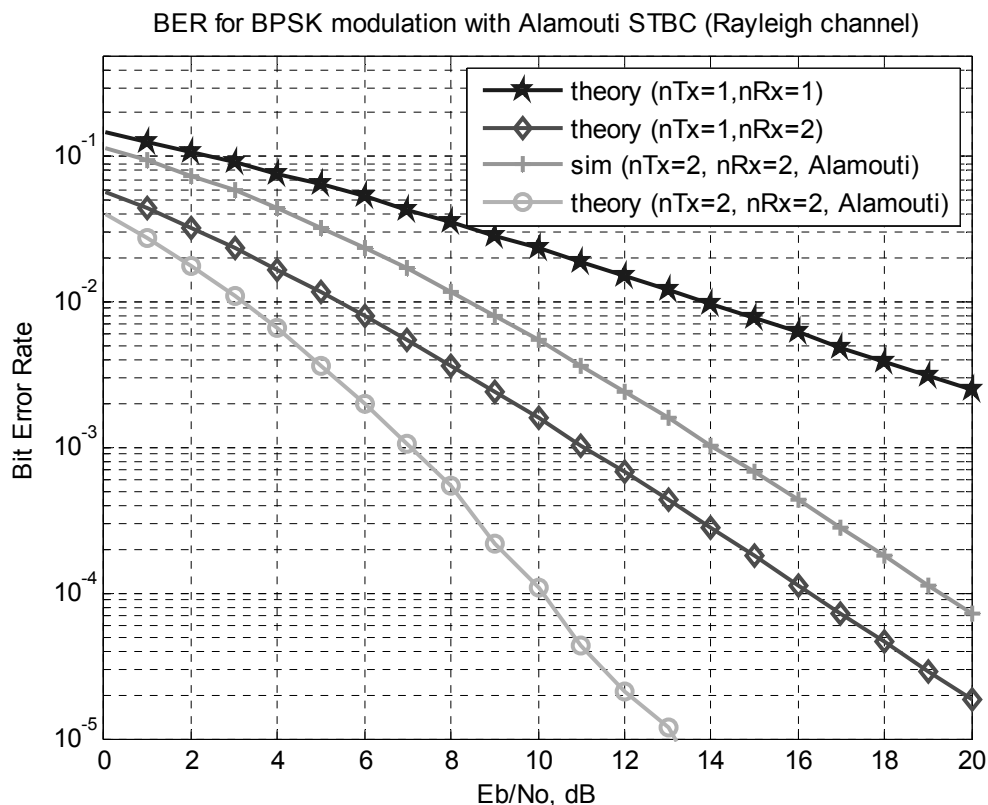


Fig 5.1 BER of Alamouti's STBC with different number of antenna

The BER performance of the MIMO system using AlamoutiSTBC is shown in the figure 5.1 for varying number of antennas. The BER is plotted for up to 2 transmit and 2 receive antenna. It can be seen from above figure that as the number of transmit antenna increase, the BER performance is also increasing and the same for increasing number of receive antenna. This figure also shows the BER obtained from theoretical formula. As a fact, the simulated BER is lower than that obtained theoretically. The value of BER for simulated AlamoutiSTBC is nearly equal to 10^{-2} at SNR equal to 8 dB for 2 transmit and 2 receive antenna whereas it is nearly equal to 0.02×10^{-3} for same SNR.

Figure 5.2 and figure 5.3 show the simulated results of BER in dB for LS and MMSE channel estimation techniques in MIMO with 4 transmit and 4 receive antennas against SNR in dB, respectively..

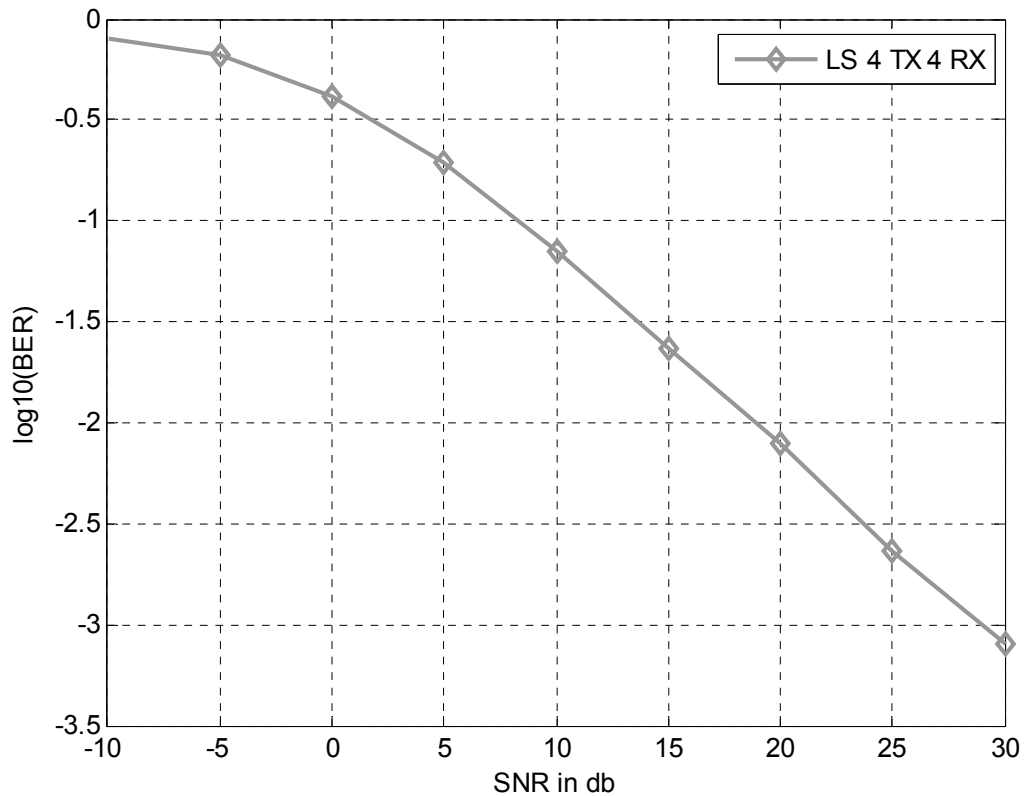


Fig 5.2 BER performance of LS scheme

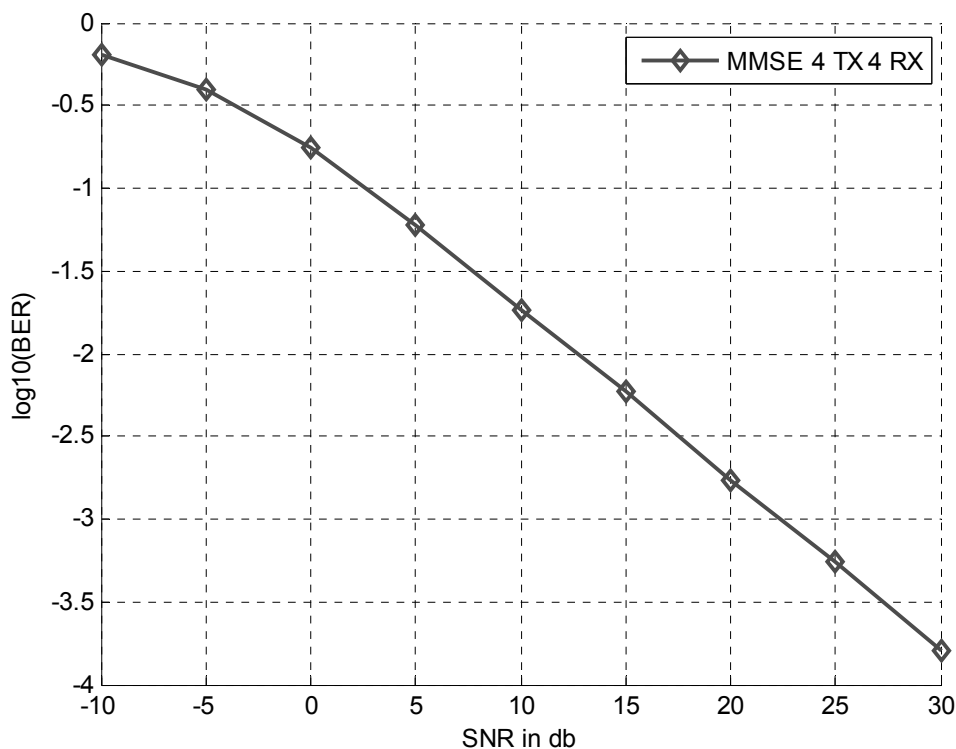


Fig 5.3 BER performance of MMSE scheme

The value of BER in LS and MMSE schemes are equal to -0.1 dB and -0.3 dB at $\text{SNR} = -10$ dB, respectively. As the value of SNR goes on increasing, the value of the BER also goes on increasing. Finally, the value of BER is equal to -3.6 dB and -3.9 at $\text{SNR} = 30$ dB. It is clear that increasing SNR gives lower value of BER resulting better BER performance and MMSE channel estimation technique provides better BER performance than LS scheme.

To get better view of LS and MMSE schemes, these two schemes are simulated under the same environment with only 2 transmit and 2 receive antenna due to memory insufficiency problem and the simulated results are shown in figure 5.4. Again, it can be seen that MMSE scheme provides better BER performance than LS scheme. The value of BER is about 0.5×10^{-1} & 0.25×10^{-1} dB at average $E_b/N_0 = 0$ dB and 0.5×10^{-3} & 10^{-5} dB at $E_b/N_0 = 20$ dB, respectively.

BER for BPSK modulation for 2x2 MIMO with LS & MMSE (Rayleigh channel)

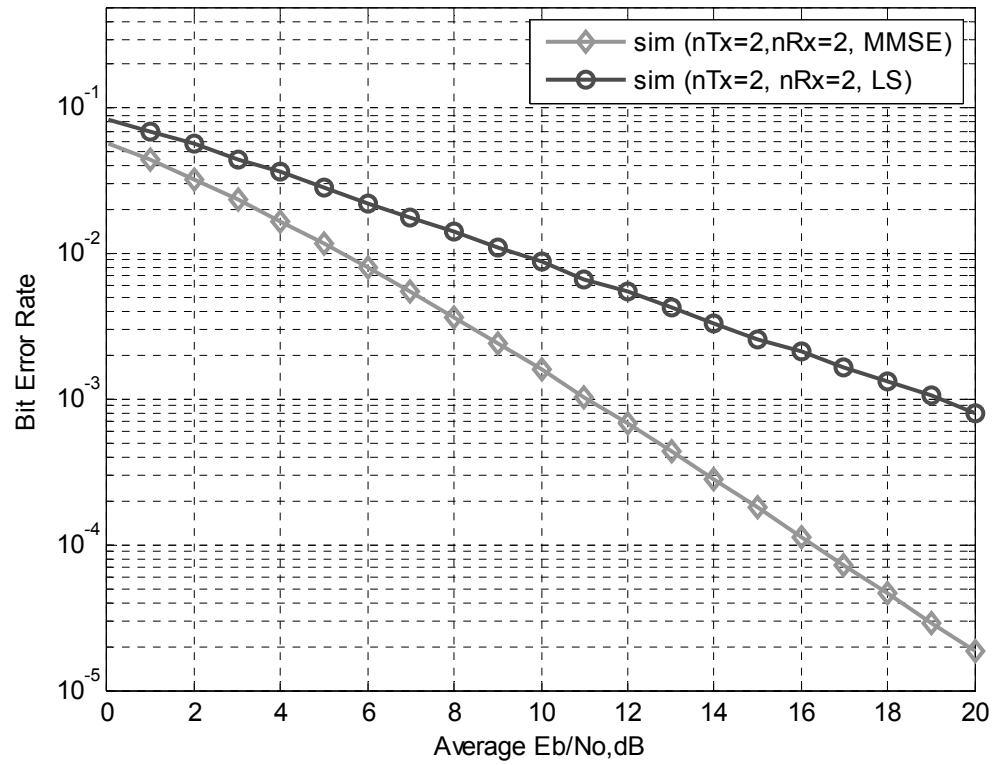


Figure 5.4 Comparison of BER performance of LS and MMSE schemes

The BER values for modified (proposed) LS channel estimation technique along with LS and MMSE techniques are simulated and plotted in figure 5.5 for 2 transmit and 2 receive antenna against different values of SNR ranging from 0 to 20 dB.

BER for BPSK modulation for 2x2 MIMO with LS & MMSE & Modified LS (Rayleigh channel)

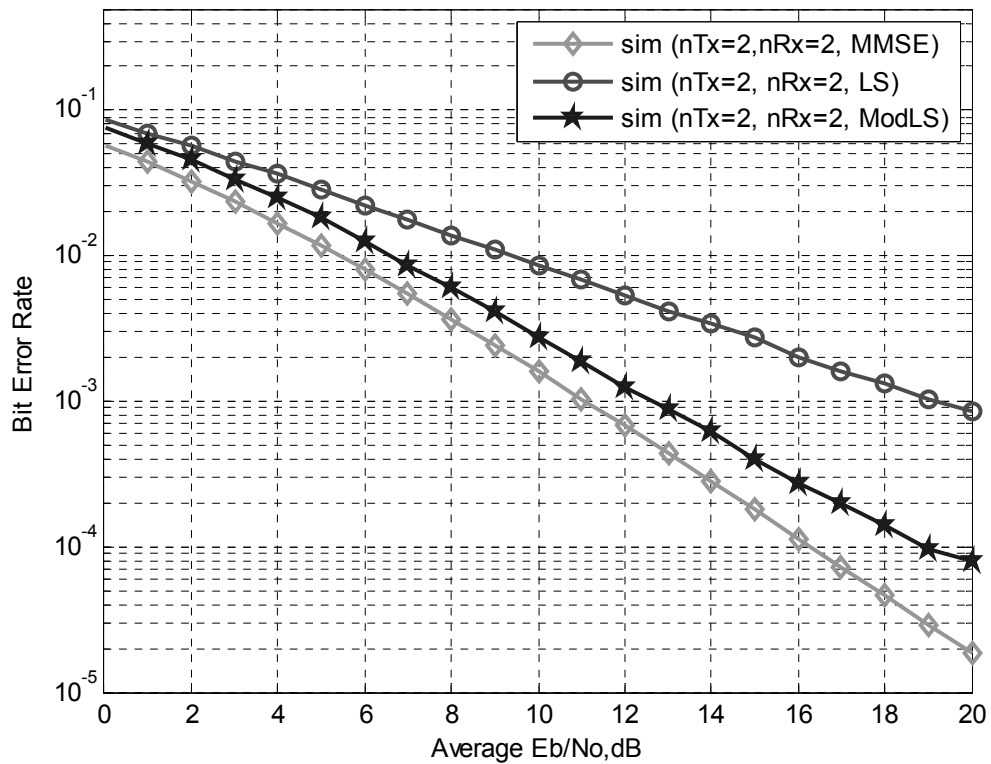


Fig 5.5 Comparison of BER Performance of Modified LS with LS and MMSE schemes

As seen from results in figure 5.5, the modified LS scheme, as expected, offers significant improvement in terms of BER performance of the channel estimation than conventional LS scheme. The value of BER is almost same at lower value of SNR, but at higher SNR as 20 dB, the modified LS scheme provides BER of about 10^{-4} dB instead of 10^{-3} dB in LS scheme. In addition, the MMSE scheme has the least values of BER than LS and modified LS schemes.

Finally, computational complexity of modified LS scheme against LS and MMSE schemes is carried out in terms of number of floating – point calculations with respect to varying number of the transmit antenna and simulated results are shown in the figure 5.6. The computational complexity is increasing with increasing the number of transmit antennas for all of these three schemes but with different rates. The rate of increase of complexity in modified LS scheme is almost linear whereas rising exponential in LS and MMSE schemes. Thus, complexity of modified LS scheme is, as expected, lower than that of LS scheme as well as MMSE scheme. In addition, the computational complexity is almost same for these channel estimation schemes up to 3 transmit antenna but then varies with higher number of transmit antennas.

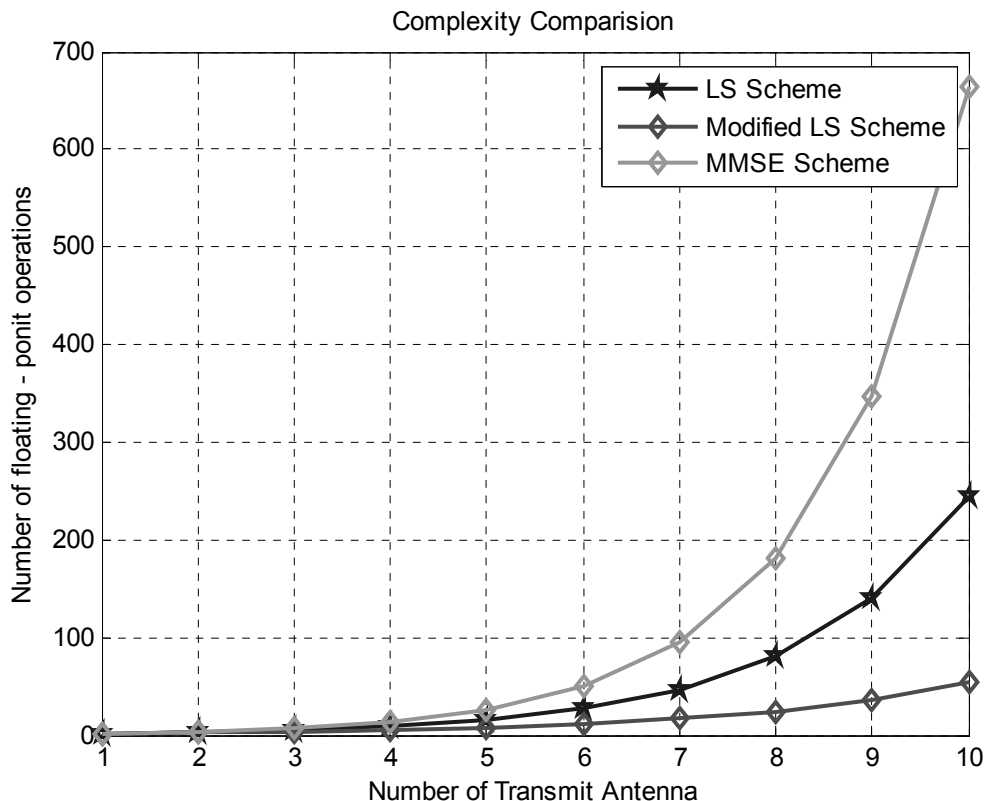


Fig 5.6 Complexity comparison between LS, MMSE and modified LS schemes

6. Conclusion

The simulation results for BER and computational complexity have been presented and discussed in the last chapter 5. From the results, it can be concluded that MMSE scheme is superior to LS and modified LS schemes in terms of BER performance and modified LS scheme is superior to LS and MMSE schemes in terms of the computational complexity.

The MMSE channel estimation technique can be chosen when very good BER performance is required in MIMO system at the cost of higher computational complexity and the LS channel estimation can be used with lesser complexity but with poor BER performance. Hence, modified LS scheme serves midway between these two schemes and can be chosen for good BER performance still having least computational complexity.

Thus, this paper, as expected, shows that modified (proposed) LS scheme offers less computational complexity but better BER performance than the LS scheme.

References

1. A. A. Abouda, and S. G. H. Äaggman, “*Effect of mutual coupling on capacity of MIMO wireless channels in high SNR scenario*”, Progress In Electromagnetic Research, PIER 65, 27-40, 2006.
2. A. A. Abouda, H. M. El-Sallabi, and S. G. H. Äaggman, “*Effect of antenna array geometry and ULA azimuthal orientation on MIMO channel properties in urban city street grid*”, Progress In Electromagnetic Research, PIER 64, 257-278, 2006.
3. J. Paulraj, D. A. Gore, R. U. Nabar, and H. Bolcskei, “*An overview of MIMO communications A key to gigabit wireless*”, Proceedings of the IEEE, Vol. 92, No. 2, 198-18, Feb. 2004.
4. R. Chen, H. Zhang, Y. Xu, and H. Luo, “*On MM-type channel estimation for MIMO OFDM systems*”, IEEE Trans. Wireless Commun., Vol. 6, No. 3, 1046-1055, May 2007.
5. Van De Beek, O. Edfors, M. Sandell, S. K. Wilson, and P. O. B. Äorjesson, “*On channel estimation in OFDM systems*”, Proc. IEEE Int. Veh. Technol. Conf., Chicago, Jul. 1995.
6. G. H. Golub, and C. F. Van Loan, “*Matrix Computations*”, 3rd edition, John Hopkins University Press, Maryland, 1996.
7. D. W. Äubben, J. Rinas, R. B. Äohnke, V. K. Äuhn, and K. D. Kammeyer, “*Efficient algorithm for decoding layered space-time codes*”, Electron. Lett., Vol. 37, No. 22, 1348-1350, Oct. 2001.
8. V. Pham, M. Le, L. Mai, and G. Yoon, “*Low complexity maximum-likelihood decoder for VBLAST-STBC scheme in MIMO wireless communication systems*”, IEEE63rd Vehicular Technology Conference, 2006, Vol. 5, 2309-2313, May 2006.
9. Z. Guo, Y. Wang, L. Li, X. Tao, P. Zhang, and H. Harada, “*A hybrid detection algorithm for MIMO systems*”, International Conference on Communications, Circuits and Systems Proceedings 2006, Vol. 2, 883-887, Jun. 2006.
10. H. Dhungana, “*Performance Evaluation of MIMO – OFDM System by PAPR Reduction and Channel Estimation*”, Thesis No. 066/MSI/607, Pulchowk Campus, IOE, TU, November 2011
11. S. K. Sharma, “*MIMO – OFDM Techniques for Wireless Communication System*”, Thesis No. IC 64615, Pulchowk Campus, IOE, TU, October 2010
12. K. P. Bagadi, Prof. Das, S., “*MIMO – OFDM Channel Estimation using Pilot Carriers* ” Jan, 2013
13. S. W. Patil, Prof. A. N. Jadhav., “*Channel Estimation using LS and MMSE Estimators*”, Jun, 2013
14. Beak, Edfors, Sandell, Wilson, Borjesson, “*On Channel Estimation in OFDM System* ”, Jan, 2012
15. T. S. Rappoport, “*Wireless Communication: Principle and Practice*”, Second Edition, Pearson, 2013
16. F. Delestre, “*Channel Estimation and Performance Analysis of MIMO – OFDM using Space – Time and Space – Frequency Coding Schemes*”, Jun 2011
17. W. Zhang, “*Channel and Frequency Offset Estimation for OFDM – Based System*”, Jun, 2010
18. Qi Wang, “*Study of Channel Estimation in MIMO-OFDM Systems for Software Defined Radio*”, LITH-ISY-EX--07/3954—SE, Linköping 2007
19. S. M. Alamouti, “*A simple transmit diversity technique for wireless communications*”, IEEE J. Select. Areas Commun., Vol. 16, 1451-1458, Oct. 1998.

POST CONSTRUCTION EFFECTIVENESS OF KATHMANDU- NAUBISE ALTERNATIVE ROAD

Anjana Bhatta

Email Address: anjana.bhatta@yahoo.com

Abstract

Transportation is the backbone of the economic development of any developing country. Therefore, Nepal has emphasized on the construction of new roads both in the rural and urban areas. But there are various types and degrees of environmental problems associated with the construction of roads in Nepal. Kathmandu-Naubise Alternative Road has been taken in the case study for the research work. The project directly deals with the Twelve Environmental issues and their performance indicators which are contain in EMAP. This study emphasizes on the mitigation measures implementation in the project. This study has evaluated the degree of effective implementation of mitigation measures.

The study has evaluated the arrangement in the project design and implementation aspects. It is concluded that the enforcement in the implementation is the key to the success of the project.

Keywords: *Transportation, EMAP, Environmental Issues, Mitigation Measures*

1. Introduction

Roads often bring significant economic and social benefits, but they can also have substantial negative impacts on communities and the natural environment. As we become more aware of these impacts, there is a growing demand for the techniques and skills needed to incorporate environmental considerations into road planning and management.

Government of Nepal has been giving priority to development of roads since the beginning of planned development programmes more than 40 years ago. With this effort, the National Road Network has altogether 15,308 km roads, including 4,522 km blacktop, 3,646 km gravel and 7,140 km earth roads. Put alternatively, the National Road Network comprises 15,308 km roads including 4,977 km strategic roads 1,984 km urban roads and 8,347 km district roads. GoN has proposed Strategic Road Network of about 12,600 km in the coming decade. Among Nepal's 75 district headquarters, only two are not connected by a motorable road. The Department of Roads is responsible for constructing and maintaining the main national lines of access through intricate, inter connected environments of Nepal. In the past, the pressure to open a road network as quickly as possible has caused to neglect many environmental considerations. The construction of Roads in Nepal which mostly has rugged topography dissected by north to south flowing rivers is not merely technical and economical challenges but also an environmental one. Although Roads are meant for the economic development of the country, there are various types and degrees of environmental problems associated with their construction. These environmental problems are not only associated with the physical environment but also related to biological, social, cultural and sometimes archaeological problems. Landslides, slope failures, soil erosion, loss of agricultural and forest land, and sedimentation into water bodies are some of the negative impacts of road construction. These adverse impacts have, in some cases, negated the objective of the development project. With the promulgation of environmental law, all the development projects are subjected to environmental screening in according with these guidelines.

Environmental Management Guidelines- 1999 was developed by Department of Roads as part of a program undertaken jointly by Government of Nepal and the World Bank under the Road Maintenance and Rehabilitation Project to implement environmental mitigation measures in the surveying, design, construction and maintenance and operation of road project.

2. Main Objective

To evaluate the effectiveness of the environmental mitigation measures, as contained in the Environmental Management Action Plan (EMAP).

Specific Objectives

- Identification of positive and negative impacts on environmental resources
- Examination of the significance of environmental implications.
- Recommend preventive and corrective measures.

3. Methodology

This study is based on both primary and secondary data. Primary data are collected through survey on expert's opinion, key informants and field observations in the project sites. Secondary data and information are collected from EIA report and related literature review.

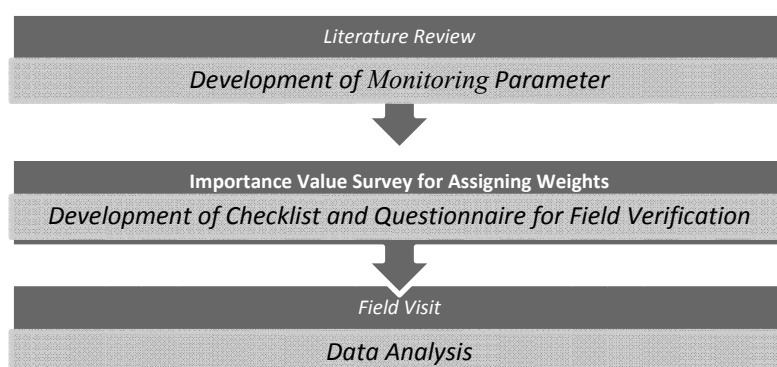


Fig 1 Schematic diagram of the methodology

During the field visit, observations were made about the contractor's activities on twelve environmental issues. Quantity as well as quality measurement of indicator judging effective implementation of mitigation measures were recorded including emerging impacts (landslides, littering, etc.) due to road construction and related activities. Line transect method was used during the observation i.e. walking along the length of the road and observing the biophysical impacts as detailed in the checklist.

The degree of effective implementation for each performance indicator obtains from site observation is then multiple with its own weight and corresponding weight of the environmental issues to get the weight degree of effective implementation. The weighted degree of individual environmental issues will be summed up to get the overall degree of effective implementation.

4. Analysis, result and discussion

4.1 Monitoring Parameter and Performance Indicator

Major twelve environmental issues that highlight all biophysical environment- oriented action in the road construction were identified and their respective performance indicator developed to monitor performance achievement of mitigation measures. Issues and their performance indicators are summarized in Table 1.

Table 1 Monitoring parameter

Environmental Issues	Performance Indicator
1.Quarries and Borrow pits	1-1 No evidence of water ponding or presence of fresh gullies and quarry spoil littering. No increased visual turbidity of surface waters 1-2 Natural contours and vegetation are restored. Engineers report testifying to completion of restoration work.
2.Spoil and Construction Waste Disposal	2-1 Presence of slides, scouring erosion or destruction of property on the valley side, disruption of water supply and irrigation systems. 2-2 Complaints from local residents 2-3 Survival rate of plants.
3.Work Camp Location and Operation	3-1 Latrines constructed; no disruption in local water supplies. 3-2 Timely and effective waste disposal and fire control 3-3 Re-plantation of the site 3-4 Natural contours and site appearance restored. Engineer's report testifying restoration of site.
4. Labour Camp location and Management	4-1 No complaints from local residents. 4-2 No disruption in local water supplies 4-3 Timely and effective waste disposal 4-4 Re-plantation of the sites. 4-5 Natural contours and site appearance restored. Engineer's report testifying restoration of site
5.Earthworks/Slope Stabilisation	5-1 Adequacy and quality of planting. 5-2 Survival of rate of plants.
6. Blasting	6-1 No major rock fracturing of the remaining hill slope. 6-2 Damage to valley side private property.
7. Stockpiling of Materials	7-1 Sufficient protection measures are provided against the washouts.
8. Explosive, Combustible and Toxic Materials Management	8-1 Hazardous materials management procedures implemented. 8-2 No visible puddles of oil or contaminated soil.
9.Retaining wall construction	9-1 No occurrence of slope instability and damage to adjust features
10. Restatement of services	10-1 Complaints Received 10-2 Full Functioning of Reinstated Water Supply Lines, Canals and

	Trials
11. Drainage/ Water management	11-1 No evidence of fresh surface erosion or presence of new gullies of the valley side. No increased visual turbidity of surface waters. 11-2 1 No evidence of loss of agricultural land and forests. No complaints from landowners.
12. Air and Noise Pollution	12-1 No complaints from local residents.

4.2 Weightage Determination

The importance value survey analysis for Weightage determination is presented. The results and discussion are as follows:

4.2.1 Weightage Distribution for each Environmental Issues

The graphical representation of weight distribution for each environmental issue is presented in Fig 2.

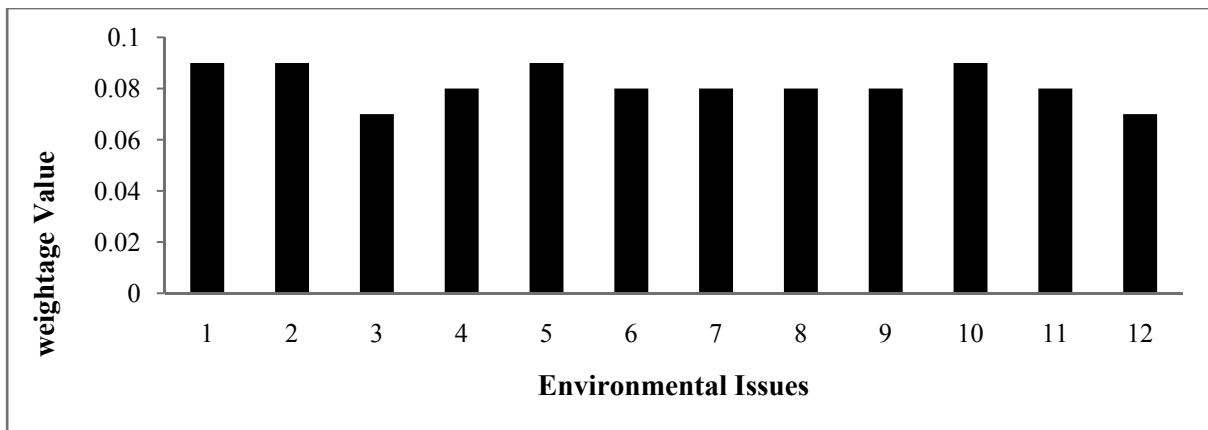


Fig 2 Weightage distributions of environmental issues

The standard deviation on weights obtained for environmental issues from various professionals is very minimal. The data’s deviation is within 14% to 27% from the mean value that signifies its relevance.

The result shows that environmental issues as; quarries and borrow pits, spoil and construction waste disposal; earthworks/ stabilization; and drainage and water management among twelve parameters carries higher weight 0.09. The result seems reasonable as the action of these environmental issues in the road construction extends a higher area of implication and directly activities service erosion and slope instability.

The weights distribution for issues as; work camp location, blasting, stockpiling of materials , explosive combustible and toxic materials management, retaining wall construction; and reinstatement of services are slightly lesser carrying similar weights of .08.

The lowest weight distribution having 0.07 values was obtained for issues as; labour camp location and management and air and noise pollution. Except for air pollution, the issues express actions supporting road construction. The impact on air pollution though significant carried low weight. This is supportive considering remoteness of the construction site.

4.2.2 Weightage Distribution for each Performance Indicator

The graphical representation of results obtained on weight distribution for each performance indicator is presented in Fig 3.

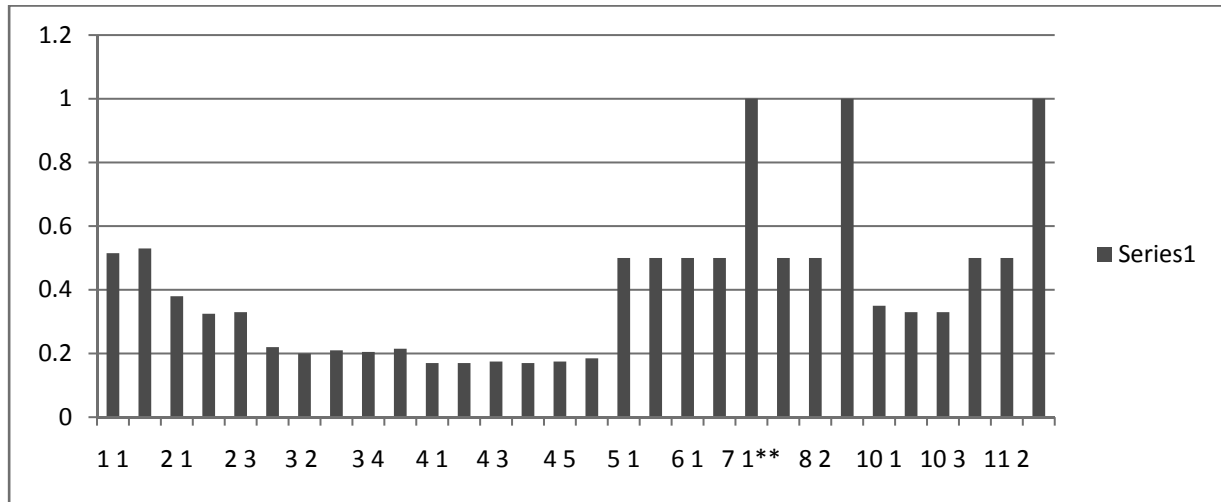


Fig 3 Weightage distribution of performance indicator

The standard deviation on weights obtained for performance indicators from various professional is also minimal. Most of the data’s deviation is within 3% to 15% from the mean value that also signifies its relevance. The distribution weight noted is in general similar for performance indicators under each environmental issue. However, is observed that the performance indicators that directly accounts on evaluation for actions caused by road construction activities were given slight higher weights than the performance indicators that bases the evaluation on public complaints.

4.3 Degree of Effective Implementation

4.3.1 Implementation Assessment of Environmental Issues

The performance rating of each indicator then were multiplied with its respective weights and summed under each issue to obtain the degree of effective implementation for each environmental issues and the details are summarized in Table 2 and the graphical representation of the results are presented in Fig4.

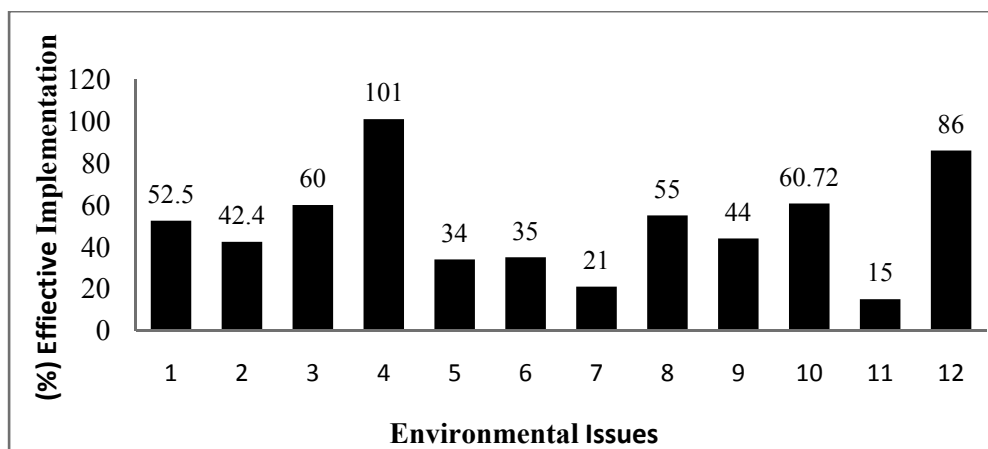


Fig 4 Effective implementation of environmental issues

4.3.2 Overall Degree of Effective Implementation

The effective implementation of each environmental issue is multiplied with its weights to obtain the weighted degree of effective implementation. The weighted degree of each issue is summed up to obtain the Overall Degree of Effective Implementation is summarized in Table 2.

Table 2 Overall degree of effective implementation

Environmental issues	Respective Weightage	Performance indicator	Respective Weightage	Effective Implementation of performance indicator (%)	Weights effective Implementation of Performance Indicator (%)	Effective Implementation of Environmental issues (%)	Weighted effective Implementation of Environmental issues (%)	Overall degree of Effective implementation (%)
A	B	C	D	E	$F = E * D * B$	$G = D * E$ & sum of each issue	H = sum of 'F' for each	I = sum of H
1	0.10	1-1	0.5	50	2.25	52.5	4.73	52
		1-2	0.5	55	2.48			
2	0.09	2-1	0.36	60	1.94	42.4	3.81	
		2-2	0.32	35	1.01			
		2-3	0.32	30	0.86			
3	0.07	3-1	0.2	100	1.4	60	7	
		3-2	0.2	100	1.4			
		3-3	0.2	100	1.4			
		3-4	0.2	100	1.4			
4	0.08	4-1	0.16	100	1.28	101	8.08	
		4-2	0.17	100	1.36			
		4-3	0.17	100	1.36			
		4-4	0.17	100	1.36			
		4-5	0.17	100	1.36			
		4-6	0.17	100	1.36			
5	0.09	5-1	0.5	30	1.35	34	3.06	
		5-2	0.5	38	1.71			
6	0.08	6-1	0.5	40	1.6	35	2.8	
		6-2	0.5	30	1.2			

7	0.08	7**	1	21	1.68	21	1.68
8	0.08	8-1	0.5	50	2	55	4.4
		8-2	0.5	60	2.4		
9	0.08	9**	1	44	3.52	44	3.52
10	0.09	10-1	0.33	53	1.57	60.72	5.46
		10-2	0.33	66	1.96		
		10-3	0.33	65	1.93		
11	0.08	11-1	0.5	20	0.8	15	1.2
		11-2	0.5	10	0.4		
12	0.07	12**	1	86	6.02	86	6.02

The graphical representation of the weighted effective implementation of each environmental issue and cumulative degree of effectiveness is presented in Fig 5.

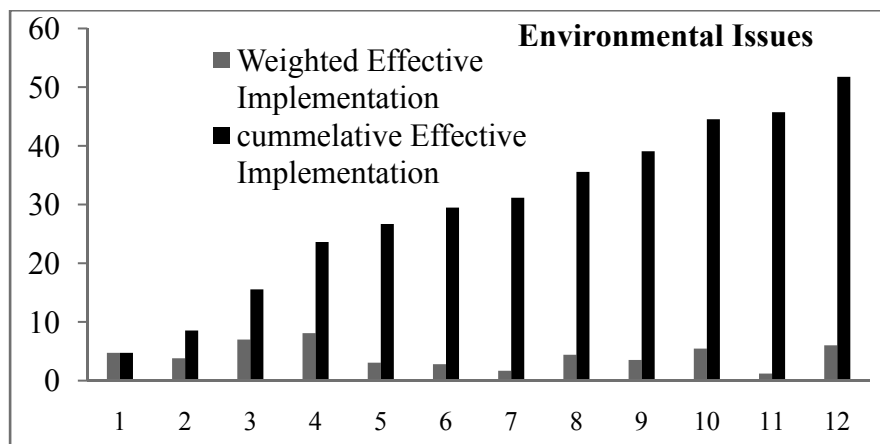


Fig 5 Overall degree of effective implementation

The result shows that the overall degree of effective implementation of mitigation measures of Naubise- Dharke Alternative Road is only about 52% with a rating notation of **Fair**.

The site observation analysis shows that the activities relating to environmental issues regarding Spoil and Construction Waste Disposal; Earthworks/Stabilization; blasting stockpiling of material; drainage and water management have been performed with a poor rating(i.e.<40).

Road construction in mountainous region requires the installation of structures i.e. retaining walls to support carriageway, toe-walls to support extra widening of road widths, flood ways to facilitate the natural cross drainage across the road length and breast walls to support the falling cut batter etc. often structural works commence after the completion of the excavation works only after disposing off much of the valuable rocks and soils down the valley. Instead these could have done earlier at

locations where its installation is required and rock source is available. Rocks are often extracted with a little or no considerations of the environmental implications of the surroundings. Quarries are often located within unsafe road right of ways and are not properly rehabilitated to safe conditions upon completion of its use. Often quarrying is undertaken without care with a common result of impoverishing the cultivated lands, especially in the vicinity and downstream. These sources in absence of adequate protective measure during and post harvesting had induced erosion and escalated its extent further. Hence these sources necessarily are closed with effective protective measures being put into so that it no longer remains a source of potential environmental degradation.

Workforces' need it camp sited with locations of minimal lead of construction alignment stretches in order to optimize their outputs. But there was not any work camp, labor camp location in the site. The local services e.g. drinking water supply lines, trials, irrigation canals etc. are also disrupted by the excavations during road constructions. The supply or access of the existing services must provisionally be maintained for its continuity during construction stage, and reinstated fully to its original capacity upon completion of the constructions. This is the concerned Supervising Consultants; especially Resident Engineer's due to for ensuring its being implemented.

While the highlights of the above issues sounds common phenomenal observations and the adverse effects resulted thereof be rectified as and where the situations calls for, it is often the practice of overlooking or not implementing completely or partially.

5. Conclusion

The overall degree of effective implementation of mitigation measures is categorised as FAIR as it has 52% of rating score. The overall result signifies that the environmental issues carrying higher weight and that involves higher mitigation costs were in general neglected by the performer. The contractor responsible for implementation has sincerely expressed their inability to perform efficiently due to cost factor due to the poor enforcement of the provision mentioned in EMAP. Serious violation was traced regarding hill slopes failures, poor drainage and water management was noted throughout the alignment. As a result, smothering of vegetation and topsoil on the valley side was immense causing scouring, erosion, slides and littering to high value and agricultural land at several locations which has much more implications on the environment. The contractor in an attempt to be competitive may not have allocated the rates to a realistic level to adequately fund environmental mitigation and protection and thus have lacked in implementing mitigation effectively. The forestation and bioengineering were arranged in the project to be carried out by other contractors after the completion of the road construction. However, environmental management of the road should have been carried out parallel with the construction.

6. Acknowledgement

I would like to express my profound gratitude to the contribution of my supervisor Prof. Padma Khadka. I am indebted to him for providing encouragement, outstanding supervision, expert guidance, consistent supports and constructive criticism throughout the thesis period.

I am pleased to acknowledge Er. Anil Marsani, (Coordinator, Masters Program in Transportation Planning, Institute of Engineering, Pulchowk Campus), for his continuous encouragement and valuable suggestions. I humbly acknowledge the support received from Prof. Gautam Bir Singh Tamrakar and guidance of SDEGhana Shyam Gautam, Department of Road, Nepal for their constant support and valuable suggestions. This study was supported by the University Grants Commission (UGC), Sanothami, Bhaktapur, Nepal. I would like to thank UGC for their support.

References

1. ESCAP/UNEP, “*Seminar on Environmental Impact Assessment of Road Transport Development*”, BANGKOK, 3-8 November 1986
2. Government of Nepal, “*Ministry of works and Transport, Department of Roads*”, Geo-Environment Unit, Environmental Management Guidelines, Reprint July 1999
3. Government of Nepal, Ministry of Works and Transport, Department of Roads, Environmental Aspect, Priority Investment Plan, “*Master Plan for strategic Road Network and Rural Transport*”, February 1997
4. Government of Nepal, Policy Document, Ministry of Physical Planning and Works, Department of Roads, Geo-Environment Unit, “*Environmental Assessment in the Road Sector of Nepal*”, January 2000
5. Koji Tsunokawa, “*Christopher Hoban Roads and the Environment*”, World Bank Technical Paper; No 376.
6. Larry W. Canter, “*Environmental Impact Assessment*”, MC. Graw-Hill. Inc., University of Oklahoma, Second Edition, 1996
7. Manoj Kumar Pandey, “*EIA Lecture Handouts*”, Environmental Engineering IOE Pulchowk, 2004
8. SMEC International Pvt. Ltd., Cooma, NSW, Australia in association with Cemat Consultants (Pvt) Ltd, Nepal. Initial Environmental Examination, “*Road Maintenance and Development Project*”, May 1999
9. SMEC International Pvt. Ltd., Cooma, NSW,, Australia in association with Cemat Consultants (Pvt) Ltd. Final Report, “*Environmental Management Action Plan for Road Upgrading*”, RMDP, June 1999

OPEN CHANNEL SURGES

Bharat Raj Pandey

Chief Engineer

Hydro-Consult Engineering (HCE)

Email Address: bharat.spbrp@gmail.com

Abstract

The open channel Surges due to sudden changes of flow depth creates Celerity (Wave Velocity) in the flow in addition to the normal water velocity of the channels. These waves travel in the downstream and sometimes upstream of the channels depending on the various situations. The propagation of the Surges becomes positives or negatives depending on its crest and the trough of the waves. Therefore on this topic, these principals are presented in the analytical methods.

Keywords: surge, dam, sluice gate

1. Introduction

The sudden changes of flow in open channel results in the increase or decrease of flow depth is called the "SURGE" in open channel. This could take place when there is a breaching of dams due to earthquake or regulating the hydropower sluice gates. Hence results in positive and negative surges in downstream river channel or in downstream tail channel of hydropower projects. This phenomenon also governs when there would be flood (unsteady flow) during monsoon period in natural river channels and the hydrograph significantly varies with rising and falling as the rainfall takes it peak period. The flood wave which generates during the positive or negative surges is called the celerity (wave velocity) of the flood in unsteady flow situation.

This positive or negative surge sometimes travels downstream or upstream depending on the situation. The increase in flow depth would become the crest of the surges and the decrease in the flow depth would become the trough of the surges.

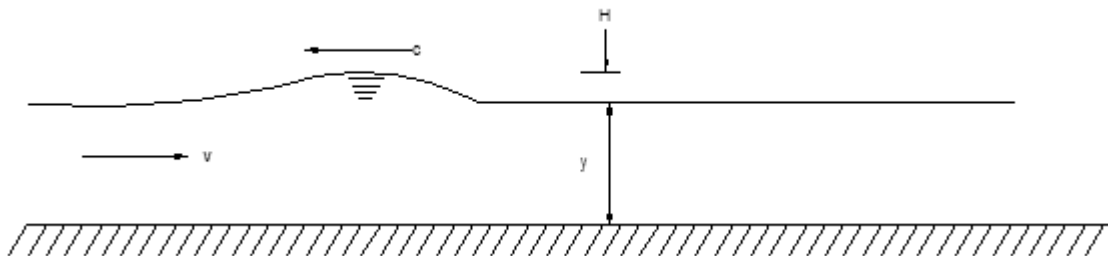


Fig 1 Propagation of low wave in channel

The celerity or speed of propagation relative to the water is given by \sqrt{gy} where y is the water depth. Therefore the velocity of the wave relative to a stationary observer is:

$$c = \sqrt{gy} \pm v \dots \dots \dots 1$$

This can be noted that the Froude number F_r , expressed by $\frac{v}{\sqrt{gy}}$ is the ratio of water velocity to wave celerity. If the Froude number is greater than unity, which corresponds with supercritical flow, a small gravity wave cannot be propagated upstream. Waves of finite height are dealt with in section of open channel surges.

The examples of Surges in downstream River Channel is when regulating the sluice gates of one of the 12MW Jhimruk Hydropower Project as shown below which is located in Puythan district of Western Region of the Nepal.



Fig 2 Downstream end showing photograph of 12MW Jhimruk Hydropower Project
(Source: Butwal Power Company (BPC))

A surge is produced in the channel by a rapid change in the rate of flow, for example, by the rapid opening or closure of sluice gates of the project. The former causes a positive surge wave to move downstream (shown in fig) and the latter produces a positive surge wave which moves upstream (shown in Fig)

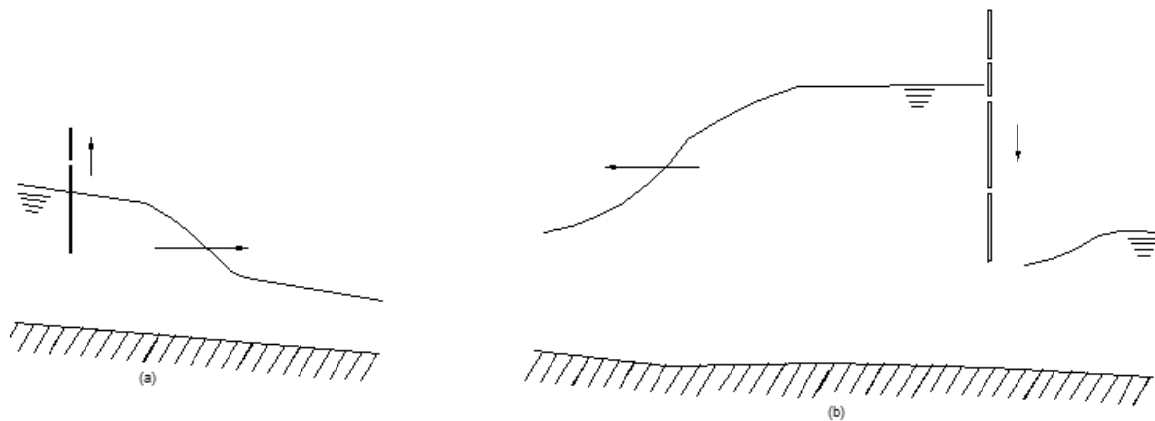


Fig 3 Positive Surge Waves

A stationary observer therefore sees an increase in depth as the wave front of a positive surge wave passes. A negative surge wave, on the other hand, leaves a shallower depth as the wave front passes. (Shown in fig)

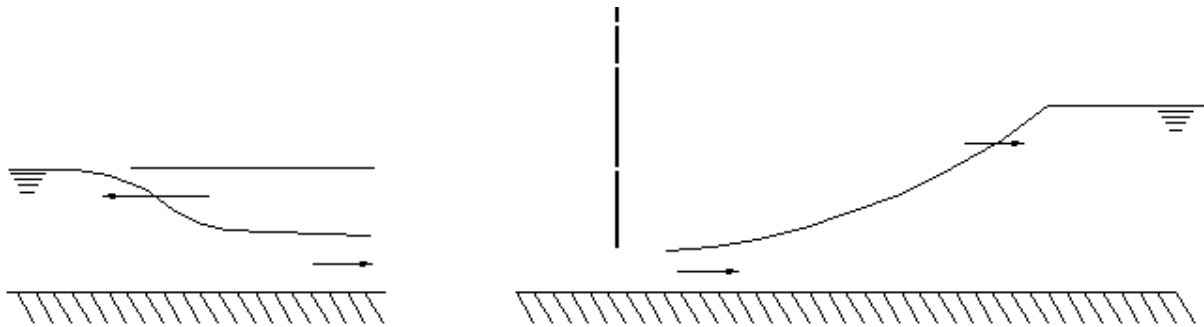


Fig 4 Negative Surge Waves

Negative Surge waves in the downstream River Channel are produced to a 12MW Jhimruk hydropower plant when the sluice gates are suddenly being closed (shown in above fig).It is illustrated from the figure that each type of surge can move upstream or downstream.

2. Analytical Methods

2.1 The upstream positive surge wave

Consider the propagation of a positive wave upstream in a frictionless channel resulting from gate closure (shown in fig)

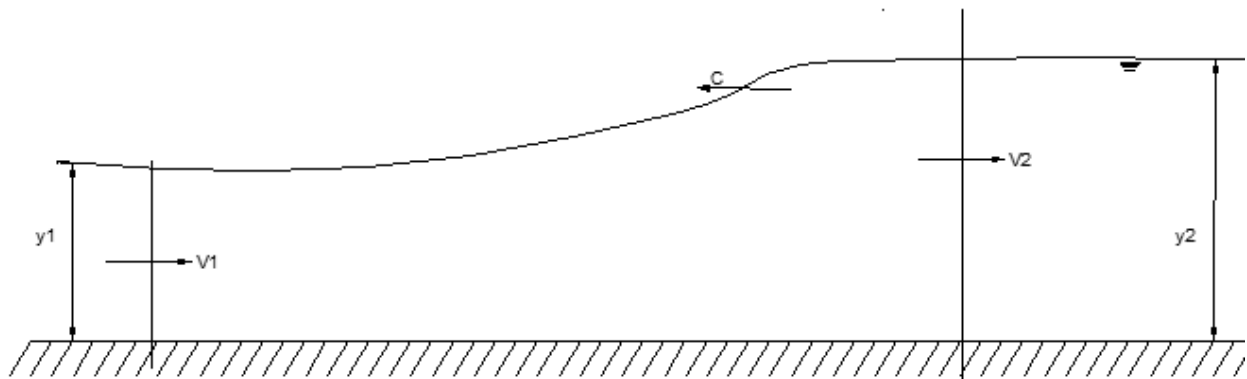


Fig 5 Upstream Positive Surges

The front of the surge wave is propagated upstream at celerity, c , relative to the stationary observer. To the observer, the flow situation is unsteady as a wave front passes; to an observer travelling at a speed, c , with the wave the flow appears steady although non-uniform. The following fig shows the surge reduced to steady state.

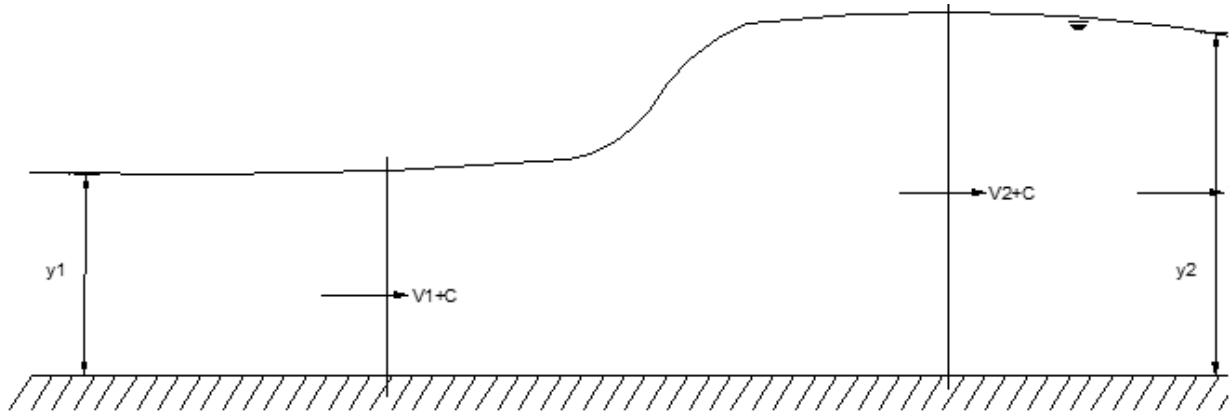


Fig 6 The continuity equation is:

$$A_1(V_1 + c) = A_2(V_2 + c) \dots \dots \dots 2$$

The momentum equation is:

$$gA_1\bar{y}_1 - gA_2\bar{y}_2 + A_1(V_1 + c)(V_1 - V_2) \dots \dots \dots 3$$

Where \bar{y}_1 and \bar{y}_2 are respective depths of the centres of area. From simplification, we get

$$c = \left[gA_2 \frac{(A_2\bar{y}_2 - A_1\bar{y}_1)}{A_1(A_2 - A_1)} \right]^{\frac{1}{2}} - v_1 \dots \dots \dots 4$$

In the special case of rectangular channel,

$$A = by: \bar{y} = \frac{y}{2}$$

From the above equation, it can be written as

$$c = \left[\frac{gy_2}{2} \frac{(y_2^2 - y_1^2)}{y_1(y_2 - y_1)} \right]^{\frac{1}{2}} - v_1$$

$$\text{then; } c = \left[\frac{gy_2}{2} \frac{(y_2 + y_1)}{y_1} \right]^{\frac{1}{2}} - v_1 \dots \dots \dots 5$$

The hydraulic jump in a stationary surge. Putting $c = 0$, in the above equation,

$$v_1^2 = \frac{gy_2}{2} \frac{(y_2 + y_1)}{y_1}$$

$$\frac{2v_1^2 y_1}{g} = y_2^2 + y_2 y_1$$

$$\text{Now } F_1^2 \{ (Froudenumber)^2 \} = \frac{v_1^2}{gy_1}$$

$$\therefore y_2^2 + y_2 y_1 - 2F_1^2 y_1^2 = 0$$

where, Jump equation is:

$$y_2 = \frac{y_1}{2} (\sqrt{1 + 8F_1^2} - 1)$$

In the case of a low wave where y_2 approaches y_1 then equation becomes

Then $c = \sqrt{gy} - v_1$ 6

And in still water ($v_1 = 0$)

$c = \sqrt{gy}$7

2.2 The downstream positive surge

This type of wave may occur in channel downstream from a slice gate at which the opening is rapidly increased. See figure below

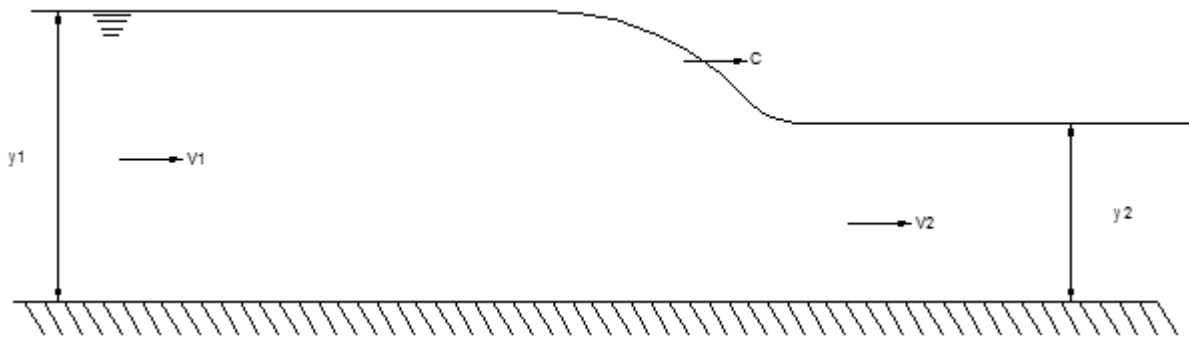


Fig 7 Downstream Positive Surges

Reducing the flow to steady state. From continuity equation:

$$(c - v_1)A_1 = (c - v_2)A_2 \dots\dots\dots 8$$

Momentum: $gA_1\bar{y}_1 - gA_1\bar{y}_2 + (c - v_2)A_2(v_2 - v_1) = 0$9

Similarly, $c = \left[\frac{gy_1}{2y_2} (y_1 + y_2) \right]^{\frac{1}{2}} + v_2 \dots\dots\dots 10$

2.3 Negative Surge Waves

The negative surge wave appears to a stationary observer as a lowering of the liquid surface. Such wave occurs in the channel downstream from the control gate the opening of which is rapidly reduced or in the upstream channel as the gate is opened. The wave front can be considered to be composed of a series of small waves superimposed on each other. Since the uppermost wave has the greatest depth it travels faster than those beneath; the retreating wave front therefore becomes flatter. Shown in fig below

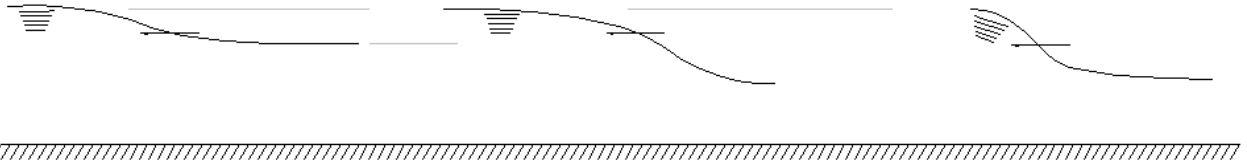


Fig 8 Propagation of Negative Surges

The above figure shows a small disturbance in a rectangular channel caused by a reduction in downstream discharge; the wave propagates upstream as described below:

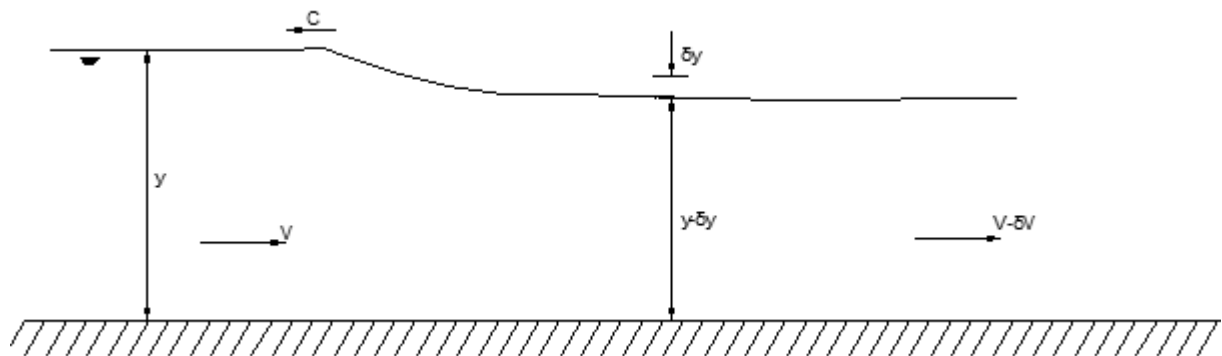


Fig 9 Neglecting the product of small quantities

$$\delta y = -\frac{y\delta v}{(V + c)} \dots\dots\dots 11$$

The momentum equation is $\frac{\rho g}{2} \{y^2 - (y - \delta y)^2\} + \rho y(v + c)\{v + c - (v - \delta v + c)\} = 0$

Where $\frac{\delta y}{\delta v} = -\frac{(v+c)}{g}$

Or $\delta y = -\frac{\delta v(V+c)}{g} \dots\dots\dots 12$

Equating the above equations;

$$\frac{y\delta v}{(v + c)} = \frac{(v + c)\delta v}{g}$$

Where, $c = \sqrt{gy} - v \dots\dots\dots 13$

Substituting for (v +c) from above equations;

$$\delta y = -\frac{\delta v}{g} \sqrt{gy}$$

And in the limit as $\delta y \rightarrow 0$

$$\frac{dy}{\sqrt{y}} = -\frac{dv}{\sqrt{g}} \dots\dots\dots 14$$

For a wave of finite height, integration of above equation yields

$$v = -\sqrt{2gy} + \text{constant}$$

When $y = y_1, v = v_1$; Where $\text{const} = v_1 + \sqrt{2gy_1}$

$$v = v_1 + 2\sqrt{gy_1} - 2\sqrt{gy} \dots \dots \dots 15$$

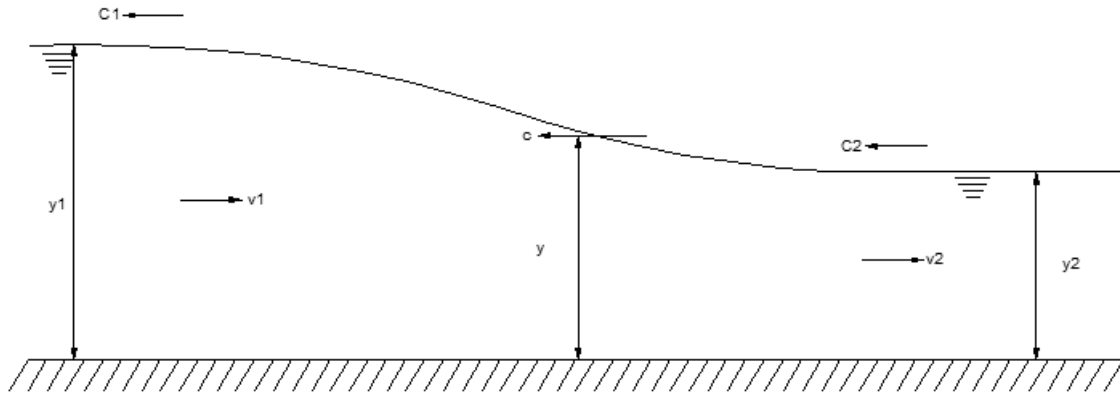


Fig 10 Negative surges of finite height

From equation $c = \sqrt{gy} - v$ and substituting in above equation then it becomes;

$$c = 3\sqrt{gy} - 2\sqrt{gy_1} - v_1; \text{The wave speed at;}$$

the crest is therefore, $c_1 = \sqrt{gy_1} - V_1$; the trough $c_2 = 3\sqrt{gy_2} - 2\sqrt{gy_1} - V_1$

In the case of a downstream negative surge in a frictionless channel as shown below a similar approach yields; $c = \sqrt{gy} + v$; again $v = 2\sqrt{gy} - 2\sqrt{gy_2} + v_2$; $c = 3\sqrt{gy} - 2\sqrt{gy_2} + v_2$;

$$c_1 = 3\sqrt{gy_1} - 2\sqrt{gy_2} + v_2$$

$$c_2 = \sqrt{gy_2} + v_2$$

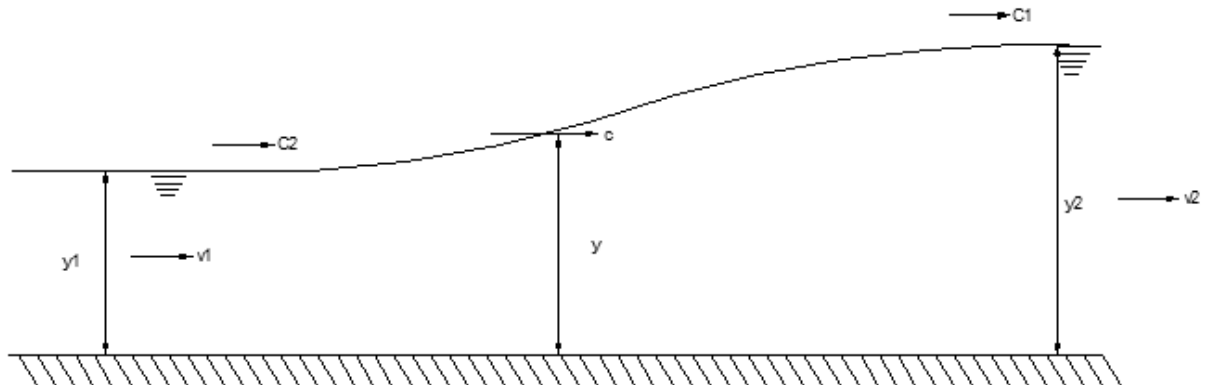


Fig 11 Downstream negative surges

2.4 The Dam Break

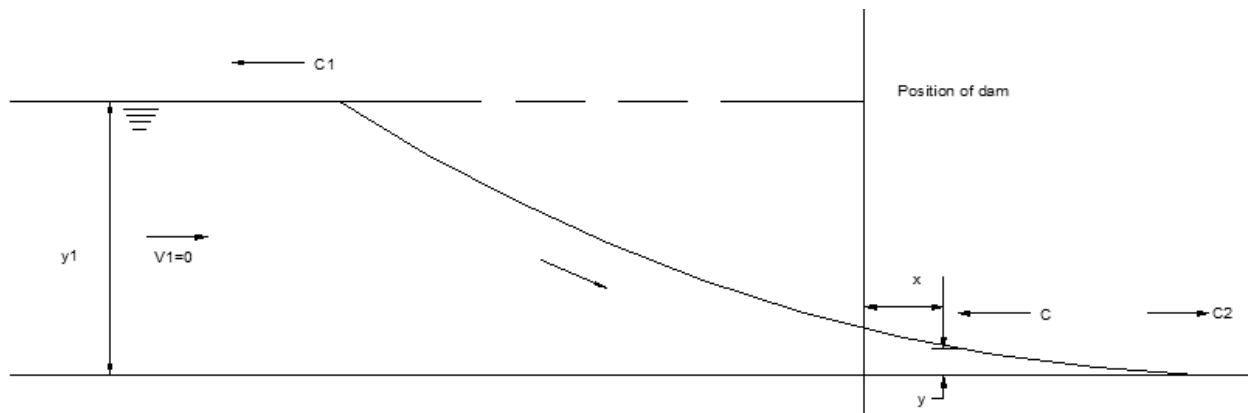


Fig 12 Dam Break illustration

The dam, or gate, holding water upstream at depth y_1 and Zero velocity, is suddenly removed.

From equation $c = 3\sqrt{gy} - 2\sqrt{gy_1}$

The equation to the surface profile is therefore

$$x = (ct) = (3\sqrt{gy} - 2\sqrt{gy_1})t$$

If $x = 0$, $y = \frac{4y_1}{9}$ and remains the constant with time. The velocity at

$x = 0$ is $v = v_1 + 2\sqrt{gy_1} - 2\sqrt{gy}$ from the above equation

i.e. $v = \frac{2}{3}\sqrt{gy_1}$, since $v_1 = 0$

3. Illustration

A rectangular tailrace channel of hydropower project, 15m wide having bed slope 0.0002 and manning roughness coefficient as 0.017 conveys a steady discharge of $45\text{m}^3/\text{s}$ from the hydropower installation. A power increase results in a sudden increase in flow to the Turbines to $100\text{m}^3/\text{s}$. Determine the depth and celerity of the resulting surge wave in the tailrace channel.

Solution:

Using Manning equation to calculate the depth of the uniform flow under initial conditions at a discharge of $45\text{m}^3/\text{s}$; the initial flow depth is then; 2.42m.

Using above equation i.e. $(c + V_1)y_1 = (c - V_2)y_2$

$$c = \frac{V_1 y_1 - V_2 y_2}{(y_1 - y_2)}$$

$$c = \frac{\frac{Q_1 y_1}{b y_1} - V_2 y_2}{(y_1 - y_2)}$$

$$V_2 = \frac{Q_2}{by_2} = \frac{45}{15 \times 2.42} = 1.24 \text{ m/s}$$

$$Q_1 = 100 \text{ m}^3/\text{s}, \text{ then; } c = \frac{6.67-3}{(y_1-2.42)} = \frac{3.67}{(y_1-2.42)}$$

Substituting this in above equation,

$$c = \left[\frac{gy_1}{2y_2} (y_1 + y_2) \right]^{\frac{1}{2}} + v_2$$

$$\frac{3.67}{(y_1 - 2.42)} = \left[\frac{gy_1}{2 \times 2.42} (y_1 + 2.42) \right]^{\frac{1}{2}} + 1.24$$

By trial and error,

$$y_1 = 2.95 \text{ m}$$

$$c = \frac{3.67}{(2.95 - 2.42)} = 6.92 \text{ m/s}$$

4. Conclusion & Recommendation

The application of the surge waves in the design of canals, especially for the hydropower & irrigation projects these principals play a vital role for the optimum design of the canals. The design depth of the flow in the canals during the surges must be able to accommodate the required amount of discharges accumulated during the propagation of the surges in downstream or upstream of the canals. Therefore, it is recommended to keep the sufficient amount of free board in the canals to accommodate the additional height of the surges in addition to the normal depth of the canal flow.

References

1. H.W. King, C.O. Wisler, J. G. Woodburn, "*Hydraulics*" John Wiley and Sons, Inc. New York 1948 (Fifth Edition)
2. Victor L. Streeter, E. Benjamin Wylie, "*Fluid Mechanics*", McGraw-Hill Kogakusha, Ltd. 1975, Japan. (Sixth Edition)
3. Ven Te Chow, "*Open Channels Hydraulics*", McGraw Hill Publishers, 1988

A One- Dimensional Bio-Heat Transfer Equation with Galerkin FEM in Cylindrical Living Tissue

Hem Raj Pandey

Faculty of Science and Technology, School of Engineering,

Pokhara University, Nepal

Email Address: rajhem2040@gmail.com

Abstract

A one-dimensional steady state bio-heat transfer model of temperature distribution in cylindrical living tissue is discussed using numerical approximation technique the Galerkin Finite element method.

we observe the effects of the thermal conductivity of the thermal system. The results show that the derived solution is useful to easily and accurately study the thermal behavior of the biological system, and can be extended to such applications as parameter measurement, temperature field reconstruction and clinical treatment.

Keywords: Pennes' Bio-heat transfer equation, Galerkin Finite Element Method.

1. Introduction

The normal body core temperature is 37°C. This body temperature is the result of equilibrium between heat production and heat loss. If the body temperature stretches so far from normal temperature, death will occur. The temperature nearly 27°C and below and nearly 42°C and above are critical, so the temperature of body should be maintained around 37°C. The maintenance of body temperature is a dynamic system. If heat is greater than heat production then the body core temperature drops. Likewise if heat loss is less than heat production then the core temperature rises. So, the rise or drop in core temperature is equally dangerous, so body temperatures are kept constant[1,3,4,5].

In this paper, we study the effect of thermal parameters of dermal part in cylindrical living tissue. The linear function is considered. The outer surface of the body is exposed to the environment and the loss of heat from the skin surface is assumed due to convection and radiation. Here, we neglected the axial and angular direction and considered only the radial direction steady state model. The numerical result(Finite Galerkin Finite Element Method[8]) obtained is exhibited graphically by applying the suitable values of physical and physiological parameters.

2. Model Formulation

Mathematical model used for bio-heat transfer is based on Pennes' equation[7]. The Pennes' model is preferable for the study of heat transfer between blood and tissue which also associates the effect of metabolism and blood perfusion. The Pennes' equation is written as;

$$\rho c \frac{\partial T}{\partial t} = \nabla \cdot (K \nabla T) + \rho_b w_b c_b (T_a - T) + q_m \quad (1)$$

where, T ($^{\circ}\text{C}$) denotes the temperature of tissue element at any time t at a distance of x measured perpendicularly into the tissue element from the skin surface, and ρ, c, k are the density (Kg/m^3), the specific heat ($\text{J}/\text{Kg}\cdot^{\circ}\text{C}$) and the thermal conductivity of tissue ($\text{W}/\text{m}\cdot^{\circ}\text{C}$) respectively. w_b is the blood perfusion rate per unit volume ($\text{Kg}/\text{s}\cdot\text{m}^3$), c_b is the specific heat of blood (Kg/m^3), q_m is the metabolic heat generation per unit volume (W/m^3), T_a represents the temperature of arterial blood ($^{\circ}\text{C}$) and T is the tissue temperature ($^{\circ}\text{C}$).

The equation (1) in the cylindrical coordinate system is

$$\rho c \frac{\partial T}{\partial t} = \frac{1}{r} \frac{\partial}{\partial r} \left(Kr \frac{\partial T}{\partial r} \right) + \frac{1}{r^2} \frac{\partial}{\partial \theta} \left(K \frac{\partial T}{\partial \theta} \right) + \frac{1}{r} \frac{\partial}{\partial z} \left(K \frac{\partial T}{\partial z} \right) + M(T_a - T) + q_m \quad (2)$$

The one dimensional steady state bio heat equation of cylindrical living tissue reduces to

$$\frac{1}{r} \frac{d}{dr} \left(Kr \frac{dT}{dr} \right) + M(T_a - T) + q_m = 0 \quad (3)$$

where boundary conditions are:

$$r=0, \quad \frac{dT}{dr} = 0$$

and

$$r = R, \quad -K \frac{\partial T}{\partial r} = h_A (T - T_{\infty})$$

where R is the radius of concerned tissue, h_A is the coefficient of heat transfer,

and T_{∞} is ambient temperature.

3 . Galerkin Finite Element Method

The Finite Element Method is a powerful numerical technique for solving the algebraic, differential, and integral equations. The finite element method provides an approximate solution. The domain of the physical problem is discretized into the finite elements. The elements are connected at points called nodes. The assemblage of elements is called finite element mesh.

Several approaches can be used to transform the physical formulation of the problem to its finite element discrete analogue. Mostly, we have Galerkin weighted residue method and variational method. There may be other ways to apply the Galerkin method, and these would not necessarily be the same as a variational method. The variational method cannot always be applied because there may be no variational principle for the problem, but the Galerkin method is always applicable because it does not depend on the existence of a variational principle.

In Galerkin approach we have the strong and weak formulation. Strong Form is the set of governing partial and ordinary differential equation with boundary condition's are the strong form. The strong solution must satisfies the differential equation and boundary conditions exactly and must be as smooth (number of continuous derivatives) as required by the differential equation. If the system under analysis consists of varying geometry or material properties, then discontinuous functions will enter into the equations of motion and the issue of differentiability can become immediately apparent. To avoid such difficulties, we can change the strong form of the governing dynamics into a weak or weighted-integral formulation. Weak form is a variational statement of the problem in which we integrate against a test (weight) function. [8]

Using weak Formulation of Galerkin Finite Element Methods(FEM)[8] with $r_a = 0$ and $r_b = R$ in the equation (3), we get

$$\int_{r_a}^{r_b} w \left[\frac{1}{r} \frac{d}{dr} \left(kr \frac{dT}{dr} \right) + M(T_a - T) + q_m \right] dr = 0 \quad (4)$$

putting $\mathbf{a} = k\mathbf{r}$ and Integrating equation (10) we get

$$\int_{r_a}^{r_b} \left[w \frac{d}{dr} \left(a \frac{dT}{dr} \right) + Mwr(T_a - T) + q_m wr \right] dr = 0 \quad (5)$$

After simplified and using the trial function into equation(11) we get

$$[K^e] \{T^e\} = \{f^e\} + \{Q^e\} \quad (6)$$

where, $K_{ij}^e = \int_{r_a}^{r_b} \left[a \frac{d\psi_i^e}{dr} \frac{d\psi_j^e}{dr} - M\psi_i^e \psi_j^e r \right] dr$, $f_i^e = \int \psi_i^e f r dr$, $f = MT_a + q_m$

Let the linear function be $\psi_1^e = \frac{r_b - r}{h_e}$ and $\psi_2^e = \frac{r - r_a}{h_e}$. Using explicit form $a = a_e r$, $f = f_e$

and $r = r_a + \bar{r}$. Thus we get

$$K_{11}^e = \frac{a_e}{h_e} \left(r_a + \frac{h_e}{2} \right) + \frac{Mh_e}{12} (4r_a + h_e), \quad K_{12}^e = -\frac{a_e}{h_e} \left(r_a + \frac{h_e}{2} \right) + \frac{Mh_e}{12} (2r_a + h_e)$$

$$K_{12}^e = K_{21}^e, \quad K_{22}^e = \frac{a_e}{h_e} \left(r_a + \frac{h_e}{2} \right) + \frac{Mh_e}{12} (4r_a + 3h_e), \quad f_1^e = \frac{f_e h_e}{6} (3r_a + h_e), \quad f_2^e = \frac{f_e h_e}{6} (3r_a + 2h_e)$$

Thus, $[K^e] = \frac{a_e}{h_e} \left(r_a + \frac{h_e}{2} \right) \begin{bmatrix} 1 & -1 \\ -1 & 1 \end{bmatrix} + \frac{Mh_e}{12} \begin{bmatrix} 4r_a + h_e & 2r_a + h_e \\ 2r_a + h_e & 4r_a + 3h_e \end{bmatrix}$ and $\{f^e\} = \frac{f_e h_e}{6} \begin{bmatrix} 3r_a + h_e \\ 3r_a + 2h_e \end{bmatrix}$ (7)

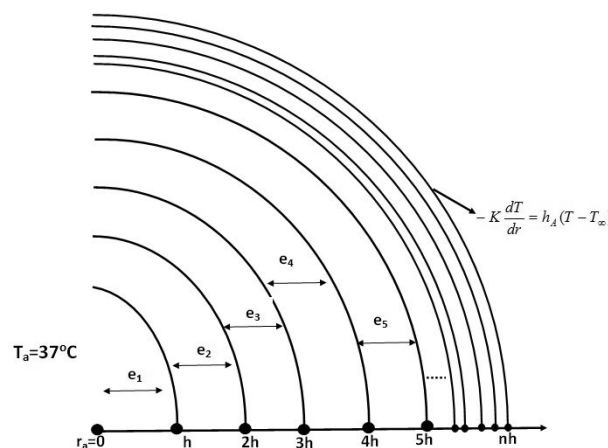


Fig 1 Finite Element Discretisation Mesh.

From the equation(7) we find the element at $r_a = 0, h, 2h, \dots, nh$ and assembling the elements in the

matrix form; $PX=Q$ (8) where, $P = \begin{bmatrix} a & c & 0 & \dots & 0 \\ c & 4b & 3c & \dots & 0 \\ 0 & 3c & 8b & 5c & 0 \\ 0 & 0 & \vdots & \ddots & \vdots \\ 0 & 0 & 0 & \dots & p \end{bmatrix}$, $X = \begin{bmatrix} T_1 \\ T_2 \\ T_3 \\ \vdots \\ T_n \end{bmatrix}$ and $Q = N \begin{bmatrix} 1 \\ 6 \\ 12 \\ \vdots \\ v_1 \end{bmatrix} + \begin{bmatrix} Q_1^1 \\ Q_1^2 + Q_2^1 \\ Q_1^3 + Q_2^2 \\ \vdots \\ Q_2^n \end{bmatrix}$

and $a = \frac{6K + Mh^2}{12}$, $b = \frac{6K + 2Mh^2}{12}$, $c = \frac{-6K + Mh^2}{12}$, $p = 6K(2n-1) + ((4n-1)Mh^2)$, $N = \frac{fh^2}{6}$, $v_1 = (3n-1)$

For the boundary condition of extreme points of each linear element

$P = \begin{bmatrix} a & c & 0 & \dots & 0 \\ c & 4b & 3c & \dots & 0 \\ 0 & 3c & 8b & 5c & 0 \\ 0 & 0 & \vdots & \ddots & \vdots \\ 0 & 0 & 0 & \dots & \alpha \end{bmatrix}$, $X = \begin{bmatrix} T_1 \\ T_2 \\ T_3 \\ \vdots \\ T_n \end{bmatrix}$ and $Q = N \begin{bmatrix} 1 \\ 6 \\ 12 \\ \vdots \\ v_1 \end{bmatrix} + \begin{bmatrix} 0 \\ 0 \\ 0 \\ \vdots \\ \beta \end{bmatrix}$

where, $\alpha = p + Rh_A T_{n+1}$, $\beta = Rh_A T_\infty$.

4. Numerical Results and Discussion

This section discusses the effects of thermal conductivity in living tissue using the Galerkin Finite element solution equation. These numerical results of these effects based on the discussed solution techniques, we consider the following parameter values[9] with normal ambient temperature(T_∞) 25^0C and number of nodes 30.

Table 1 Values of Parameters for Theoretical Analysis.

w_b Kg /s.m ³	c_b J/Kg. ⁰ C	K W/ m. ⁰ C	h_A W/ m ² . ⁰ C	q_m W/m ³	T_a ⁰ C	R m
3	3850	0.48	10.023	1085	37	0.0285

Effects of the Thermal Conductivity

The various value of thermal conductivity of dermal part are taken as 0.24 W/m^0C , 0.48 W/m^0C and 0.72 W/m^0C for the observation of the thermal conductivity effects in living tissue. Figure(1) represent the graph of thickness verses body temperature obtained by using FEM solution.

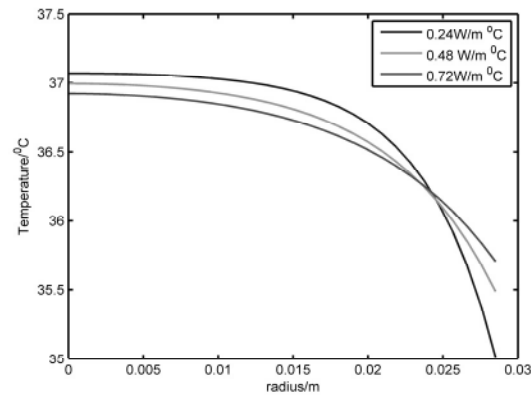


Fig 2 Effects of the Thermal Conductivity.

The observed results in Figure shows that the temperature distribution in living tissue is decreasing smoothly and then temperature falls sharply nearly the skin surface due to the conduction process at the outer surface of the living tissue. The value of temperature at any point of dermal part near core at high thermal conductivity is less than the temperature at low thermal conductivity. The results obtained from Figure exhibit approximately the same value of temperature distribution at a given thickness of dermal part measured from the body core.

5. Conclusion

In this study we use the different thermal parameters with their different values of thermal conductivity of the dermal part of living tissue. The effects of different thermal parameters are discussed by using Galerkins FEM solution method in the cylindrical bio-heat equation. The effects of thermal conductivities have the significant and more remarkable effects in temperature variation in living tissue.

The solution obtained can be used for the measurement of thermal parameters, reconstruction of the temperature field and thermal diagnosis and in the treatment that maximizes the therapeutic effect while minimizing unwanted side effect. It may also be useful to design medical devices to perform within a special range of temperature rate of heating and cooling.

References

1. S. Acharya and D. B. Gurung, “*Five Layered Temperature Distribution in Human Dermal Part*”, Nepali Mathematical Sciences Report 31, (2011) , no. 1–2, pp. 15–28.
2. T. E. Cooper and G. J. Trezek, “*A Probe Technique for Determining the Thermal Conductivity of Tissue*”, J. Heat transfer, ASME, 94(1972)133.
3. D. B. Gurung, “*Mathematical Study of Abnormal Thermoregulation in Human Dermal Parts*”, Ph. D. Thesis, (2007).
4. D. B. Gurung ,V. P. Saxena, and P. R. Adhikari , “*Finite Element Approach to One Dimensional Unsteady State Temperature Distribution in the Dermal Parts with Quadratic Shape Function*”, J. Appl. Math & Information, (2009), 27, pp. 301–313.
5. C. Guyton and E. Hall , “*Text Book of Medical Physiology*”, Elsevier, India, (2009).
6. M. N. Ozisik, “*Heat conduction*”, John Wiley & Sons Inc., Second Edition (1993), pp. 436–495.
7. H. H. Pennes , “*Analysis of Tissue and Arterial Blood Temperature in Resting Human Forearm*”, A Journal of Applied Physiology, (1948), 1(2), pp. 657–678.
8. J. N. Reddy, “*An Introduction to Finite Element Method*”, McGraw Hill Publishing Company Limited, Third Edition , (2006), pp. 1–180.
9. K. Y. X. Zhang and F. Yu, “*An Analytic Solution of One-Dimensional Steady-State Pennes Bioheats Transfer Equation in Cylindrical Coordinates*”, Journal of thermal Science, (2004), 13(3), pp. 255–258.

FUZZY CLUSTERING BASED BLIND ADAPTIVE OFDM SYSTEM

Krishna Sundar Twayana¹, Shashidhar Ram Joshi²¹Department of Electronics and Computer Engineering, Advanced College of Engineering & Management, Kopundole, NepalEmail Address: krishna.twayana@acem.edu.np²Department of Electronics and Computer Engineering Institute of Engineering, Pulchowk CampusEmail Address: sashi@healthnet.org.np**Abstract**

This paper present blind adaptive modulation for OFDM system. Automatic recognition of the modulation level of detected signal and blind estimation of SNR is a major task of an intelligent receiver presented here. In this paper, modulation classification is performed by fuzzy c-means clustering followed by new approach of modulation classification, fuzzy template matching considering the constellation of the received signal. In addition, SNR estimation and modulation order for the next transmission is carry out by Fuzzy Logic Interface based upon heuristics. The simulation that has been conducted shows high capability of recognition of modulation level, almost perfect estimation of SNR and adaptive with considerable BER in an Additive White Gaussian Noise channel. The performance of proposed system is simulated in computer simulation tool, MATLAB 7.0.

Keywords: *Adaptive modulation, SNR estimation, Fuzzy c-means clustering, Fuzzy template matching.*

1 Introduction

Adaptive transmission is real-time balancing of the link budget through adaptive variation of the transmitted power level, symbol transmission rate, constellation size, coding scheme, or combination of these parameters without sacrificing the BER. These schemes provide a higher average link spectral efficiency, which require channel estimation at the receiver.

In modern wireless digital communication, the precise knowledge of SNR is important. Many algorithms require the knowledge of SNR for their optimal performance. In data-aided (DA) SNR estimation also known as pilot symbol assisted modulation (PSAM), SNR of the signal through rapid fading environment is detected by periodically inserting known symbols [1], from which the receiver derives its amplitude and phase reference. However, the training sequence limits system throughput rate. Where as in non-data aided (NDA) SNR estimation system [2, 3], instantaneous SNR is compute from the received signal and the receiver feedback appropriate transmission parameter to adapt into future channel conditions.

Clustering algorithms have been studied for a long time, and are used nowadays for a large number of applications. They are successfully in use in systems for information access, data mining or computer vision. Different algorithms have been developed using different approaches

and considering different underlying assumptions on the data and on the final set of clusters. Fuzzy clustering [4, 5] is one of the well known robust and efficient approach to reduce computation cost to obtain the better results. Fuzzy clustering can obtain not only the belonging status of objects but also how much the objects belong to the clusters. The boundaries between clusters could not be defined precisely, some of the data could belong to more than one cluster with different positive degrees of memberships. This clustering method considers each cluster as a fuzzy set and the membership function measures the degree of belonging of each feature in a cluster. So, each feature may be assigned to multiple clusters with some degree of belonging. The aim of modulation classification (MC) [4, 5, 6, 7] is to identify the modulation type of a communication signal. This is a challenging problem, especially in non-cooperative environments, where no prior knowledge on the incoming signal is available.

2 Methodology

2.1 Complete System

The proposed system as shown in Fig 1, is based on a statistical ratio of observables over a block of data. Average deviation, which has direct impact on bit error rate, determine the appropriate modulation order for the next transmission frame. Rules are defined in such a way that modulation order switch to new one based on bit error rate for particular modulation order at given SNR. The receiver feedback appropriate modulation level to the transmitter for subsequent data transmission through the channel.

The proposed technique has been designed so that it would be capable of recognizing the types: 4-QAM, 8-QAM, 16-QAM, 32-QAM, 64-QAM, 128-QAM and 256-QAM. In order to reduce complexity, all the received symbols have been mapped and 64 cluster center have been randomly initialized in the first quadrant. Fuzzy c-means clustering compute the centroids of a cluster as being the mean of all points weighted by their degree of belonging to the cluster iteratively until program reach some termination condition. Upon completion of the fuzzy algorithm centroids are obtained and then fuzzy template matching process is done for modulation classification. The automatic recognition of the modulation format of a detected signal is the intermediate step between signal detection and demodulation, which is a major task of an intelligent receiver.

2.2 Fuzzy Logic SNR and Modulation Estimation

The non data aided fuzzy logic SNR estimator and modulation order controller for QAM signals is derived base on a statistical ratio of observables over a block of data. The average deviation of real and imaginary components from its likelihood values and present modulation order obtained after modulation classification, Fuzzy Inference System (FIS) estimates the SNR value and best modulation order for next transmission frame to maintain BER below 10^{-3} from rules and membership functions defined for average deviation and present modulation order.

2.3 Fuzzy C-Means Clustering

Fuzzy c-means (FCM) is a method of clustering which allows one piece of data to belong to two or more clusters. This method is frequently used in pattern recognition. It is based on

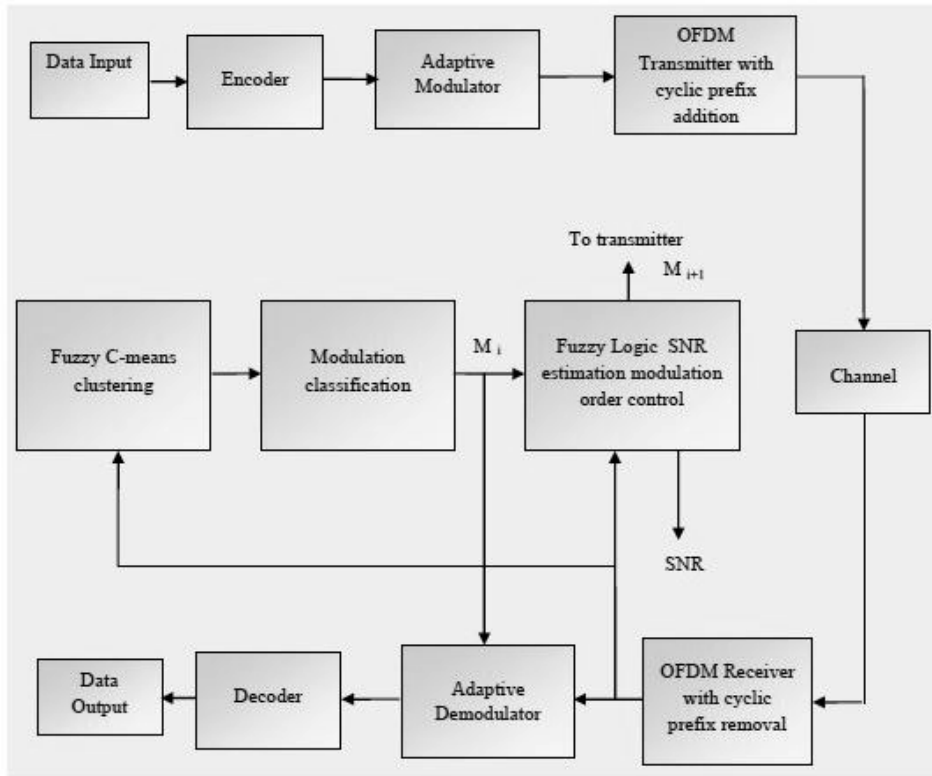


Fig 1: Complete Diagram of Proposed System

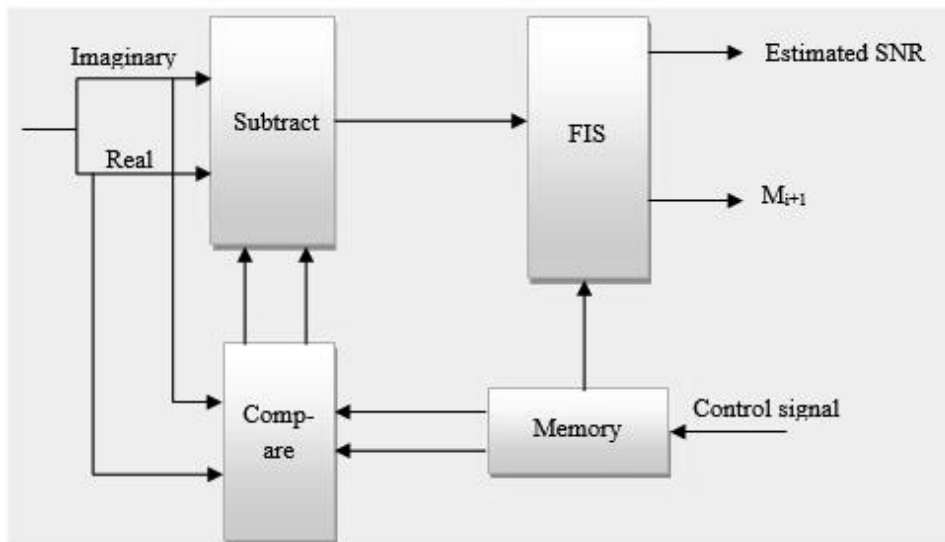


Fig 2: Fuzzy Logic SNR Estimation and Modulation Control

minimization of the following objective function:

$$J = \sum_{k=1}^N \sum_{i=1}^C \mu_{ik}^m \|x_k - c_i\|^2, \quad 1 \leq m < \infty \quad (1)$$

where m is any real number greater than 1, μ_{ik} is the degree of membership of x_k in the cluster c_i , x_k is the i^{th} of D-dimensional measured data, c_i is the D-dimension center of the cluster, and $\|*\|$ is any norm expressing the similarity between any measured data and the center. Fuzzy partitioning is carried out through an iterative optimization of the equation 1, with the update of membership μ_{ik} and the cluster centers c_i as steps shown below:

- i. Initialize $U = [\mu_{ik}]$ matrix, $U^{(0)}$
- ii. At j step: calculate the centers vectors $C^{(j)} = [c_i]$ with $U^{(j)}$

$$c_i = \frac{\sum_{k=1}^N \mu_{ik}^m * x_k}{\sum_{k=1}^N \mu_{ik}^m} \quad (2)$$

- iii. Update $U^{(j)}$, $U^{(j+1)}$:

$$\mu_{ik} = \frac{1}{\sum_{j=1}^c \left(\frac{\|x_k - c_i\|}{\|x_k - c_j\|} \right)^{\frac{2}{m-1}}} \quad (3)$$

- iv. Calculate $J^{(j)}$ from equation 1
- v. If $\|J^{(j)} - J^{(j-1)}\| < \varepsilon$ then STOP; otherwise return to step ii.

2.4 Fuzzy Template Matching

The main idea in this method is assessment of resulted cluster centers from fuzzy c-means clustering based on relative similarity that exist between different kind of standard QAM modulations with predefined levels. In the beginning for every kind of QAM modulation family, the ideal centriods in first quadrant have been defined. It must be mentioned that, since the value of the objective function decrease naturally as the number of clusters increases, which in turn causes an error in recognition of the actual number of cluster, the value of the objective function is multiplied by a weight proportional to the number of clusters to prevent producing error. After multiplication of the weights, the number of clusters corresponding to the cost function with minimum value is chosen as the final number of cluster. After the final clusters on the first quadrant are obtained, these clusters are extended to the whole constellation diagram.

Fuzzy Template Matching algorithm for modulation classification:

- i. Initialize ideal cluster centers for M-QAM C_j , $1 \leq j \leq \frac{M}{4}$
- ii. Calculate the Euclidean distance of the clusters pair-wise between C_j and cluster centers from fuzzy c-means clustering c_i , $1 \leq i \leq 64$

$$d_{ij} = \|c_i - C_j\| \quad (4)$$

iii. Compute membership values

$$\mu_{ji} = \frac{1}{\sum_{k=1}^C \left(\frac{\|c_i - C_j\|}{\|c_i - C_k\|} \right)^{\frac{2}{m-1}}} \quad (5)$$

iv. Evaluate cost function:

$$cost_fun = \min(d(i,:)) * \max(\mu(:,i)) * \frac{M}{4} \quad (6)$$

v. Repeat steps i to iv for all considered modulation order

vi. Select the modulation order corresponding to the minimum cost function

3 Result and Discussion

3.1 Overall Simulation Result

In order to evaluate the performance of the proposed system, simulation has been performed for various SNR values and different levels of QAM modulations on randomly generated binary data stream. Channel model apply for this system is assumed quasi-stationary AWGN channel, and it is assumed that there is no time and/or frequency synchronization error also. Fuzzy c-means clustering algorithm has been used for constellation recovery and modulation classification is performed to achieve the actual number of cluster centers. SNR estimation and change of modulation order are carried out by FIS. Simulation result in command window is shown in Fig 3.

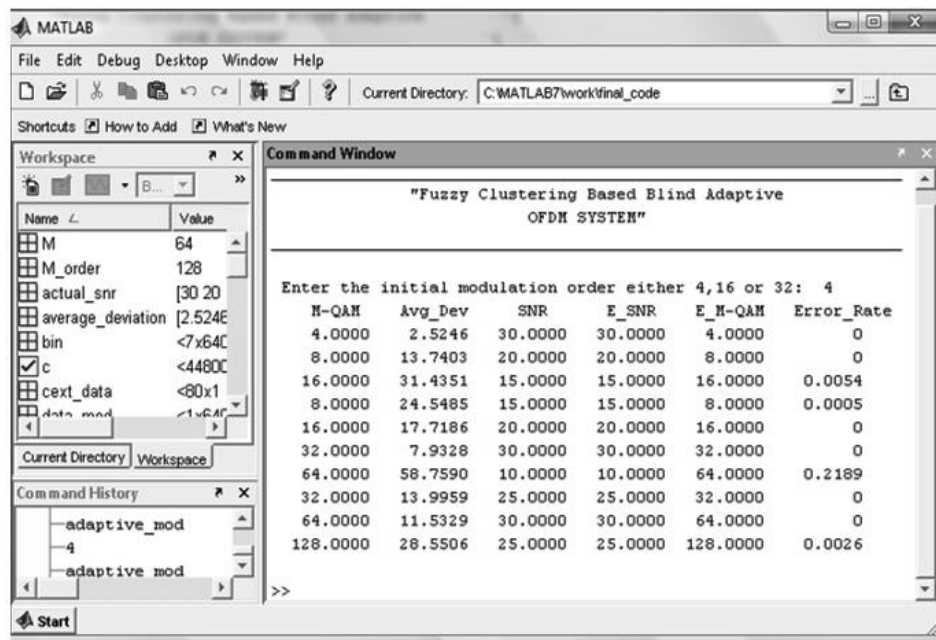


Fig 3: Overall Simulation Result

3.2 SNR Estimation

Non data aided SNR estimation implemented in this paper is based on average deviation of in-phase and quadrature component of received signal at given modulation level. Using fuzzy logic in decision making is a good choice because ordinary (non fuzzy) system is controlled by plain if and else statements, for example if estimated SNR = 10dB for average deviation in (26, 24) range is declared in the algorithm and if we get average deviation 26.1, using plain rule based system will yields an error whereas using fuzzy logic system will yield output SNR near to 10dB. So the estimated SNR by fuzzy logic is more likely to the actual SNR value in contrast to that by non fuzzy system as shown in Fig 4.

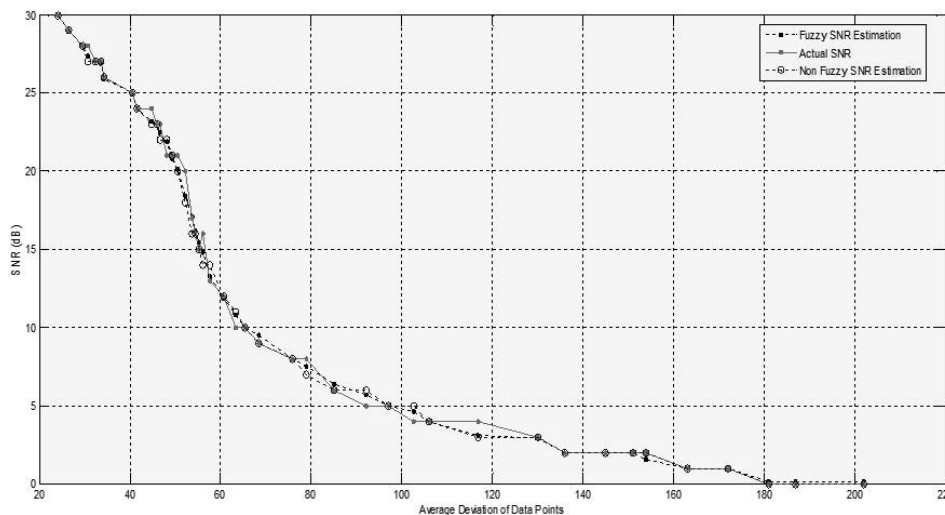


Fig 4: Comparison of Estimated SNR and Actual SNR

3.3 Modulation Classification

After the centroids are obtained from fuzzy c-means clustering, modulation type is recognized by evaluating the amount of matching with the standard templates of QAM modulation. Simulation result shows the proposed method have good recognition performance even in low SNR condition. The performance of the FCM algorithm depends on the selection of the initial cluster center and/or the initial membership value and fuzzifier m determines the level of cluster fuzziness. In this paper the initial number of clusters has been set to 64 in the first quadrant randomly and fuzzifier m is set to 2 for clustering. Fig 5 below shows simulation results of recognition of 16-QAM modulation levels with 5dB SNR value by taking 500 samples where captions are:

- a. Centroids in the first quadrant obtained from fuzzy clustering
- b. Values of the objective functions for possible clusters in first quadrant
- c. Centroids of the clusters in whole constellation diagram
- d. Extended clusters and their centroids in whole constellation diagram

The accuracy of recognition versus SNR ratio for different modulation types of QAM family is shown in Fig 6. This method can recognize all the 4-QAM modulations with 100% accuracy

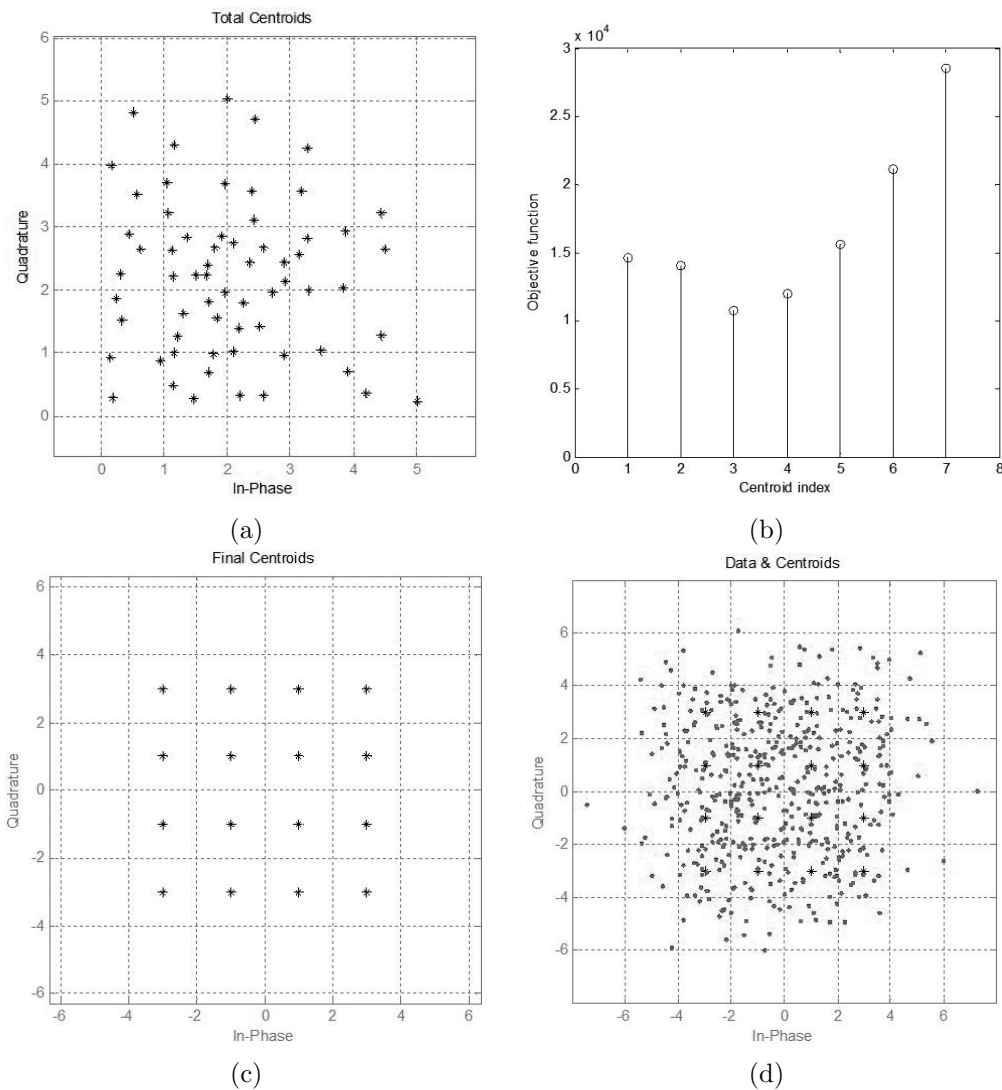


Fig 5: Recognition of 16-QAM with SNR=5dB

and its recognition truth does not depend on the signal to the noise, and it can also identify this modulation type with SNR=0dB. Similarly, this method can identify all the 16-QAM modulation with SNR=7dB with 100% accuracy. Nevertheless, accuracy of recognition of 64-QAM and 128-QAM for the SNR 10dB and higher than that is 100% and for a level lower than it is less. Accuracy of recognition of 256 QAM is better than other modulation levels except of 4 QAM.

4 Conclusion

The results of computer simulation shows that almost perfect SNR estimation and modulation recognition even in low SNR condition and system is adaptive with noise condition. In the new fuzzy template matching algorithm, there is no restriction on order of assessment to be started from highest level of 256 QAM and end at lowest level 4 QAM as in normal template matching. This approach could be extended and modified to recognize other types of digital modulations in different fading channels.

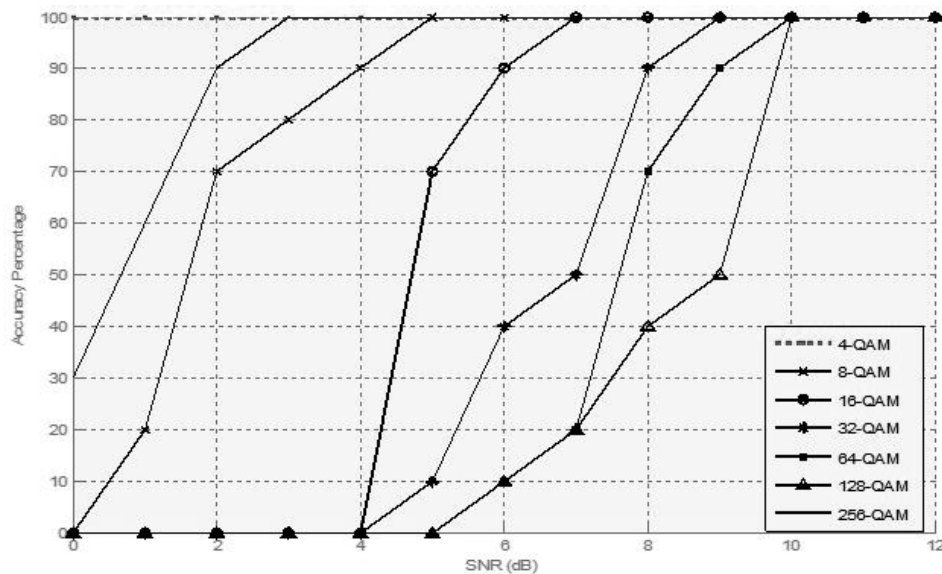


Fig 6: Accuracy of QAM Modulation Recognition Versus SNR

References

- [1] K.Seshadri Sastry, Dr. M.S.Prasad Babu, "Adaptive Modulation for OFDM system using Fuzzy logic interface." *IEEE Conference proceedings, IEEE International Conference in Software Engineering and Service Sciences*, Beijing , China.
- [2] K.Seshadri Sastry, Dr. M.S.Prasad Babu, "SNR Estimation For QAM signals Using Fuzzy Logic Interface." *IEEE Conference proceedings, IEEE International Conference in Computer Science and Information technology*, Chengdu , China.
- [3] K.Seshadri Sastry , Dr. M.S.Prasad Babu, "Fuzzy logic based Adaptive Modulation Using Non Data Aided SNR Estimation for OFDM system," *International Journal of Engineering Science and Technology*, vol. 2(6), pp. 2384–2392, 2010.
- [4] Bijan G Mobaseri, "Constellation shape as a robust signature for digital modulation recognition," *Military Communications Conference Proceedings, MILCOM IEEE*, 1:442-446, 1999.
- [5] Bijan G Mobaseri, "Digital Modulation Classification using Constellation Shape," *signal processing*, 1:442-446, 1999.
- [6] Negar Ahmadi, Reza Berangi, "A Template Matching Approach to Classification of QAM Modulation using Genetic Algorithm," *Signal Processing: An International Journal*, vol. 3 Issue 5, pp. 95–109, 2009.
- [7] Negar Ahmadi, Reza Berangi, "Symbol Based Modulation Classification using Combination of Fuzzy Clustering and Hierarchical Clustering," *Signal Processing: An International Journal*, vol. 4, Issue 5, pp. 95–109, 2010.

SOME CLASSICAL SEQUENCE SPACES AND THEIR TOPOLOGICAL STRUCTURES

Narayan Prasad Pahari

Central Department of Mathematics, Tribhuvan University,

University Campus, Kirtipur, Kathmandu, Nepal

Email Address: nppahari@gmail.com

Abstract

The aim of this paper is to study some of the basic scalar and vector valued sequence spaces. We also study the topological structures of some of the basic sequence spaces when topologized through a norm or a paranorm.

Keywords: Function Space, Sequence Space, Paranormed Space, Orlicz Sequence Space.

2010 AMS Subject Classification: Primary - 46A45, Secondary - 46B 15.

1. Introduction

Functional Analysis is an abstract branch of Mathematics, that deals with the study of linear spaces endowed with some kinds of limit-related structures like topology, norm, inner product etc. and the operators or functions acting upon these spaces. By a function space we mean a linear space of functions defined on a certain set with respect to pointwise addition and scalar multiplication.

The study of sequence spaces is in fact a special case of the more general study of function spaces if the domain is restricted to the set of natural numbers \mathbf{N} . The set ω of all functions from the natural numbers \mathbf{N} to the field \mathbf{K} of real \mathbf{R} or complex numbers \mathbf{C} , can be turned into a vector space. In other words, let ω be the set of all (real-or) complex valued sequences $\{x_n\}_{n \in \mathbf{N}}$. i.e., $x_n \in \mathbf{C}$ under the operations of point wise addition and scalar multiplication given by

$$\{x_n\}_{n \in \mathbf{N}} + \{y_n\}_{n \in \mathbf{N}} = \{x_n + y_n\}_{n \in \mathbf{N}}$$

$$\text{and } \lambda \{x_n\}_{n \in \mathbf{N}} = \{\lambda x_n\}_{n \in \mathbf{N}},$$

for every $x_n, y_n \in \mathbf{C}$ and scalar λ , form a vector space over \mathbf{C} . Any subspace X of ω is then called a **sequence space**. In other words, a sequence space is a vector space whose elements are **infinite scalar** sequences of real or complex numbers and is closed under the coordinatewise addition and scalar multiplication. If it is closed under coordinate wise multiplication as well, it is called a **sequence algebra**. Sequence spaces when equipped with a linear topology form **topological vector spaces**.

Several workers like Kamthan and Gupta (1980), Maddox (1980), Ruckle (1981), Malkowski and Rakocevic (2004) etc. have made their significant contributions in developing the theory of vector and scalar valued sequence spaces in various directions, when sequences are taken from a Banach space or from a locally convex space. Literatures concerning the theory of sequence space can be

found in any standard text books and monographs of Functional Analysis, for instance we refer a few; Lindenstrauss and Tzafriri (1977), Wilansky(1978), Kamthan and Gupta (1980), Rao and Ren (1991) etc.

2. Topological Structures of Some Basic Sequence Spaces

We shall study the topological structures of sequence spaces when topologized through a norm or through a paranorm generalize and unify various existing sequence spaces. The concept of paranorm is closely related to linear metric spaces. It is a generalization of that of absolute value of real numbers or modulus of a complex number.

A paranormed space (X, G) is a linear space X together with a function $G : X \rightarrow \mathbf{R}_+$ (called a paranorm on X) which satisfies the following axioms:

$$PN1: G(\theta) = 0;$$

$$PN2: G(x) = G(-x) \text{ for all } x \in X;$$

$$PN3: G(x + y) \leq G(x) + G(y) \text{ for all } x, y \in X; \text{ and}$$

$$PN4: \text{ if } (\alpha_n) \text{ be a sequence of scalars with } \alpha_n \rightarrow \alpha \text{ as } n \rightarrow \infty \text{ and } (x_n) \text{ be a sequence in } X \text{ with } G(x_n - x) \rightarrow 0 \text{ as } n \rightarrow \infty, \text{ then } G(\alpha_n x_n - \alpha x) \rightarrow 0 \text{ as } n \rightarrow \infty \text{ (continuity of scalar multiplication).}$$

A paranormed space (X, G) is said to be *complete* if (X, d) is complete with metric

$$d(x, y) = G(x - y).$$

Every paranormed space becomes a linear pseudometric space with $d(x, y) = G(x - y)$ which is translation invariant. Thus each paranormed space is a topological linear space. Moreover a pseudometric linear space must be a paranormed space, i.e., a paranorm can be defined on the space which induces an equivalent pseudometric.

The studies on paranormed sequence spaces were initiated by Nakano and Simons at the initial stage. Later on it was further studied by Maddox [1969] and many others. Bhardwaj and Bala [2007], Khan [2008], and many others studied paranormed sequence spaces using Orlicz function.

We shall discuss the topological structures of some of the important classes of the basic sequence spaces when topologized through a norm or through a paranorm, which in fact, generalize and unify various existing sequence spaces. Among them, sequence spaces $c_0(p)$, $c(p)$, $\ell_\infty(p)$ appear in the work of Lascarides and Maddox (1971) and others while $c_0(X)$, $c(X)$, $\ell_\infty(X)$, $\ell_p(X)$ are used by Leonard (1976), Maddox (1980) and others. Let $x = (x_k) = (x_k)_{k=1}^\infty$ be the sequences and ω denote the class of all sequences $x = (x_k)$, $k \geq 1$, over the field \mathbf{C} of complex numbers. Let $p = (p_k)$ be any sequence of strictly positive real numbers (bounded in general) and $\lambda = (\lambda_k)$ be any sequence of non zero complex numbers. Here we deal with the topological structures of the following sequence spaces.

A. The spaces $c(p)$, $c_0(p)$, c and c_0 .

With $\{p_k\}$ as above, define

$$c_0(p) = \{x = \{x_k\}: |x_k|^{p_k} \rightarrow 0 \text{ as } k \rightarrow \infty\}; \text{ and}$$

$$c(p) = \{x = \{x_k\}: |x_k - l|^{p_k} \rightarrow 0 \text{ as } k \rightarrow \infty \text{ for some } l \in \mathbb{C}\}.$$

$c(p)$ and $c_0(p)$ form metric spaces with the metric

$$d(x, y) = \sup_k |x_k - y_k|^{p_k/M}, \text{ where } M = \max \{1, \sup p_k\}.$$

Note that the set $c(p)$ and $c_0(p)$ are complete with its metric topology. But it is not normed space. In fact, the set $c(p)$ forms a paranormed space with paranorm

$$\|x\| = \sup_k |x_k|^{p_k/M} \text{ if and only if } \inf p_k > 0.$$

The set $c_0(p)$ is a linear metric space paranormed by

$$\|x\| = \sup_k |x_k|^{p_k/M}, \text{ where } M = \max \{1, \sup p_k\}.$$

If $p_k = p$ for all k , then we write c and c_0 for $c(p)$ and $c_0(p)$ respectively. c and c_0 are respectively the sets of all convergent sequences and null sequences. Note that c and c_0 are metric spaces as well as Banach spaces with the metric and norm respectively given by

$$d(x, y) = \sup_k |x_k - y_k| \text{ and } \|x\| = \sup_k |x_k|.$$

B. The spaces $l_\infty(p)$ and l_∞ .

Let $\{p_k\}$ be as in the above. We define

$$l_\infty(p) = \{x = \{x_k\}: \sup_k |x_k|^{p_k} < \infty\}.$$

Note that $l_\infty(p)$ is complete metric space with its metric topology with the metric

$$d(x, y) = \sup_k |x_k - y_k|^{p_k/M}, \text{ where } M = \max \{1, \sup p_k\}.$$

But it is not normed space. In fact, the set $l_\infty(p)$ is paranormed space with paranorm

$$\|x\| = \sup |x_k|^{p_k/M} \text{ if and only if } \inf p_k > 0.$$

If $p_k = p$ for all k , then we write l_∞ for $l_\infty(p)$. l_∞ is the set of all bounded sequences $x = \{x_k\}$ of real (or complex) numbers and forms a metric space and Banach space with the natural metric and norm respectively given by

$$d(x, y) = \sup_k |x_k - y_k| \text{ and } \|x\| = \sup_k |x_k|.$$

C. The spaces $l(p)$ and l_p .

Since $\{p_k\}$ be a bounded sequence of strictly positive real numbers, so that $0 < p_k \leq \sup p_k < \infty$. We define

$$l(p) = \{x = \{x_k\}: \sum_{k=1}^{\infty} |x_k|^{p_k} < \infty\}.$$

Then, $l(p)$ becomes a metric space with metric

$$d(x, y) = \left(\sum_{k=1}^{\infty} |x_k - y_k|^{p_k} \right)^{1/M}, \text{ where } M = \max \{1, \sup p_k\}.$$

The space $l(p)$ is complete metric space in its metric topology but it is not a normed space.

If fact, the set $l(p)$ is paranormed by

$$\|x\| = \left(\sum_{k=1}^{\infty} |x_k|^{p_k} \right)^{1/M}.$$

In particular, if $p_k = p$ for all k , then we write l_p for $l(p)$, which consists of the p -power summable sequences with p -norm.

Observe that if $1 \leq p < \infty$, l_p forms a metric space and Banach space with the metric and norm respectively given by

$$d(x, y) = \left(\sum_{k=1}^{\infty} |x_k - y_k|^p \right)^{1/p} \text{ and } \|x\| = \left(\sum_{k=1}^{\infty} |x_k|^p \right)^{1/p}.$$

Similarly for $0 < p < 1$, l_p forms a metric space and complete p -normed space with the metric and p -norm respectively given by

$$d(x, y) = \sum_{k=1}^{\infty} |x_k - y_k|^p \text{ and } \|x\| = \sum_{k=1}^{\infty} |x_k|^p.$$

D. Orlicz Sequence Space ℓ_{Φ}

The study of Orlicz sequence spaces was initiated to study Banach space theory. An *Orlicz function* is a function $\Phi : [0, \infty) \rightarrow [0, \infty)$ which is continuous, non decreasing and convex with

$$\Phi(0) = 0, \Phi(u) > 0 \text{ for } u > 0, \text{ and } \Phi(u) \rightarrow \infty \text{ as } u \rightarrow \infty.$$

Lindenstrauss and Tzafriri (1977) used Orlicz function to construct the sequence space

$$\ell_{\Phi} = \left\{ x = (x_k) \in \omega : \sum_{k=1}^{\infty} \Phi\left(\frac{|x_k|}{\rho}\right) < \infty \text{ for some } \rho > 0 \right\}$$

of scalars, which forms a Banach space with Luxemburg norm defined by

$$\|x\|_{\Phi} = \inf \left\{ \rho > 0 : \sum_{k=1}^{\infty} \Phi\left(\frac{|x_k|}{\rho}\right) \leq 1 \right\}.$$

The space ℓ_{Φ} is called an Orlicz sequence space and is closely related to the space ℓ_p with

$\Phi(x) = x^p, (1 \leq p < \infty)$. They have very rich topological and geometrical properties that do not occur in ordinary ℓ_p spaces.

Bhardwaj and Bala (2007), Khan (2008), Kolk (2011), Pahari and Srivastava (2011),(2012), and many others, have been introduced and studied various sequence spaces using Orlicz function as a generalization of well known sequence spaces.

E. Other Sequence Spaces

We shall denote e and $e^{(n)}$ ($n = 1, 2, \dots$) for the sequences such that $e_k = 1$ for $k = 1, 2, \dots$ and

$$e_k^{(n)} = \begin{cases} 1, & (\text{for } k = n) \\ 0, & (\text{for } k \neq n). \end{cases}$$

Let m be any nonnegative integer, we denote the m -section of a sequence $x = \{x_k\}$ by $x^{[m]}$, i.e.

$$x^{[m]} = \sum_{k=1}^{\infty} x_k e^{(k)}.$$

Further CS , l_1 and BS denote for the sets of all convergent, absolutely convergent and bounded series as described below:

The space of bounded series BS is the space of sequences X for which $\sup_n \left| \sum_{k=1}^n x_k \right| < \infty$.

The space BS , when equipped with the norm

$$\|x\|_{BS} = \sup_n \left| \sum_{k=1}^n x_k \right|,$$

forms a Banach space isometrically isomorphic to l^∞ , via the linear mapping

$$(x_n)_{n \in N} \rightarrow \left(\sum_{k=1}^n x_k \right)_{n \in N}.$$

A sequence space X with a linear topology is called a **K-space** provided each of the maps $p_k : X \rightarrow \mathbb{C}$ defined by $p_k(x) = x_k$, $x \in X$ is continuous for all $k = 1, 2, \dots$

A K -space X is called an **FK-space** provided X is a complete linear metric space. A normed FK space is called a **BK-space**.

Further, l_1 is a BK space with respect to the norm

$$\|x\|_1 = \sum_{k=1}^{\infty} |x_k|,$$

c_0 , c and l_∞ are BK spaces with respect to the norm

$$\|x\|_\infty = \sup_k |x_k|,$$

and cs is a BK space with respect to the norm

$$\|x\|_{cs} = \sup_n \left| \sum_{k=1}^n x_k \right|, \text{ see, Malkowski (1999).}$$

A *FK* space $X \supset \phi$ is said to have **AK-space** if every sequence $x = \{x_k\}_{k=1}^{\infty}$ in X has a unique representation of the form $x = \sum_{k=1}^{\infty} x_k e^{(k)}$, i.e. $x^{[m]} \rightarrow x$ (as $m \rightarrow \infty$). For examples, the spaces l_1, c_0 and *CS* form *AK* spaces.

A sequence $(x^{(k)})_{k=1}^{\infty}$ in a linear metric space X is called a **Schauder basis** (see, Malkowski ,1999), if for every $x \in X$ there exists a uniquely determined sequence $\{\lambda_k\}_{k=1}^{\infty}$ of scalars such that

$$x = \sum_{k=1}^{\infty} \lambda_k x^{(k)}.$$

A complex sequence $\{x_k\}$ is called an **analytic sequence** if the sequence $\{|x_k|^{1/k}\}$ is bounded and an **entire sequence** if $|x_k|^{1/k} \rightarrow 0$ as $k \rightarrow \infty$. The set of all analytic and entire sequences are respectively denoted by \mathfrak{a} and Γ , see Rao (1999).

3. Conclusion

In this paper, we have characterized the topological structures of some of the basic scalar and vector valued sequence spaces. In fact, these structures can also be used to explore further properties of the generalized sequence spaces by topologizing through a norm or a paranorm.

References

1. V. N. Bhardwaj, and I. Bala, “Banach space valued sequence space $\ell_M(X,p)$ ”, *Int. J. of Pure and Appl. Maths*, 41(5),617–626, 2007.
2. P. K. Kamthan, and M. Gupta, “Sequence and series, lecture notes”, Marcel Dekker Inc., 1980.
3. V. A. Khan, “On a new sequence space defined by Orlicz functions”, *Common. Fac. Sci. Univ. Ank-series*; 57(2) , 25–33, 2008.
4. E. Kolk, ” *Topologies in generalized Orlicz sequence spaces*”, *Filomat*, 25(4), 191-211, 2011.
5. Lascarides, C.G. and Maddox, I.J. “A study of certain sequence spaces of Maddox and generalization of a theorem of Iyer”; *Pacific. J. Math* ; 38, 481-499, 1971.
6. I. E. Leonard, “Banach sequence space”; *J. Math Anal. Appl.*54(1), 245-265, 1976.
7. J. Lindenstrauss, and L. Tzafriri, “Classical Banach spaces”, Springer-Verlag, New York/Berlin, 1977.
8. I. J. Maddox, “Some properties of paranormed sequence spaces”, *J. Math. Soc. London.* 2(1), 316-322, 1969.
9. E. Malkowski, “On Generalized Matrix Domains; Sequence Spaces and Applications”; Narosa Publishing House, New Delhi, 35-37, 1999.
10. E. Malkowski, and V. Rakocevic, “An introduction into the theory of sequence spaces and measures of non-compactness”, 2004.
11. N.P. Pahari, and J. K. Srivastava, ”On Banach space valued paranormed sequence space $\ell_M(X, \bar{\lambda}, \bar{p}, L)$ defined by Orlicz function”; *South East Asian J.Math. & Math.Sc.*; 10(1), 45-57, 2011.
12. N. P. Pahari, and J. K. Srivastava, “On vector valued paranormed sequence space $c_0(X, M, \bar{\lambda}, \bar{p})$ defined by Orlicz function”; *J.Rajasthan Acad. of Phy. Sci.*; 11(2),11-24, 2012.
13. K. C. Rao, “The Space of Entire Sequences; Sequences Spaces and Application”, Narosa Publishing House, New Delhi, 4-8, 1999.
14. M. M. Rao, and Z. D. Ren, “The Theory of Orlicz Space”, Marcel Dekker Inc., New York, 1991.
15. W. H. Ruckle, “Sequence spaces”, Pitman Advanced Publishing Programme, 1981.
16. S. Simons, ”The sequence spaces $l(p_j)$ and $m(p_j)$ ” ; *Proc. London Math. Soc.* (3),15, 422-436, 1965.
17. A. Wilansky, “Modern methods in topological vector spaces”, McGraw-Hill Book Co. Inc. New York, 1978.

OPTIMAL MATERIALIZED VIEW MANAGEMENT IN DISTRIBUTED ENVIRONMENT USING RANDOM WALK APPROACH

Purushottam Bagale¹, Shashidhar Ram Joshi ²

¹Department of Electronics and Computer Engineering, Advanced College of Engineering &
Management, Kopundole, Nepal

Email Address: purushottam.bagale@acem.edu.np

²Department of Electronics and Computer Engineering Institute of Engineering, Pulchowk Campus

Email Address: sashi@healthnet.org.np

Abstract

Materialized View selection and maintenance is a critical problem in many applications. In large databases particularly in distributed database, query response time plays an important role as timely access to information and it is the basic requirement of successful business application. The materialization of all views is not possible because of the space constraint and maintenance cost constraint. Materialized views selection is one of the crucial decisions in designing a data warehouse for optimal efficiency. Selecting a suitable set of views that minimizes the total cost associated with the materialized views is the key component in distributed database environment. Several solutions have been proposed in the literature to solve this problem. However, most studies do not encompass search time, storage constraints and maintenance cost. In this research work two algorithms are depicted; first for materialized view selection and maintenance in distributed environment where database is distributed, Second algorithm is for node selection in distributed environment.

Keywords: *Materialized View Selection and Maintenance, Query Optimization, Distributed Database, Optimization, Random Walk Approach, Gossip Protocol, Node Selection Approach.*

1 Introduction

Materialized view (MV), proven to be an excellent technique in decision support applications, would continue to be useful in this scenario to preserve the integrated data to ensure better access, performance and high availability. MV must be maintained when the sources change. This has been extensively studied in the past few years, however, it is not sufficiently explored in distributed environment. Materialized view can significantly improve the query performance of relational databases. MVs are a well known technique to reduce the response time of complex queries in database management systems (DBMS). MVs can improve the query performance by avoiding re-computation of expensive query operations. In a distributed DBMS, MVs can materialize query results near to the query issuer and reduce network transmissions. On the other hand, MVs have to be recomputed when the underlying relations are updated, and various resource constraints have to be considered. Thus, it is far from trivial to find the optimal set of MVs in complex, distributed environment [1, 2].

The motivation for using materialized views is to improve performance but the overhead associated with materialized view management can become a significant system management problem.

The common materialized view management activities include; identifying which materialized view to create; indexing the materialized view; ensuring that all materialized views and materialized view indexes are refreshed properly each time the database is updated; checking which materialized views have been used; determining how effective each materialized view has been on workload performance; measuring the space being used by materialized views; determining which existing materialized views should be dropped; archiving old detail and materialized view data that is no longer useful. The distributed model is quickly becoming the preferred medium for file sharing and distributing data over the internet. A distributed network consists of numerous peer nodes that share data and resources with other peers on an equal basis. Unlike traditional client-server models, no central coordination exists in a distributed system; thus, there is no central point of failure [3, 4].

The selection of views to materialize is the important issue in distributed environment. In this thesis work, outlined a methodology whether the views created for the execution of queries is beneficial or not by considering the various parameters: cost of query, cost of maintenance, net benefit and storage space. Here, proposed methodology for selecting views to materialized so as to achieve the best combination good query performance. These algorithms are found efficient as compared to other strategies.

2 Methodology

2.1 Complete System

The optimization model of this research involves the process of selection and update of materialized view with tree based approach and determining the best node for executing the query using node selection strategy.

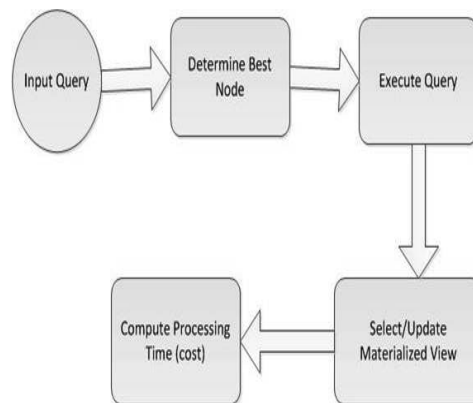


Fig 1: Complete Diagram of Proposed System

In the proposed system as shown in Fig: 1 queries are taken as input. Since our system is for distributed environment, best node is then determined where query is to execute. Then Query is executed using node selection strategy. Then the creation and maintenance of materialized view is done by using tree based approach. Then the Processing Time (Cost) is computed. This computed cost will be used for the evaluation of our system.

2.2 MV Selection and Maintenance, RWA

2.2.1 Materialized View Selection

The Materialized view selection is to select an appropriate set of views that minimizes total query response time and the cost of maintaining the selected views, given a limited amount of resource, e.g., materialization time, storage space, etc. There are mainly two classes of materialized view selection. First is materialized view selection under a disk space constraints and the second is materialized view selection under a maintenance time constraints. The problem of utilizing the limited resources disk space or maintenance time to minimize the total query processing cost comes under the materialized view selection with resource constraints [5].

2.2.2 Materialized View Maintenance

Materialized views are stored in data warehouse to enable users to quickly get search results for analysis. When the remote basic data source changes, the materialized views in data warehouse are also updated in order to maintain the consistency, this causes the need for handling the problem of materialized view maintenance [6].

Data sources in a distributed environment are typically owned by different information providers and function independently from one another. The relationship between materialized views and such autonomous data sources hence must be loosely coupled. That is, the source updates are committed without any concern of how and when the view manager will incorporate them into the view. This causes problems which we called maintenance anomalies: View maintenance, view synchronization, and view adaptation[7]. View maintenance maintains the materialized view extent under source data updates. In contrast, view synchronization aims at rewriting the view definition when the source schema has been changed. Thereafter, view adaptation incrementally adapts the view extent again to match the newly changed view definition.

2.2.3 Random Walk Approach

Random walk approach is a mathematical formalization of a path that consists of a succession of random steps. It is the stochastic (non-deterministic) process formed by successive summation of independent, identically distributed random variables. In this thesis work, basic of random walk approach is used for determining the best node in which the materialized view is created or updated. [8]

2.3 Algorithm

2.3.1 Node Selection Algorithm

This algorithm decides the nodes in the distributed environment for which materialized view should be created, updated or to be maintained.

The random walk algorithm is used as base for designing the node selection algorithm and gossip protocol is used to find the best set of the nodes. Where, M = Total number of nodes

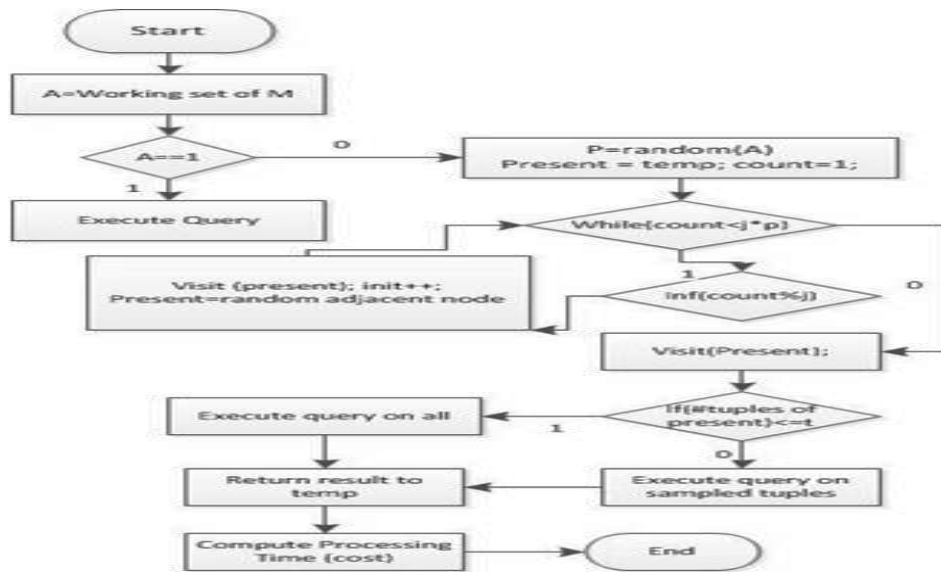


Fig 2: flow chart of node selection algorithm

in network A = Number of Active nodes $Init$ = node where query is initiated P = number of nodes to visit $Temp$ = Node where query is initiated Q = Query with selection condition j = jump size for randomly selecting nodes t = max tuples to be processed per node

The Random Walk Algorithm will be used for node selection. Initially it will check the available nodes. If there is only one node then the query will be executed on the same node otherwise the random nodes will be identified from the available active nodes on which the query will get executed [9]. This algorithm will decide the nodes in the distributed environment for which materialized view should be created, updated or to be maintained. RWA will be used as base for designing the node selection algorithm and gossip protocol will be used to find the best set of the nodes.

2.3.2 Materialized view creation and maintenance Algorithm

The tree based approach will be used for creating and maintaining materialized views. Flow chart of the materialized view creation and maintenance is given in fig.2 where T = Total records in database TR = threshold for number of records. V = Set of Materialized Views

The middle record will be selected as root element of tree. The records will be then splitted till the threshold doesn't reach so that the leaf of tree should contain the number of records that will be present in materialized view. Then the materialized view will be created for each leaf node indirectly each leaf represent materialized that has to be created and maintain. The materialized view will be selected as per the query the records for which the query is intended the materialized view for those records will be selected for the processing. This will minimize the total execution cost.

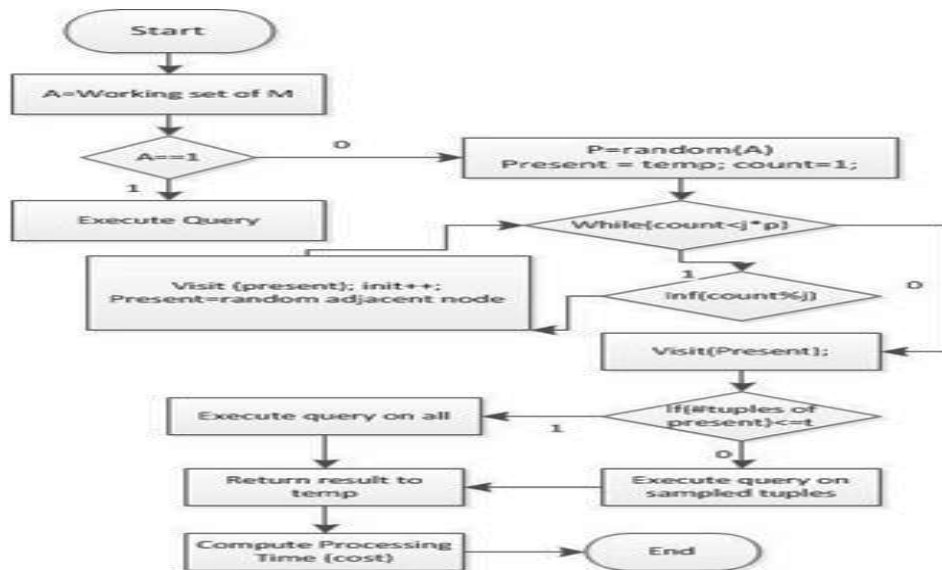


Fig 3: flow chart of materialized view creation and maintenance algorithm

3 Result and Discussion

3.1 Comparison of QPC, MC and SC for four strategies

The simulation model is designed to implement our Optimized Materialized view management in distributed environment using random walk approach. For our experiments, java prototype of the algorithms described in section 3 is programmed. The simulated distributed database environment including computing nodes, database tables and cost-based query optimizer is implemented for Optimized Materialized view management in distributed environment using random walk approach. The cost model for the optimizer will be described in the next section. The total cost is calculated on the basis of query processing, maintenance and storage cost for four strategies. Result is shown in Fig 4.

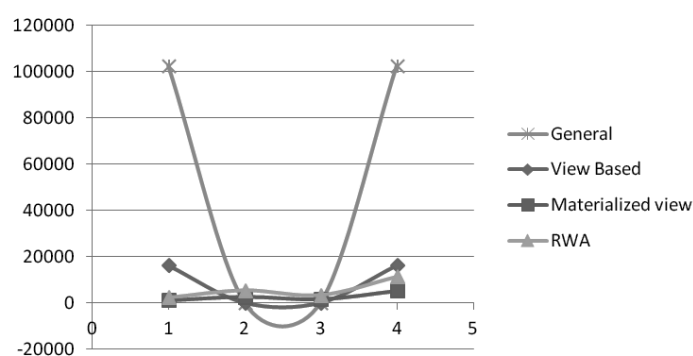


Fig 4: Comparison of QPC, MC and SC for four strategies

Here we found that the total cost computed from the query processing cost, maintenance cost and storage cost in four different strategies shows that though the maintenance cost is not applied for general query and view based, the total cost is very high because it searches for the base table for the result. The total cost for RWA is higher than the general MV but lower than general and view based strategies. The total cost for materialized view is lowest among all.

3.2 Total Cost Comparison

In Fig 5, the total cost comparison of all the four strategies along with proposed random walk approach materialized view is given.

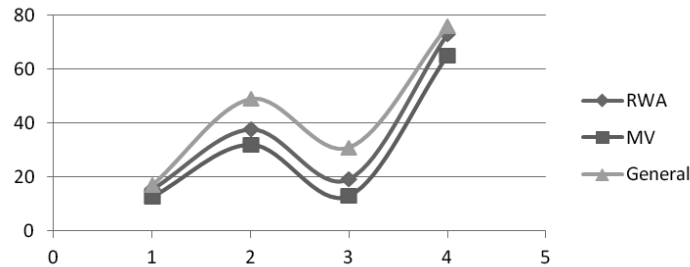


Fig 5: total cost comparison of all four strategies

3.3 Response time comparison

In Fig 6, the response time taken by all the four strategies along with proposed random walk approach materialized view is given. The response time is given in terms of milliseconds. Here the comparison is implemented using the proposed methodology with general, view based and materialized view based strategy on the basis of response time and it is observed that proposed method requires a minimum time for execution and response and this minimizes the total cost of query for processing. Although the maintenance cost and maintenance cost for our proposed method is high, the response time taken by proposed method is best.

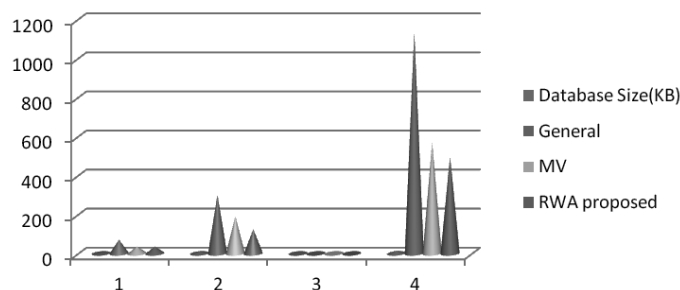


Fig 6: Response time comparison of all four strategies

4 Conclusion

This research given a optimal way to manage materialized view in distributed environment using random walk approach. Thus it is concluded that this approach provide simple and cost-effective guidelines to the engineers, scientists, and researchers in the field of materialized view in distributed environment.

The same concept can be deployed in the future by extending the domain size and environment to the cloud computing

References

- [1] D. P. P.Kalnis, N. Maumoulis, “View selection using randomized search,” *Internatioanl Journal of Information Technology*, 2002.
- [2] A. R. V. Harinarayan and J. Ullman, “Implementing data cubes efficiently,” *Proceedings of ACM SIGMOD 1996 International Conference on Management of Data, Montreal, Canada*, pp. 205–216, 1996.
- [3] A. Bauer, W. Lehner, “On Solving the View Selection Problem in Distributed Data Warehouse Architectures.” *IEEE(1099-3371)*, year = 2003.
- [4] G. D. B. Babcock, S. Chaudhuri, “Dynamic sample selection for approximate query processing,” pp. 539–550, 2003.
- [5] C. Zhang, X. Yao, J. Yang, “An Evolutionary Approach to Materialized Views Selection in Data warehouse Environment,” *IEEE*, 2001.
- [6] F. H. LWF Chaves, E Buchmann, “Towards materialized view selection for distributed database,” *International conference on extending database Technology*, 2009.
- [7] H. Jiang, D. Gao, W. Li., “Exploiting Correlation and Parallelism of Materialized View Recommendation for Distributed Data Warehouse,” *IEEE*, 2007.
- [8] Wikipedia, “Random walk.”
- [9] C. Gkantsidis, M. Mihail, A. Saberi, “Random Walks in Peer to Peer Networks,” *Proc. IEEE INFOCOM*, 2004.
- [10] B. Liu, E.A. Rundensteiner, “Cost-Driven General Join View Maintenance over Distributed data source,” *IEEE*, 2005.
- [11] S. Chen, X Zhang, E.A. Rundensteiner, “A Compensation based approach for view maintenance in distributed environment,” *Signal Processing: An International Journal*, 2006.
- [12] A. Benjamin, D. Gautam, G. Dimitrios, K. Vana, “Efficient Approximate Query Processing in Peer-to-Peer Networks,” *IEEE Trans on Knowledge and Data Engg.*, 2007.
- [13] J. Shantanu, J. Christopher, “Materialized Sample Views for Database Approximation,” *IEEE Trans of Knowledge and Data Engg.*, 2008.
- [14] D. R. B. B. Ashadevi, “Optimized cost effective approach for selection of materialized views in data warehousing,” *International Journal of Information Technology*, 2009.
- [15] V. T. p.p.karde, “Selection and maintenance of materialized view and its application for fast query processing,” *International Conference on extending database Technology*, 2010.
- [16] Wikipedia, “Java remote method invocation.”
- [17] Wikipedia, “Materialized view.”

EARTHWORK PLANNING AND VISUALISATION OF TIME-LOCATION INFORMATION IN ROAD CONSTRUCTION PROJECTS

R. K. Shah

Senior Lecturer, School of the Built Environment, Faculty of Technology and Environment, Liverpool John Moores University, Liverpool, L3 3AF, United Kingdom

Email Address: r.shah@ljmu.ac.uk

Abstract

Accurate information of locations from visual aspect is vital for efficient resource planning and managing the workspace conflicts in the earthwork operations, which are missing in the existing linear schedules. Hence, the construction managers have to depend on the subjective decisions and intangible imagining for resources allocation, workspace conflicts and location-based progress monitoring in the earthwork projects. This has caused uncertainties in planning and scheduling of earthworks, and consequently delays and cost overruns of the projects. To overcome these issues, a framework of computer based prototype model was developed using the theory of location-based planning. This paper focuses on the case study experiments to demonstrate the functions of the model, which includes automatic generation of location-based earthwork schedules and visualisation of cut-fill locations on a weekly basis. The experiment results confirmed the model's capability in identifying precise weekly locations of cut-fill and also visualising the time-space conflicts at the earthwork projects. Hence, the paper concludes that the model is a useful decision supporting tool to improve site productivity and reduce production cost of earthworks in the construction projects like roads and railways.

Keywords: *Earthworks, cut-fill sections, location-based scheduling information, productivity, visualisation*

1. Introduction

In comparison with other production industries, the construction industry has distinctive features in terms of one-off projects, site production, and temporary organisation [1]. The planning and scheduling process of a construction project is a challenging task and the decisions taken in this stage have the foremost impact on the successful execution of a project from its early conceptual stage to the project completion and operational stage [2]. Planning and scheduling involve careful allocation of resources, particularly along linear construction projects when and where necessary throughout the construction operations. Failure to decide on the optimum work activities with the required resources from location aspects have an adverse impact on the project cost, time, quality, space conflicts, and safety of site works in the construction projects [3].

Arditiet *al.* [4] suggested that earthworks projects require a separate planning task for each project due to the distinctive characteristics of earthworks. The effective application of planning and scheduling techniques: such as CPM and PERT are limited because the activities associated with linear construction projects like roads, railways and pipelines are fundamentally different from the general building and housing projects. Most of the activities in road projects are linear activities and needs linear scheduling method. A linear scheduling method has the potential to provide significant enhancement in terms of visual representation from the location aspects, and to progress monitoring because the method allows the project schedulers and construction managers to plan road construction projects visually and determine the controlling activity path and locations [5]. Hence, a new methodology with a computer-based model is introduced in this paper to overcome the above issues.

This paper presents a computer-based prototype model that generates automatically location-based earthwork schedules, and provides a platform for visualising the scheduling information of earthworks from the location viewpoints, particularly in linear construction projects like road and railways. The research devises a decision-support tool that aids to the construction and planning managers, mainly in resource scheduling and progress monitoring more effectively, and assists them in communicating the scheduling information from the location aspects throughout earthwork operations. In this paper, the location-based scheduling is dubbed as “time-location plan”. The remainder of the paper outlines literature review, design a conceptual framework, and details of the prototype model development that includes inputs, processes and outputs. The key outputs of the model are automatic generation of location-based schedules (time-location plan and time-space congestion plan) with optimised quantities of earthworks, particularly in the linear construction projects. Finally, case study experiments from a road construction project were used to demonstrate the purposes of the model.

2. Literature review

Generally, at the early stages of construction project, earthworks take place and they have unique characteristics, particularly in linear construction projects like roads, railways and pipelines. They constitute a major component in construction and absorb high costs, and there is a need to deal with haul distances for balancing cutting and filling quantities of earthworks in a cost effective approach [6]. For example, a study of 145 road projects found that earthworks constituent was represented around 19.58% of the monetary value of the project [7]. The earthworks activities also have direct effects in the sequencing of the rest of road activities since earthwork contributes higher percentage in a project monitoring value. Hence, decisions taken during the planning stage of the earthwork operations have high impact on the overall performance of the project [3].

Mattila and Abraham [8] stated that the subjective division of the repetitive activities from location to location, the inability to schedule the continuity of resources and display the activity rates of progress, and failure to provide any information of the performed works on a project are the key limitations of the Critical Path Method (CPM). Mawdesley *et al.* [3] pointed out that CPM networks are more suitable for large complex projects, however, line of balance and linear scheduling methods are more practical for the repetitive and linear construction projects. A linear schedule is used to reduce the interruption of continuous or repetitive activities, to maintain resource continuity, and to determine locations of the activities on any given day from the schedule.

Arditiet *al.* [9] (2001) suggested that the line of balance technique is an example of linear scheduling method, which is based on the hypothesis that the productivity for an activity is uniform or linear. In other words, the productivity (production rate) of an activity is linear when time is plotted on the vertical axis, and location of an activity on the horizontal axis (or vice versa). The production rate of an activity is the slope of the production line, and is expressed in terms of units/linear meter per time. Scheduling methods such as line of balance, repetitive scheduling method, time-location matrix model, time-space scheduling method, linear scheduling methods, time-distance diagram and linear-balance diagram are known as ‘location-based scheduling’. These methods are based on the theory of location-based planning in the management of construction projects [10, 11]. This method is important because it provides vital information of working locations throughout the earthwork operations, with the aim of reducing the dependency on the subjective decisions. The correct working locations and timing assist construction managers and planners in resource planning, mobilisation of heavy equipment at require locations and controlling site progress more effectively from location aspects. The linear scheduling methods, however, do not provide exact information of working locations and time throughout the earthwork construction.

Kenley and Seppanen [10] pointed out that there are mainly two types of scheduling methodologies: an activity-based and a location-based methodology. The location-based methodology is also subdivided into two types: unit-production and location-production scheduling. It is known as an alternative methodology of location-based scheduling, which is based on tracking the continuity of crews working on production tasks. On the other hand, DynaRoad [12] developed commercial software for a construction schedule and controlling the earthwork activities in linear projects. This provides the location-based scheduling information for a whole section but lacks to provide weekly information of locations. TILOS, which is time-location planning software for managing linear construction projects, assists in visualising the repetitive tasks from location aspects. It also provides the flow of scheduling data in terms of time and location on a construction plan [13]. However, existing time-distance charts, produced by DynaRoad and TILOS do not provide weekly information of locations.

This is imperative for effective planning of resources and reducing the space conflicts at construction sites. Consequently, construction managers depend on the subjective decision for earthwork scheduling due to the limited information of the working locations. Taking into account previous studies, it is concluded that location-based scheduling, which is based on the theory of location-based methodology, is an effective way of representing the planning and scheduling information of earthwork activities in road projects. From the reviewed literature, it was established that the existing time-distance chart is incapable of providing scheduling information of locations. Therefore, this research examined a new methodology for the automatic generation of location-based scheduling that is capable of providing the weekly or daily location information of earthworks. The next section discusses a framework of a computer-based prototype.

3. Framework of a prototype

A general specification of the framework of prototype of earthwork scheduling and visualisation is designed as shown in Fig 1, taking into account of the findings from the literature and industry review [14]. The framework is a state-of-the-art, which is designed by integrating the road design data, sectional quantities, productivity rates and unit cost of cut/fill quantities, and an arithmetic algorithm. This helps to generate location-based schedules of earth work automatically and visualise the weekly scheduling information from the location aspects. The developed prototype has the capability of generating terrain modelling, cut/fill optimisation, weekly progress profiles, and time-space congestion plans, cost profiles and cost S-curves of earthworks in the linear construction projects.

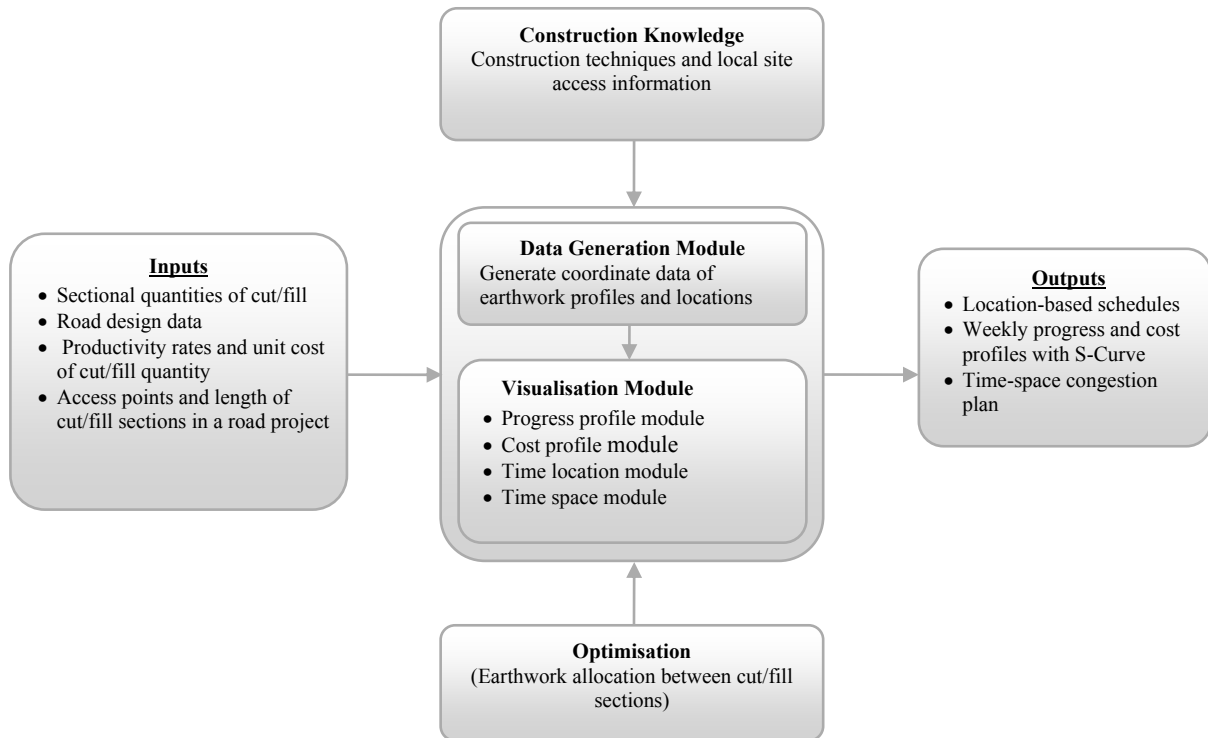


Fig 1 Framework of a prototype of earthwork scheduling and visualisation

This research, however, presented a computer-based prototype model and focused on the case study experiments with the model under scenarios at the construction site. A case study from road projects was utilised for the automatic generation of location-based schedules of earthworks using the algorithm underpinned in the prototype model [15]. Although the prototype model is capable of generating weekly progress profiles, cost profiles and S-curve, this paper discusses mainly the methodology and algorithm, which aid to generate location-based schedules automatically for earthworks. The paper also demonstrates the functions of the model with a case study experiments in a road project. The overall explanations of the model components: inputs, processes and outputs are discussed in the next sections.

3.1 Prototype model

This section describes the key components of the prototype model. The sectional quantities of cutting or filling activities, productivity and construction site knowledge base are inputs of the model. The cutting or filling quantity at each station is calculated using road design data including longitudinal section and cross sections. The productivity rate produced by the “RoadSim” simulator is integrated into the model as a main input. The soil characteristics, types of available equipment sets, haulage distance of soil, access road conditions and working efficiency of crew were incorporated within the “RoadSim” simulator. However, earthwork for rock excavation is excluded from this study since the nature of rock excavation is fully different from the normal earthwork operations. The construction knowledge encapsulated from planners and managers was utilised to select the right construction methods under different terrain conditions and soil characteristics considering the available equipment sets for earthworks. The site operational rules and knowledge allow in establishing the sequential relationships amongst listed work activities during the construction operations. The knowledge and operational rules were incorporated within algorithm for the generation of a location-based schedule.

Moreover, an optimisation algorithm was also developed and integrated with the model for optimum allocation of earthworks and the movement direction between cuts and fills, borrows to fills or cut to

landfills considering economical haulage unit costs. The optimisation algorithm was designed by integrating the characteristics of mass haul diagram, unit cost simulated by “RoadSim” simulator, and Excel solver. The solver was built within MS Excel using a Simplex algorithm for linear optimisation problems. Before producing a location-based schedule, it is vital to identify the possible sources and destinations of earthwork quantities, required for filling and cutting operations in the linear projects. The processes of the prototype include four modules: data generation module, visualisation module, cost profile module and a time-location module. Data generation module processes the input data to generate the coordinate data of weekly locations of the cutting and filling activities, incorporating different production rates. The time location module processes the coordinate data and generates location-based plans for earthwork activities. The next section discusses the generation of location-based scheduling.

3.2 Generation of location-based earthwork scheduling

Location-based scheduling is a planning tool, which is widely applicable in the earthwork planning tasks. The location-based scheduling is also known as time-distance planning, time-chain age planning and linear scheduling method. It enables the design and display of planning and scheduling information of earthwork activities in two dimensions: Location in X-axis and Time in Y-axis or vice versa together with topographical information of a road project. The slope of activities displayed in time location chart represents a rate of production of the earthwork activities. If the slopes of planned activities are compared with the slope of actual activities, they provide visual information of early indication regarding possible of conflicts or overlap between activities during the course of activity progress.

The proposed methodology in the prototype model is original and intelligent to identify the starting and ending location as well as the start and end period of cutting and filling activities at planning stage. It also helps to find the actual information of weekly locations, which ultimately assist to planners and managers for planning the necessary resources more efficiently. The methodology is designed with an arithmetical algorithm that tracks the locations (stations) along a road section which are broken down into weekly or daily schedules, satisfying the linearity characteristics (start and end locations having equal production rate) in the earthwork operations. The equation 7 developed by Shah *et al.*[15], is being used for identification of the station numbers at each layer throughout the earthwork operations by incorporating the ‘variable’ productivity data. The productivity data produced by RoadSim [16] are incorporated in the developed equation. The factors that influence the productivity of earthworks are incorporated within the RoadSim programme and produce hourly productivity based on the selected sets of resources and construction equipment.

$$V_r = \left[\left\{ \sum_{i=1}^{i=n} (V_i) - P \right\} / n \right] \quad (7)$$

Whereas,

V_r = Remaining earthwork quantities after progress at each week

V_i = Quantity of earthwork at each station along the selected road section, $i = 1, 2, 3, \dots, n$.

n = number of working stations along the road section

P = Productivity used to progress the earthworks

This process is repeated at each layer of cutting or filling sections to achieve the remaining volume (V_r) at each station is equivalent to zero (at the design level of road) at the selected working sections along a road project. At each layer, the starting and ending stations are identified and their lengths between the two stations are determined by the algorithm, designed in the model with help of VBA

programming language. These lengths, at each layer between working stations, increase from the first to the last layer at both cutting and filling sections of the earthwork operation. Similarly, cutting and filling sections are selected according to the earthwork schedule to complete the earthwork operations throughout the construction of a road section. If the cutting or filling sections are longer, these sections are divided into manageable sections and these processes are repeated to achieve the design level of the road.

In this model, two input variables: Productivity rate (P) of earthwork activities produced by “RoadSim” and working length (X) determined by “mass haul diagram” were integrated with the model to search the coordinate of starting and ending locations of working section. The algorithm assists to calculate the coordinate of working locations considering “variable” productivity data throughout the construction operations in a road project. Therefore, coordinates of weekly or daily locations directly depends on the value and unit of productivity i.e. weekly or daily productivity by assuming 40 hours per week or 8 hours per day as standard working time.

The identified coordinate data of locations and time of earthwork activities are stored in a table at first and then exported the coordinate data by programme to generate location-based scheduling. The location-based scheduling has generated automatically. The automatic generated location-based schedule, which is key outputs of the model, provides accurate information of working locations, in the earthwork planning and scheduling. The location-based schedule assists to planners and construction managers in allowing the visualisation and analysis of the status of construction activities on a particular location along the road sections. The next section describes the visual function of the model that assist to planning in visualising the information about weekly locations and space congestion in earthwork operations.

3.3 Visualisation of time-space scheduling information

This section presents the development of a visualisation component of the prototype model. This provides the visual information of earthwork scheduling, space congestion, progress profiles, and communicates the construction process sequences with consideration given to location aspects. The Visualisation Module (VM) processes the coordinate data of location-based schedules and transforms them into a visual format to visualise earthwork scheduling information. The VM was developed using the C# and VBA programming language on MS Excel platform. The required input data was stored in MS Excel worksheets and used as database. Several VBA macros were designed to process input data and generate into visual outputs of the model. The VM imports data using Structured Query Language (SQL) inquiry, and transforms the imported data into a visual representation of scheduling information of earthworks activities in a tabular and graphical format.

A snapshot of the visual outputs of the model is shown in Fig2, which includes weekly progress and cost profiles, cost S-Curve, location-based scheduling information and time-space congestion plan of earthworks in road projects. The location-based plan provides information related to the congested locations and pavement activities such as sub-base, base course and top road surfacing (see Fig 2). The visualisation component also provides tabular information of starting and ending locations on weekly basis throughout the construction operations of earthworks and pavement. The following section describes a case study experiment to evaluate the model’s functions (generation and visualisation of location-based scheduling information of earthworks) using real site data from a road project.

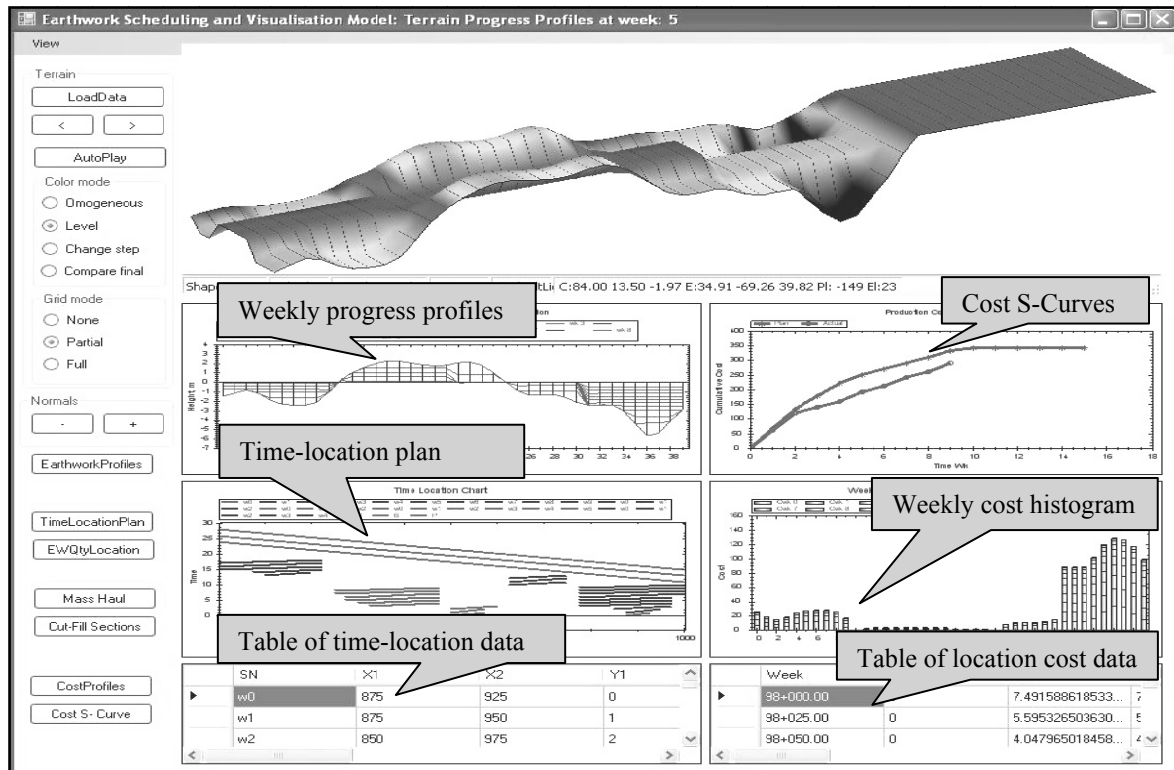


Fig 2 Snapshot of the visual outputs of model showing the location-based scheduling information

4. Case Study Experiments

A case study involving 1.0 kilometer of road section of lot no. 3 road project in Portugal was selected to demonstrate the functionalities of the model. Actual road design data including L-section and X-section is considered, and the sectional quantity of earthwork is calculated assuming typical trapezoidal section at 25m intervals along the selected road section. The productivity data of cutting or filling activities is considered as a key factor that affects the construction duration, working locations and numbers of construction layers required to complete earthwork operations. Since the model outputs directly depend on the accuracy of the productivity data, the case study experiment was run to compare the variations in the productivity values between actual site progress and model used values of earthwork activity. The case study results revealed that the actual productivity was lower by 2% compare to the productivity value produced by the model to generate a location-based schedule for earthwork activity in road projects. The outputs of the model are automatic generation of earthwork progress profiles, 4D terrain surfaces, cost profiles, production cost S-curve and location-based work schedules and visualisation of scheduling information from the location aspects.

A 7 km road section was selected with the assistance of a company for the validation of the time–location plan (location-based scheduling) produced by prototype model. The duration of earthworks shown in a time–location plan provided by the company was compared with the duration shown in the time–location plan generated by the prototype model. The comparative results including detailed information of weekly working lengths/locations of a road section, earthwork quantities, productivity, and total duration of the earthworks are presented in Table1.

Table 1 Comparison of between company-provided and model-generated time-location plan

S. N.	Road section	Sectional Length (m)	E/W Qty. (m ³)	Cut/Fill Activity	Used Production Rate m ³ /wk	Company-produced Results		Model-generated Results		Variation in Time
						Time (wk)	Locations	Time (wk)	Locations	Time %
1	0+000 to 0+925	925	32,400	Cutting	2309	14.03	0+000 & 0+925	15	Fig 3	6.45%
			34,433	Filling		14.91		15		0.58%
2	0+925 to 2+675	1750	64,700	Cutting	3464	18.68	0+925 & 2+675	21	Fig 3	11.06%
			51,352	Filling		14.82		16		7.35%
3	2+675 to 3+600	925	23,357	Cutting	5196	4.50	2+675 & 3+600	5	Fig 3	10.10%
			36,204	Filling		6.97		8		12.90%
4	3+600 to 7+000	3400	204,294	Cutting	10392	19.56	3+600 & 7+000	22	Fig 3	10.64%
			213,168	Filling		19.64		23		10.81%

The comparison results (presented in Table 1) show that model simulated production duration of earthworks is higher by 8.7% (average) than the company estimated production duration of earthwork for both cutting and filling operations. The duration was calculated by rounding the values for each cut/fill section in case of the model-generated schedule, whereas, the duration was calculated by dividing whole quantities with productivity (production rate) of earthworks for each section in case of the company produced schedule (Table 1). Figure 3 represents a time-location plan of the road project, which includes both the model generated time-location plan in colour limes whereas dotted line represents the company produced and utilised time-location plan. The plan was produced by dividing the road section into four sub-sections (0+000 to 0+925, 0+925 to 2+675, 2+675 to 3+600 and 3+600 to 7+000). Each section was planned with different sets of equipment separately at different production rates (Table 1).

Moreover, several experiments about generating time-location plan for earthworks were carried out at lot no. 5 section in a road construction project in Portugal. The experiments revealed that the actual production time was lower by 2.34% than the model-simulated production time of earthworks due to variation of soil characteristics at the cutting sections along the road project, which is presumed as a minor variation in earthworks.

Hence, it is concluded that the model-produced location-based schedules or time-location plans are acceptable for earthworks in road construction projects. Consequently, these plans support in improving resource planning and scheduling information of weekly work locations, mobilising sets of construction equipment and required materials including gang size of labours from the location aspects.

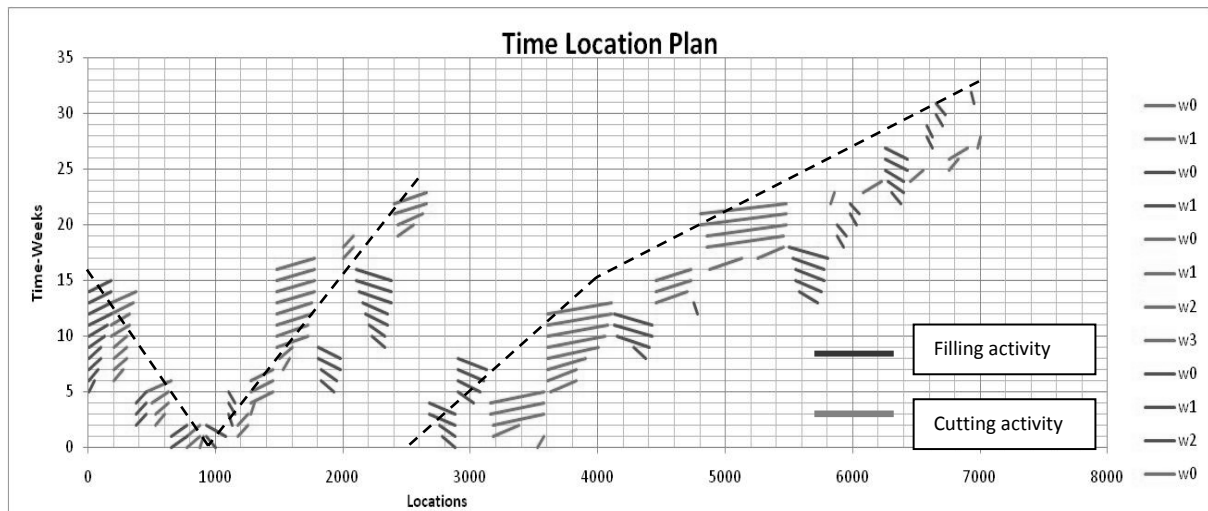


Fig 3 Model-generated time-location plans of a 7 km road project

5. Conclusion

The paper presents the development of a framework and a computer-based prototype model. The model was designed by integrating the road design data; sectional earthwork quantities, productivity rates and unit cost of cut/fill sections and arithmetic algorithms. The model generates automatically the scheduling information of weekly work locations, space congestion plans and resource allocation information for the earthwork projects. A case study experiment was run to demonstrate the functions of the model using site data from road projects. The experiment results revealed that the model provides weekly information of working locations and required resources such as quantity of materials, sets of construction equipment and crew size in earthwork operations. The evaluation from road experts also recommended that the model is a useful tool in supporting the strategic decisions at the planning stage, and helpful to provide the scheduling information more precisely from the location aspects. Running various strategies with the model would allow optimisation of resources, including sets of the construction equipment and crew size, in the earthwork operations at a particular section of a road or railway project.

The findings from the case study experiments found that the model-generated location-based plans are satisfactory and applicable in the linear construction projects like roads or railways, particularly for the earthwork operations. The time-space congestion plan said to identify space congestion in advance and the possibility of equipment being idle at a particular location along the road section. Finally, the paper concluded that the model is a valuable decision supporting tool that assists to the construction and planning managers in mobilising construction equipment more efficiently and visualising the scheduling information of earthworks from the locations aspects. Consequently, the tool is helpful in resource scheduling, progress monitoring, reducing space conflicts and communicating the scheduling information more effectively from the location aspects in earthwork projects like roads and railways.

References

1. L. Koskela, "*An exploration towards a production theory and its application to construction*", *PhD Thesis*, 200, VTT Publications.
2. F. W. Ahmed and Y. T. Walid, "*A Virtual Construction Environment for preconstruction planning*", *Journal of Automation in Construction*, Vol. 12, pp 139-154, 2002.
3. M. J. Mawdesley, W. H. Askew and S. H. Al-Jibouri, "*Site layout for earthworks in road projects*", *Journal of Engineering Construction and Architectural Management*, Vol.11(2), pp 83-89, 2004.
4. D. Arditi, B. O. Tokdemir and K. Suh, "*Challenging in Line-of-Balance Scheduling*", *Journal of Construction Engineering and Management*, Vol. 128(6), pp 545-556, 2002.
5. D. J. Harmelink and R. A. Yamin, "*Development and application of linear scheduling techniques to highways construction projects*", Technical report of FHWA/IN/JTRP-2000/21, October, pp 8-69, 2000.
6. S. Kim and J. S. Russell, "*Framework for an intelligent earthwork system Part I system architecture*", *Journal of Automation in Construction*, Vol. 12, pp 1-13, 2003.
7. S. Castro, "*Integrated simulation models applied to road construction management*", PhD Thesis, University of Teesside, Middlesbrough, UK, 2005.
8. K. G. Mattila and D. M. Abraham, "*Linear scheduling: past research efforts and future directions*", *Journal of Engineering, Construction and Architectural Management*, Vol. 5 (3), pp 294- 303, 1998.
9. D. Arditi, B. O. Tokdemir and K. Suh, "*Effect of learning on line-of-balance scheduling*", *International Journal of Project Management*, Vol. (19), pp 265-277, 2001.
10. R. Kenley and O. Seppanen, "*Location based management of construction projects: part of a new typology for project scheduling methodologies*", *Proceedings of the 2009 winter simulation conference*, pp 2563-2570, Dec 13-16, 2009, Austin, Texas, USA
11. R. Kenley and O. Seppanen, "*Location based management for construction projects: planning, scheduling and control*", First edition, 2010, Spon Press, Abingdon, UK.
12. DynaRoad, "*DynaRoad: plan, schedule and control*", available online at <http://www.dynaroad.fi/pages/index.php>. 2006. [Accessed at 15 Jan 2015].
13. TILOS, "*Linear Project*", TILOS, available online at http://www.tilos.org/software_en.html 2009, (Accessed at 15 Jan 2015).
14. R. K. Shah and N. Dawood, "*An innovative approach for generation of a time-location plan in road construction projects*", *Journal of Construction Management and Economics*, 29(5), pp 435-448, 2011.
15. R. K. Shah, N. Dawood and S. Castro, "*Automatic Generation of Progress Profiles for Earthwork Operations using 4D Visualisation Model*", *Journal of Information Technology in Construction*, Vol (13), pp 491-506, 2008.
16. S. Castro and N. Dawood, "*Automating road construction planning with a specific-domain simulation system*", *ITcon Vol. 14*, p556-573, 2009.

3D Flow Modeling of the First Trifurcation Made in Nepal

Radha Krishan Mallik¹, Paras Paudel²

¹RND Center Pvt.Ltd.

Email Address: rkmallik@gmail.com

²Nepal Airlines

Email Address: paras.paudel@gmail.com

Abstract

The foremost objective of the study was to find out the most efficient profile of trifurcation in given constraints of pressure, velocity and layout of the overall geometry. The study was done for the 3.2 MW Madi Khola Hydropower Project of Gandaki Hydropower Development Co. Pvt. Ltd. The 3 Dimensional Flow modeling of the trifurcation was based on the application of Computational Fluid Dynamics (CFD).

The loss in the Trifurcation greatly depends upon its geometrical configuration. The research started with a general profile and the flow pattern generated inside it was studied with the help of 3 Dimensional Flow modeling. The extent of vortex zone formation inside the trifurcation indicates the loss inside trifurcation. The profile of the trifurcation was hence changed to reduce the vortex formation as far as possible, till we get minimum possible loss. The profile under study should meet maximum flow efficiency under the physical constraints of fabrication. The flow efficient profile was then analyzed to capture the stress amplification near junction. The reinforcing element in the form of steel T-section was added of different sectional values till the stress was within allowable limits under severe conditions.

Keywords: *CFD, FLOTRAN, Trifurcation*

1. Introduction

Project layout and powerhouse orientation decide what kind of penstock branching would be most suitable for the highest safety and minimum head loss. Usually in case of branching for 3 or more units, a number of unsymmetrical bifurcations are used one after another along the penstock alignment. It involves relatively less analytical works during design and is easy to fabricate. But project layout can dictate the other way around, as in case of 3.2MW Madi Khola Hydropower Project in Kaski district, which is already nearing the completion of construction. In this project orientation of the powerhouse with respect to the penstock alignment is such that only a symmetrical trifurcation can be used to feed water to three equal capacity Pelton turbines. Madi trifurcation has become the first trifurcation designed and fabricated within Nepal.

Design of an element of water conveyance system constitute of hydraulic and structural analyses. Hydraulic analysis for penstock branching (bifurcation and trifurcation) is considered unimportant and is found mostly avoided in small hydropower projects of Nepal. But the fact is that hydraulic analysis here is as important as structural analysis. Structural analysis optimizes the initial cost through right selection of steel thicknesses, whereas hydraulic analysis minimizes the head loss through selection of best possible geometry. Head loss in the branching entails a constant loss of money for as long as the plan runs, and this loss, in long run, is many times higher than the cost of the structure itself. Large

hydropower projects do not only conduct hydraulic analysis but also go for model tests. But small project of capacities 1-10 MW are recommended at least to conduct hydraulic analyses for the critical components of water conveyance system. Bifurcation and trifurcation are among such components. They are used near the powerhouse under high pressure head added by pressure surge due to water hammer. Besides, in case of Pelton turbines, there are free water jets downstream to the manifold, which convert almost all of the available head into velocity head. Under this condition the water exerts force on manifolds due to change in momentum of water and can be evaluated from principle of conservation of momentum. This net force must be resisted by the manifold system and the concrete block holding manifold.

The structural analysis of the manifolds is necessary but not sufficient if we consider the long term operational benefits in terms of power outcome and the performance of the plant. The vibration problem caused due to unnecessary eddies developed can cause huge losses of pressure head downstream of the manifold. The profile of the manifolds affects the loss in the available water head significantly. This loss can decrease the potential plant capacity. The profile selection process can be done either by experimental analysis on reduced scale manifolds model test at lab or by numerical modeling of the fluid flow. The former option is rather expensive and may not be feasible every time. It is preferable to select best profile by tuning it with CFD solver and then follow reduced scale model test for the confirmation of flow parameters.

At the time of valve closure the velocity reduces to zero within time interval of valve closure. This phenomenon now converts velocity head to pressure head again. The pressure magnifies due to abrupt change in the velocity. The magnified pressure moves to upstream with certain velocity which depends up on bulk modulus of water and its density. The trifurcation has to resist this magnified pressure. The hoop stresses and longitudinal stress and the combined stress due to increased pressure must be below the tolerable limit as specified in Steel Structure Design Codes. At the zone of the junction of bifurcation the simple analysis approach can not catch the local stress concentration and there are chances of underestimation of such valuable stress concentration. Finite element method can be used to capture Stress Concentration near junction of trifurcation using finer mesh near junction.

2. Design & Analysis Criteria

The pressure losses at junction in manifolds are not analyzed and neglected which is the normal practice in hydropower of Nepal. These losses are significant in obtaining high plant capacity. Before starting design and analysis of the trifurcation; the constraining parameter, such as space available and the position of turbine from the existing site condition, are used to select the trifurcation layout. The normal practiced profile is first used in detailed numerical analysis to understand how the profile affects the losses. The outcomes in analyzing such manifolds provide necessary data for modification. A number of trial and errors to minimize loss was carried out. Finally the best profile was adapted and was used for the stress analysis to minimize the stress below the allowable limit at the junction by adding reinforcement at junctions.

Computational Fluid Dynamics is used for the analysis of the velocity and pressure distribution at different section of manifolds. The pressure and velocity distribution will then be used as a criteria modifying profile of manifold body.

Flotran CFD features of the Ansys v11 is used for the mathematical modeling of the flow through the profile. AutoCad 2006, Ansys Workbench 11 features is used for the mesh generation of the water volume inside the manifolds. The volume is imported in Ansys Flotran CFD for the analysis.

The jet velocity was expected as a output from the analysis

If the neat head of water and discharge at inlet is h and Q respectively then from the continuity equation for the equal discharge among three branching pipe,

Expected Discharge through each nozzle = $Q/3$

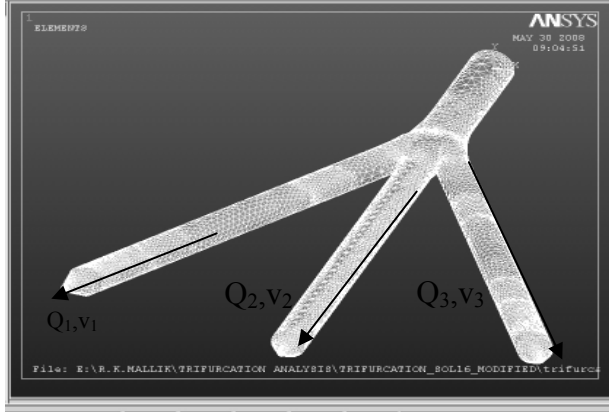


Fig 1 Ansys meshing of the trifurcation fluid control volume

For no loss in the manifold system the velocity at each outlet nozzle = $\sqrt{2gh}$

Corresponding area of the nozzle, $A = Q_i / \sqrt{2gh}$

Corresponding dia. of each nozzle = $\sqrt{4A / \pi}$

This is the dia. of nozzle for no loss condition.

But due to losses in junction the neither all three velocity neither equal nor it is $\sqrt{2gh}$

The evaluation of the real velocity at the outlet of the jet can help us to evaluate the loss by using the energy equation

Inlet Energy = outlet energy + Loss in energy

Loss in energy = Outlet energy-inlet energy

Inlet energy per unit time = Work done by pressure per unit time+ kinetic energy = $PQ + \frac{\rho Q v^2}{2}$

Outlet energy per unit time

$$= \frac{\rho Q_1 v_1^2}{2} + \frac{\rho Q_2 v_2^2}{2} + \frac{\rho Q_3 v_3^2}{2}$$

Where ρ : density of water

Q : Discharge in branching upstream

Q_1, Q_2, Q_3 : Discharge in Branching

v_1, v_2, v_3 : Velocities in branching

Q, ρ, P are known input parameters, while Q_1, Q_2, Q_3 and v_1, v_2, v_3 can be determined from the Ansys Flotran CFD output by surface integral of velocity distribution of cross section near jet.

3. ANSYS FLOTRAN CFD

Types of FLOTRAN Analyses

We can perform these types of FLOTRAN analyses:

- Laminar or turbulent
- Thermal or adiabatic
- Free surface
- Compressible or incompressible
- Newtonian or Non-Newtonian
- Multiple species transport

These types of analyses are *not* mutually exclusive. For example, a laminar analysis can be thermal or adiabatic. A turbulent analysis can be compressible or incompressible. To solve our problem we need to consider any analysis involving the flow of fluid, use either of the Laminar Flow Analysis Turbulent Flow Analysis Laminar and turbulent flows is considered to be *incompressible* since density is constant or the fluid expends little energy in compressing the flow.

3.1 FLOTRAN CFD Analysis

Determining the Problem Domain

The analysis of the losses in penstock pipe line up to trifurcation upstream was done to evaluate pressure and velocity as a inlet boundary condition for trifurcation. Boundary condition at out let of trifurcation is rather difficult process. It is preferable to model up to nozzle where there is free jet condition. Such modeling requires excessive computer memory almost difficult to solve with normal PC. If we focus on the losses due to trifurcation only then logically we can locate free jet zone somehow near to the junction provided that it will not affect the junction velocity and pressure distribution.

Determining the Flow Regime

We need to estimate the character of the flow. The character is a function of the fluid properties, geometry, and the approximate magnitude of the velocity field. The Reynolds number can be used to decide whether the flow will be laminar or turbulent. Similarly mach no criteria can be used to evaluate the compressible and incompressible flow.

Reynolds number = inertial force/viscous force, it should be greater than 2000 for turbulent flow. Mach no = Velocity of fluid/velocity of sound in fluid, which should be greater than 0.7 to activate the compressible flow model.

Creating the Finite Element Mesh

For the most accurate results, we should use mapped meshing. It more effectively maintains a consistent mesh pattern along the boundary. In some cases, we can use hexahedral elements to capture detail in high-gradient regions and tetrahedral elements in less critical regions. For flow analysis, especially turbulent, we should not use pyramid elements in the region near the walls because it may lead to inaccuracies in the solution.

In our case free meshing with tetrahedral element was used for simplicity in meshing it leads some degree of mass imbalance. The mass imbalance can be controlled by further fine meshing

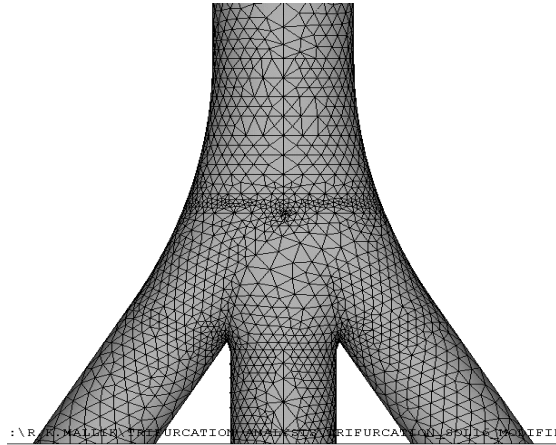


Fig 2 Tetrahedral meshing of fluid control volume near junction

Applying Boundary Conditions

The free body diagram of the manifolds was considered for the analysis.

- The pipe wall was replaced by the zero velocity constrained.
- The net pressure near inlet surface of the manifold was directly applied (177m water head).
- The trial velocity at inlet is applied directly as 3m/sec, 4m/sec..... the velocity to generate input discharge corresponding to plant capacity.

The nozzle of the different trial dia. was attached with the trifurcation outlet. This helps us to apply pressure boundary condition at nozzle outlet as zero equivalents to atmospheric pressure.

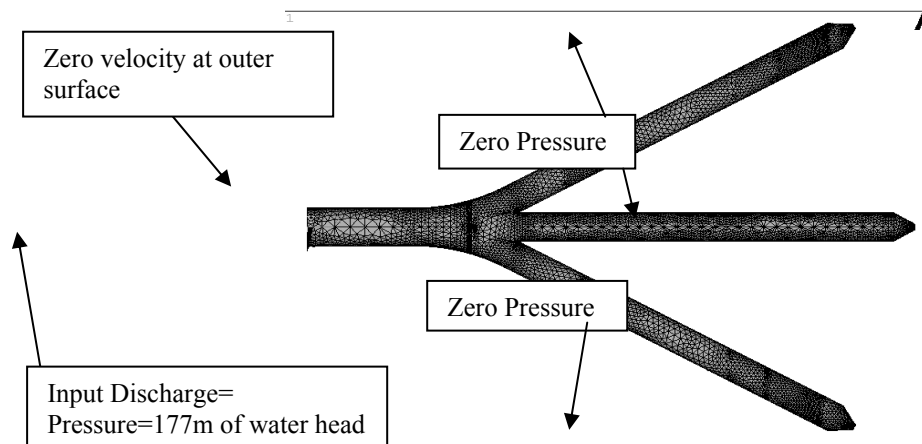


Fig 3 Boundary condition for most efficient trifurcation control volume

Setting FLOTRAN Analysis Parameters

This step includes selection of the flow models as laminar incompressible, laminar compressible, turbulent incompressible, turbulent compressible etc. The number of iteration, convergence option, and fluid properties should also be assigned in this step.

Solving the Problem

This step includes the solving process. We can monitor solution convergence and stability of the analysis by observing the rate of change of the solution and the behavior of relevant dependent variables. These variables include velocity, pressure, temperature, and (if necessary) turbulence quantities such as kinetic energy (degree of freedom ENKE), kinetic energy dissipation rate (ENDS), and effective viscosity (EVIS).

Examining the Results

The results are in the form of velocity distribution and pressure distribution and turbulence quantities distributions. The numerical integration is used to convert velocity distribution to average velocity at outlets. The average velocity at inlet and outlets are then used to evaluate the loss in manifold.

The loss in energy is made as small as possible by adjusting the geometrical profile of manifold at joint.

This is the trial and error process. The modification is made till the loss in the manifold is equivalent to 0.42%.

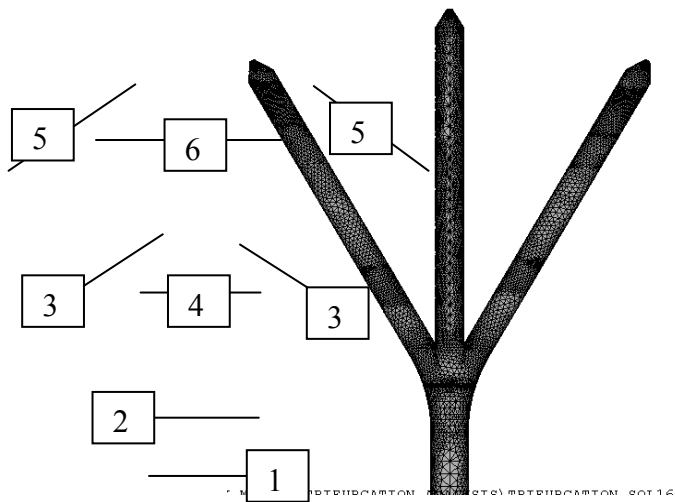


Fig 4 Different section of interest for recording output data

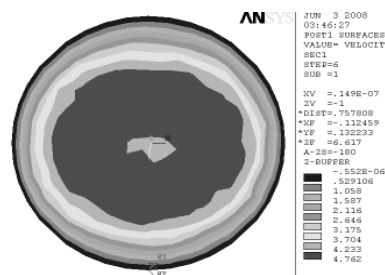


Fig 5 Velocity distribution at section 1-1

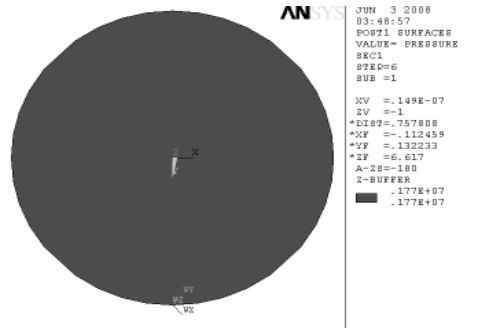


Fig 6 Pressure Distribution at section 1-1
Uniform pressure of 177m water head

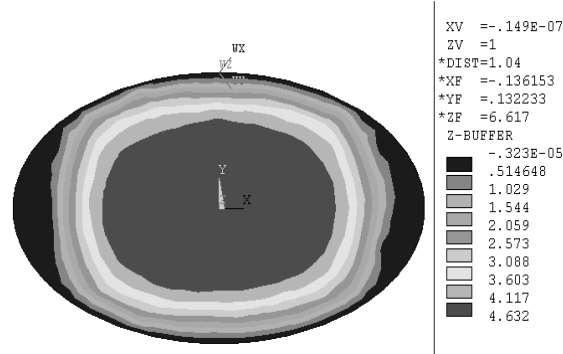


Fig 7 Velocity distribution between section 1 and 2

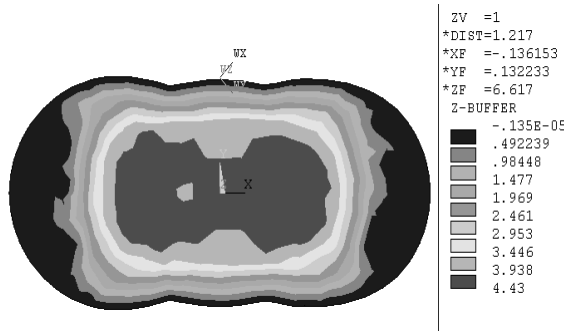


Fig 8 Velocity distribution between section 1 and 2

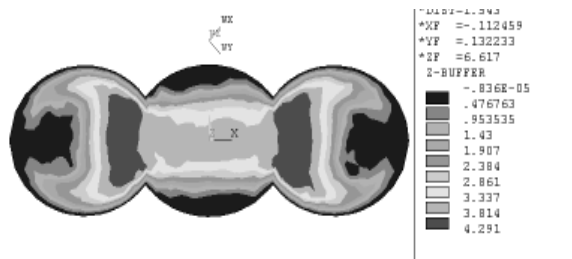


Fig 9 Velocity distribution in section 2-2

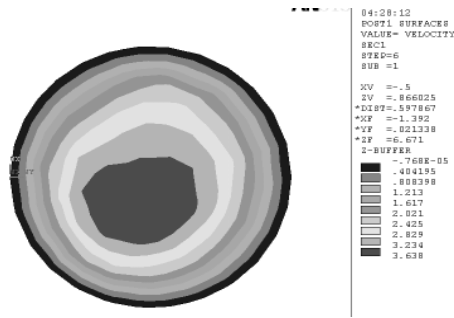


Fig 10 Velocity distribution in sections 5-5

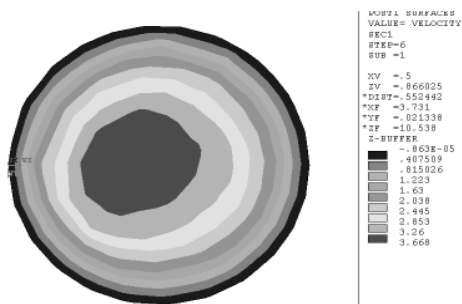


Fig 11 Velocity distribution in sections 5'-5'

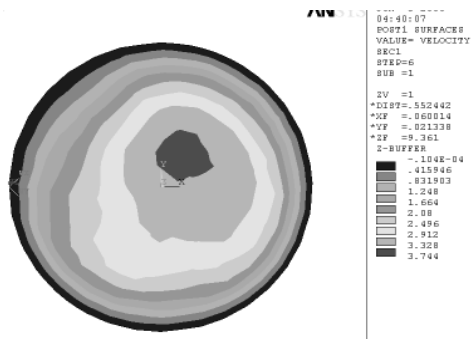


Fig 12 Velocity distribution in sections 6-6

The velocity distribution profile for section at junction indicates the causes of loss of energy near junction. These velocity profiles are for the most possible efficient geometry of the trifurcation junction.

Conclusions from most efficient profile

Left jet			Energy
Area	0.022532	m ²	
Discharge	1.303	m ³ /sec	
Velocity	57.846	m/sec	2180739 J
Velocity head	170.552	m	

Right jet			
Area	0.022532	m ²	
Discharge	1.307	m ³ /sec	
Velocity	58.006	m/sec	2198827 J

Velocity head 171.494 m

Middle jet			
Area	0.022532	m ²	
Discharge	1.295	m ³ /sec	
Velocity	57.494	m/sec	2141131 J

Velocity head 168.481 m

Main Pipe			
Area	1.125	m ²	
Discharge	3.677	m ³ /sec	
Velocity	3.268	m/sec	6548275 J

Velocity head 0.544 m
Pressure 1770000 N/m²

Pressure head	177	m
total energy u/s to trifurcation	177.545	m
Total output energy	6520696.58	J
Total input energy	6548275.47	J
Total Loss	27578.89	J
% Loss	0.421	%
loss in terms of head	0.748	m

3.2 Stress Analysis at Junction

According to the ASME Code, the non-embedded penstock pipe may be designed under the following condition.

Normal condition:

This condition gives the allowable stress = **138.67** Mpa

Intermittent condition:

This condition gives the allowable stress = **184.89** Mpa

Emergency condition:

This condition gives the allowable stress = **250** Mpa **Exceptional conditions:**

It includes malfunctioning of control equipment in most adverse manner and shall not be used as the basis of design.

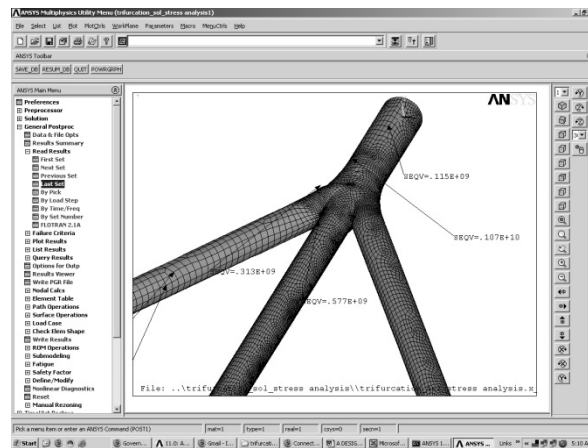


Fig 13 Mesh generation of manifold with shell 181 element, for stress analysis.

If the maximum stress does not exceed the specified minimum ultimate tensile strength, the structural integrity of the penstock is reasonably assured.

Precautions must be taken to minimize the probability of occurrence and effects of the exceptional condition.

In this analysis the stress was supposed not to increase above 138 Mpa in normal water pressure + water hammer pressure. For the combination of normal flow condition and the earthquake effects the whole penstock unit should be studied.

The von-mises stress criterion was used for checking the yield at the zone of stress concentration

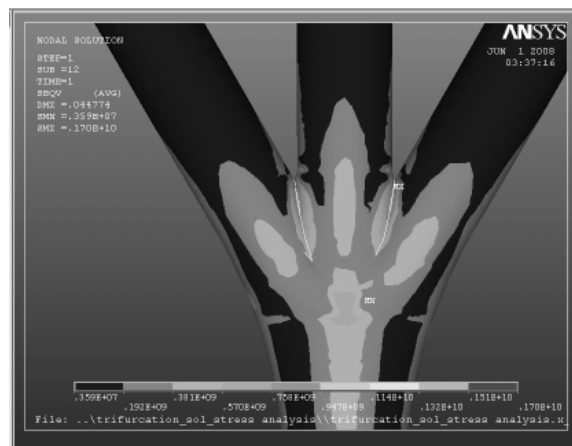


Fig 14 Von-mises stress distribution, showing stress concentration near junction. Stress near junction exceeds yield strength of mild steel for water pressure below normal water pressure

Examining the Results

The stress at the junction of the manifold was observed exceeding at normal running condition. The problem was resolved by adding extra reinforcing plate at junction in the form of T section

4. Conclusions

Around 20 models were checked for the loss of the head due to geometry of manifold between common profiles to most efficient profile. Only result for the most efficient profile is presented in this paper.

The Study indicates that the profile can be better tuned with the finite element application for fluid flow (Computational fluid dynamics).

The flow distribution in case of common profile is rather disturbed to longer zone of the trifurcation system. In case of most efficient profile the flow distribution is disturbed slightly to smaller length of the trifurcation system.

The second profile was taken for the fabrication to limit loss in head less than 1 m head of water

References

1. "ANSYS Fluid Analysis Guide", ANSYS Release 10.0.002184, ANSYS, Inc. South point 275 Technology Drive Canonsburg, PA 15317, August 2005.
2. Y.S. Chen, S.W. Kim, "Computation of turbulent flows using an extended $k-\epsilon$, Turbulence closure model", NASA CR-179204, 1987.
3. I. Buntić Ogor, S. Dietze, A. Ruprecht, "Numerical Simulation of the Flow in Turbine-99 Draft Tube", Proceedings of the third IAHR/ERCOFTAC workshop on draft tube flow 8-9 December 2005, Porjus, Sweden.
4. T.J. Chung, "Computational Fluid Dynamics", University of Alabama in Huntsville, CAMBRIDGE UNIVERSITY PRESS, First published at 2002.
5. Arne Kjølle, "Hydropower in Norway", Mechanical Equipment, A survey prepared by, Emeritus Norwegian University of Science and Technology. December 2001.
6. Xiaodong Wang, "On Mixed Finite Element Formulations for Fluid-Structure Interactions", PhD Thesis in Applied Mechanics, MIT, June 1995
7. F. Nobile, "Numerical approximations of fluid-structure interactions with applications to hemodynamics", Ph. D. Thesis, EPFL Lausanne (CH), 2001.
8. Ellen Kock, Lorraine Olson, "Fluid-structure interaction analysis by the finite element method-a variation approach", International, Volume-31, Issue-3, 24 June 2005.
9. University of Alberta ANSYS Tutorials - www.mece.ualberta.ca/tutorials/ansys.
10. P. Colella and E.G. Puckett, "Modern Numerical Methods for Fluid flow", UC Berkeley E266A course notes.
11. Thomas H. Pullia, "Solution Methods in Computational fluid dynamics", Based on notes from a VKI lecture series in 1986.

Life Cycle Assessment of Municipal Solid Waste Management System in Kathmandu, Nepal

Ramesh Ranabhat

Mechanical Department, Institute of Engineering, Pulchowk Campus, T. U. Nepal

Email Address: ramesh.ranabhat@ioe.edu.np

Abstract

Due to rapid urbanization, ever increasing population, limited resources and industrialization all-inclusive, the environmentally habitual management of municipal solid waste has become a global challenge. According to report of the National Population Census 2011, growth rate of Nepalese Population is 1.4 percent per annum with population density estimated at 181 per sq. KMs. Solid waste management in Nepal, the current practice of the illegal dumping of solid waste on the river banks has created a serious environmental and public health problem. The focus of this study was to carry out the magnitude of the present SWM problems by identifying the sources, types, quantities, dangers and opportunities they pose. It will be helpful to examine the adequacy of the existing institutional arrangements and implement a strategic and operational plan for SWM and to establish the EASEWASTE data base of municipal solid waste management system in Kathmandu City, Nepal.

Keywords: EASEWASTE, Solid Waste Management, LCA, SWM

1. Introduction

Due to limited resources, ever increasing population, rapid urbanization and industrialization the environmentally habitual management of municipal solid waste has become a global challenge. The urban population in industrialized country is 74% of the total population in those countries, whereas the urban population in developing nations accounted for 44% of the total 7 billion population of the world in 2011. However, urbanization is occurring rapidly in many less developed countries. It is expected that 70 percent of the world population will be urban by 2050, and that most urban growth will occur in less developed countries (UNPF).

Nepal is undergoing a population explosion in its urban areas in recent times especially due to rural

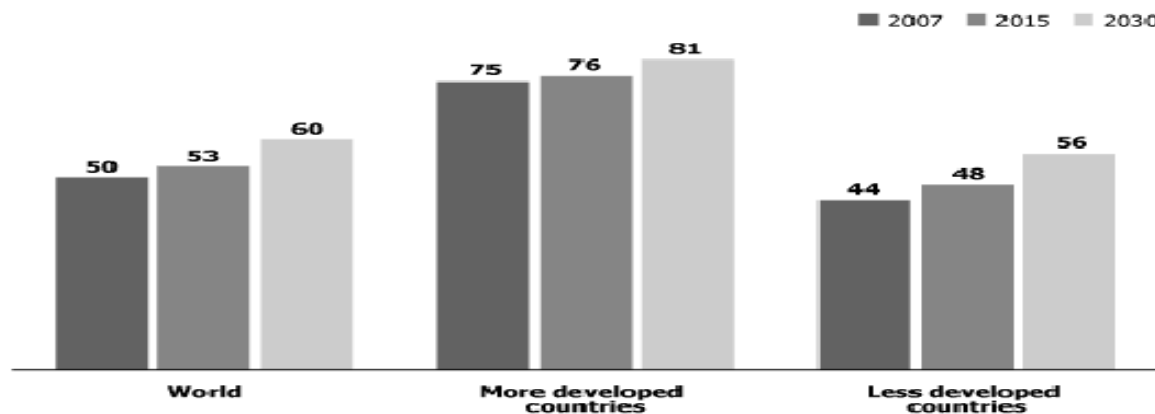


Fig 1 Percent of world urban population, 2007, 2015 and 2030(UNPF)

migrants seeking employment, business and other opportunities in the cities. The urban population of Nepal constitutes about 17 percent of the total population in 2011 compared to 14 percent urban population in 2001, which is low when compared with other developing nations. However, compared to the land area of the country and the available resources, this small urban population has become an enormous burden for the government in terms of environmental health, sanitation and environmental management.

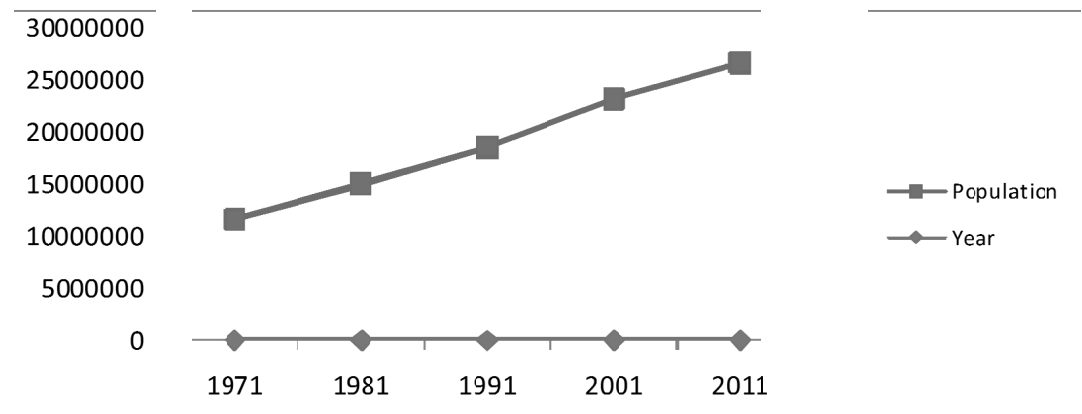


Fig 2 National populations according to censuses (CBS 2011)

Urbanization in Nepal is rapid and haphazard, creating problems in delivering services and facilities. Solid waste management has become a major challenge in most urban centers. Open waste piles are a common site and the work of municipalities' is often limited to sweeping the streets and dumping the waste in the nearest river or vacant land. The produced municipal solid waste (MSW) varies within Nepal and its municipalities. It is estimated that the total amount of municipal waste generated in Nepal is about 500,000 tons per year (Dangi, 2009). Solid waste was not such a big problem in the old days in the Kathmandu Valley. People in the Kathmandu Valley had their own method of managing their household waste, including circulation of organic waste between city and rural areas nearby. In line with increasing population in the Valley and changing life style and consumption habits, SWM has been increasingly recognized as one of the major environmental issues in the Valley as a result of the increasing amount of waste generated and the change of waste compositions. Gradually, the collection and disposal of solid waste started in some systematic way especially in KMC and LSMC, along with the operation of Gokarna Landfill (LF) which was developed in 1986. However, after closure of Gokarna LF in 2000 due to the opposition of the surrounding local people, final disposal could not stop going to river side dumping on a temporary basis, e.g. Bagmati River dumping

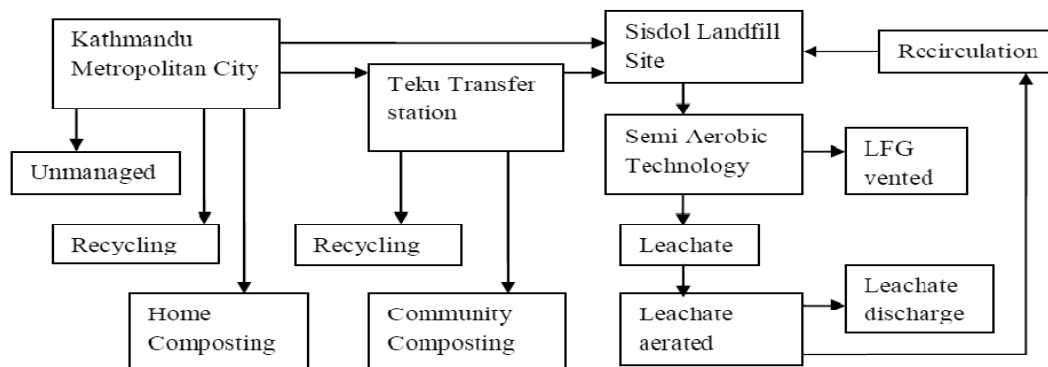


Fig 3 Solid waste management system of Kathmandu Valley

Leachate Treatment System:

The leachate collected in the pond is regularly aerated through proper aerator system, which can be regarded as biological aerobic treatment. The aerated leachate is further re-circulated by means of a pump to spray the leachate over landfill cells for a simple anaerobic biological treatment. The recirculation assists the waste to be more reactive and decompose faster than its normal rate. Hence, accelerating the rate of the methane and leachate production the Fig 4 below demonstrates the longitudinal profile of Leachate treatment plant.

Typical Longitudinal Profile : Landfill Area - Leachate Treatment Plant

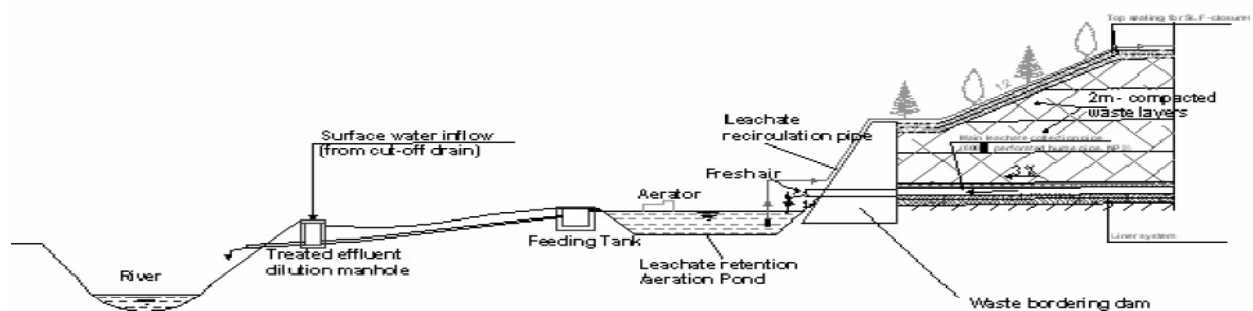


Fig 4 Leachate treatment plant in Sisdol landfill Site.

2. Methodology

For the Kathmandu case study, data have been collected mainly from Kathmandu Metropolitan City Office, Solid Waste Management and Resource Mobilization Center(SWMRMC), associated references and bibliographies. Some data which were unavailable were taken from the default database in EASEWASTE and it was utilized to represent a life-cycle inventory, a characterization of impacts and a normalized impact profile. System boundaries from the point of waste generation and source separation to the point after final disposal of the waste residuals are defined below with collected data and information.

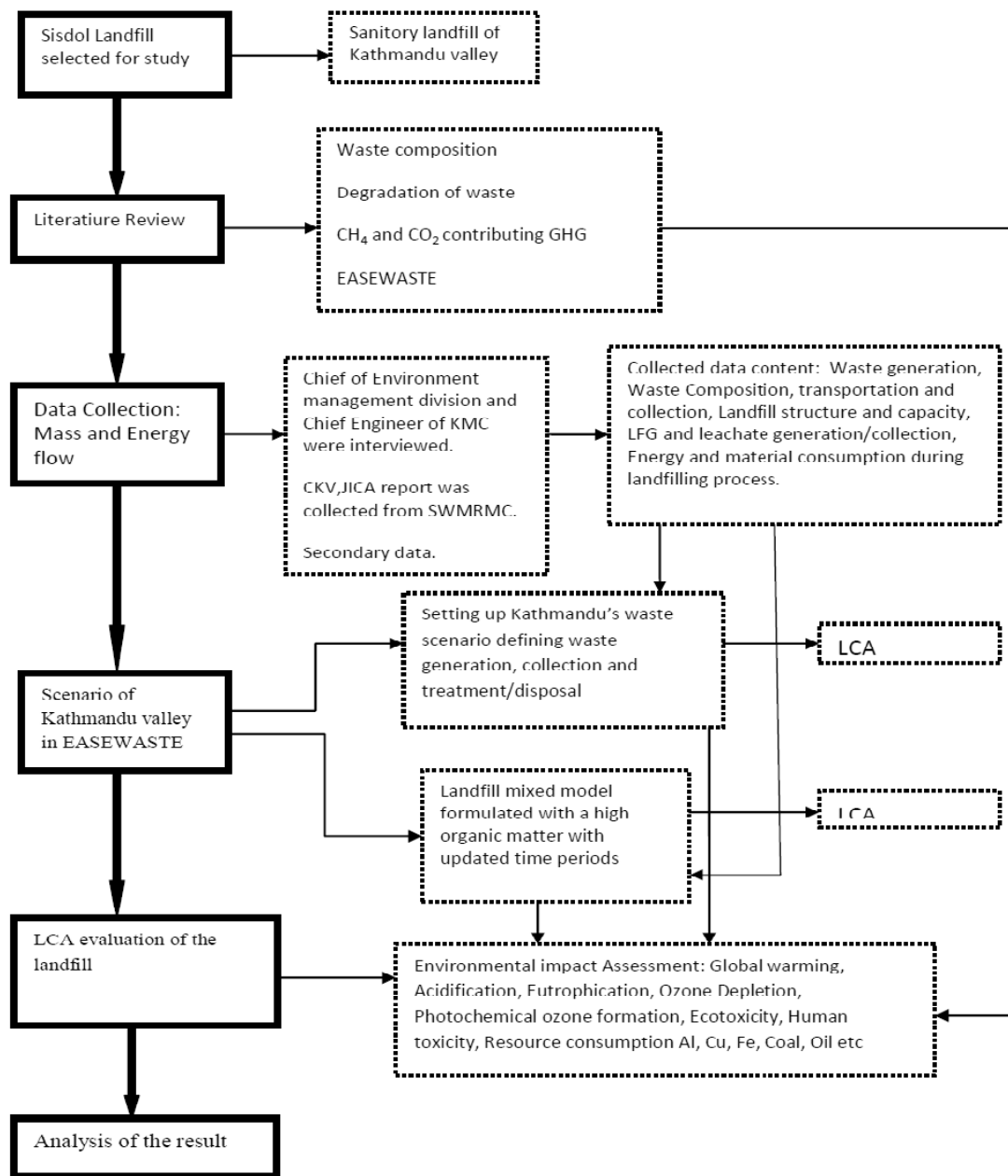


Fig 5 Flow chart of methodology

System Boundaries of the waste management system

Kathmandu is a metropolitan city located in the Central Development Region of Nepal and approximately 2,20,000 inhabitants lived in the City of Kathmandu in 2009, (Pradip Raj Pant).The housing is dominated by two to three storied multi-family Houses. The unit generation rate of waste was 0.4 kg per person per day, and the total amount of municipal solid waste was approximately 400 tons per day (KMC).The composition of solid waste used in this research is shown in the Fig 6.

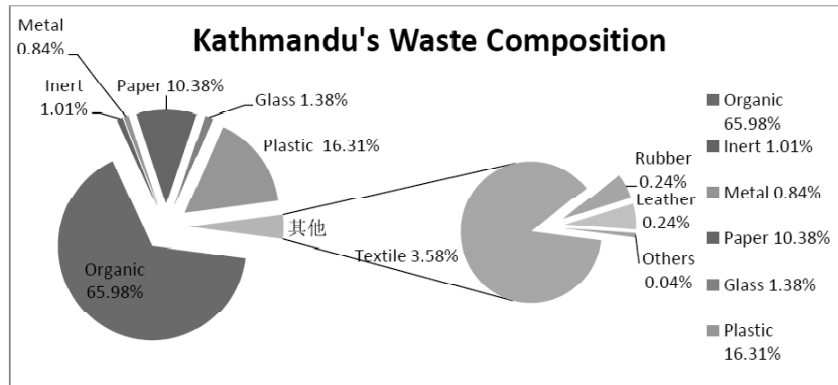


Fig 6 waste composition of Kathmandu valley(source: KMC 2001)

The total amount of solid waste was 146,000 tons per year, of which 96,360 tons per year was Organic waste which was individually collected from door to door, including 16,060 tons per year of waste paper, 24,820 tons of waste plastic, 1898 tons of waste glass and so on. The sorting efficiencies of the recycled materials of the waste including plastics, paper, and glass were assumed as 20%, 60% and 80% respectively. The integrated solid waste system of the city is represented in the Fig 7.

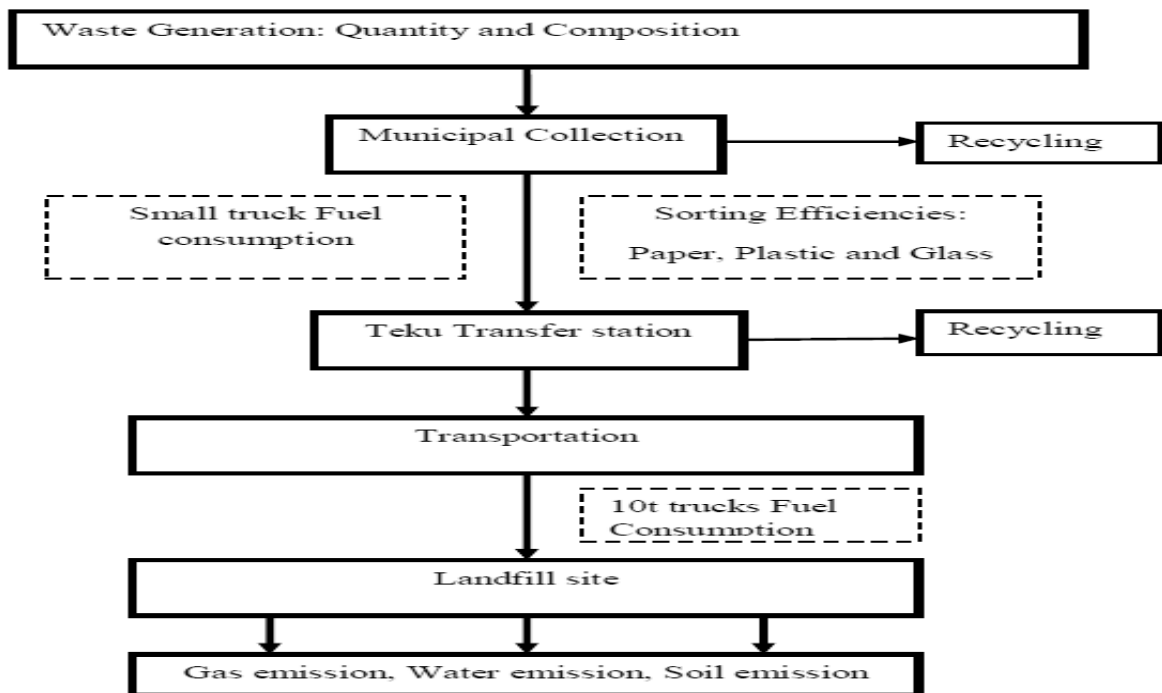


Fig 7 Municipal solid waste flow of Kathmandu City, Nepal (KMC)

Scenarios

The environmental assessment was based on three scenarios, in which the first two (scenarios 1 and 2) addresses the landfill treatment technologies and scenario 3 assesses the environmental impacts from composting all the organic matters generated from households of Kathmandu.

Scenario 1 is the current waste management system in Kathmandu, in which the mixed waste after recycling is sent to the landfill where land fill gas (LFG) emissions are not treated.

Scenario 2 is based on utilizing the LFG generated from the landfill for electricity production. All the data is exactly the same with scenario 1 except in scenario 2 the LFG is recovered and utilized.

Scenario 3 considers all the Organic waste generated from Kathmandu City is sent for composting and the remaining waste is sent to the landfill.

3. Result and Discussion

The results for all three scenarios were calculated as normalized potential impacts according to the normalized environmental impacts potential reference of Life Cycle Inventory Assessment (LCIA) method, EDIP 1997 (Wenzel et al. 1997). Normalization provides a relative expression of the environmental impact or resource consumption compared to the impact from one average person.

3.1 LCA evaluation of Kathmandu’s waste with and without Electricity production:

Figure 8 shows the non toxic environmental impacts caused by scenario 1 where it can be seen that the highest impacts during 100 year period are on Global Warming and Stratospheric Ozone depletion. The major contribution (direct impact) is due to disperse emissions (through landfill gas) of CH₄ and CFC12. The total quantity of CO₂-eq substances emitted that caused Global Warming is 249,148.724 kg per year with reference to EDIP97

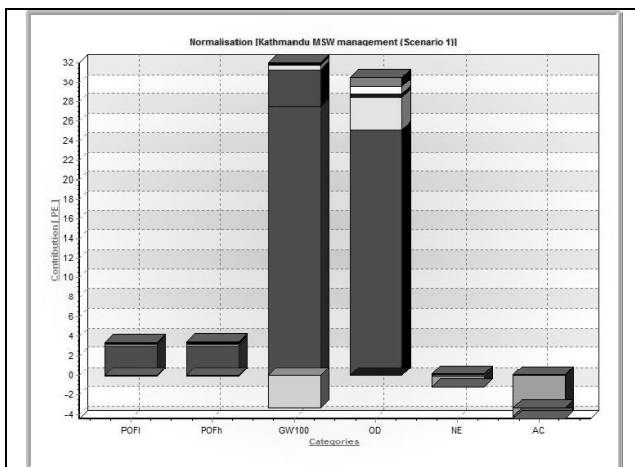


Fig 8 Normalized potential impacts for scenario 1

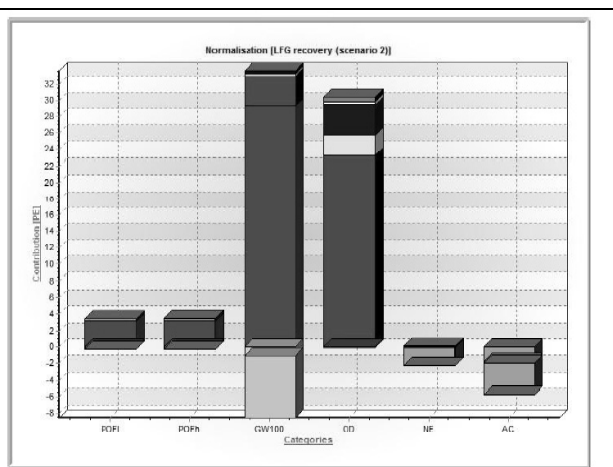


Fig 9 Normalized potential impact for scenario 2

The Fig 9 shows the non toxic environmental impacts caused by scenario 2 that has more or less similar trend of the impacts as of scenario 1. The figure 10 displays the compared graph of scenario 1 and scenario 2. In all the impact categories, scenario 2 i.e. the landfill with LFG recovery system demonstrated the better result than scenario 1, without LFG recovery. The total amount of non toxic environmental impacts of both the scenarios, are demonstrated in the table 1

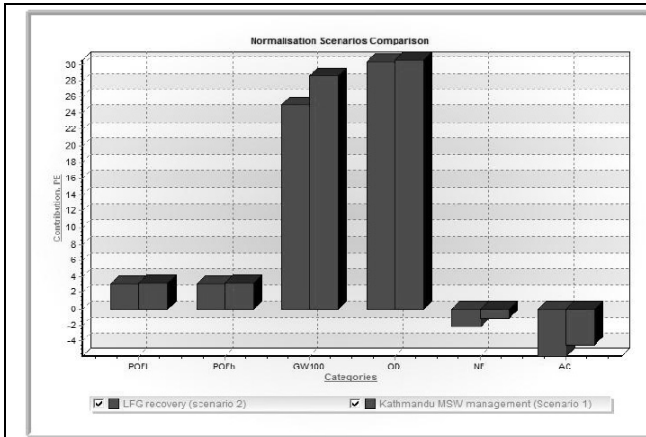


Fig 10 Normalized potential impact of scenario 1 and scenario 2

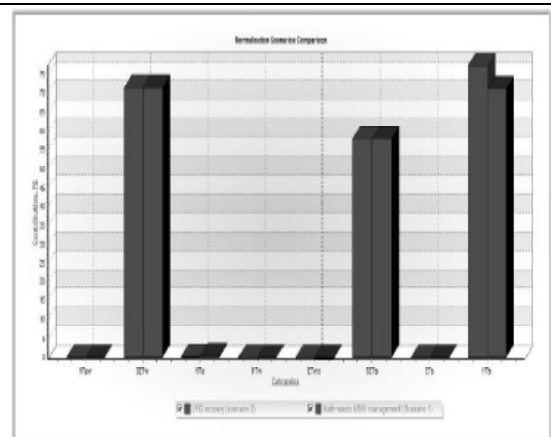


Fig 11 Normalized potential impact of scenario 1 and scenario 2(toxic)

Table 1 Environmental Impacts (toxic) of scenario 1 and 2

Photochemical Ozone Formation, Low NOx [kg C2H4-eq]	Photochemical Ozone Formation, High NOx (EDIP97): [kg C2H4-eq]	Global Warming NOx [kg (EDIP97): [kg CO2-eq]	Stratospheric Ozone Depletion (EDIP97): [kg CFC11-eq]	Nutrient Enrichment (EDIP97): [kg NO3-eq]	Acidification (EDIP97): [kg SO2-eq]
80.282	81.586	249,148.724	3.144	-	-
79.035	80.793	215,875.606	4.258	133.028	327.64
				308.462	469.521

3.2 Environmental Assessment of Composting compared with Landfill with and without Recovery

Figure 11 shows environmental impacts caused by scenario 3, the scenario where all the organic contents of the city is assumed sending for composting instead of land filling. The impact on Nutrient enrichment is high due to high quantity of Ammonia (NH3) and Phosphate (PO4) discharged from composting. Emission of 23,246 kg of CO2-eq contributes to the impact on Global warming which is 90% less than the actual scenario of Kathmandu City and 75% from scenario 2.

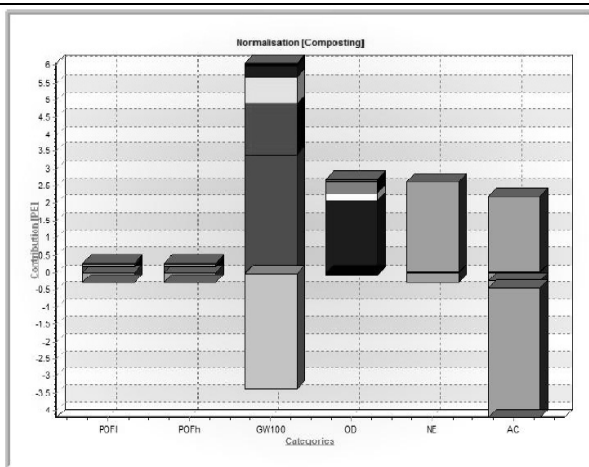


Fig 12 Normalized Environmental impacts of scenario 3

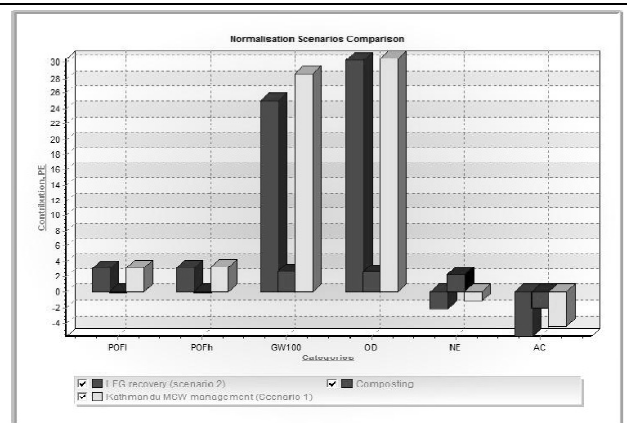


Fig 13 Normalized environmental impacts of Scenario 1, scenario 2 and scenario 3

The fig12 demonstrated that composting scenario was regarded as one of the best alternatives for the management of solid waste according to the Life-Cycle perspective. Impact on Global warming is significantly reduced by 91.6% compared to scenario 1 and 91.4% compared to scenario 2 because reduced amount of CFCs were generated from the landfill due to the absence of Organic waste.

Table 2 Comparison of scenario 1 and scenario 2

Impacts	Scenario 1 PE	Scenario 2 PE	Difference in PE	Remarks
Global Warming	28.638	25.018	-3.62	Scenario 2 is marginally better than scenario 1
Photochemical Ozone formation Stratospheric zone depletion	3.263	3.177	-0.086	Scenario 2 is marginally better
Nutrient Enrichment	-1.118	-2.128	-1.01	Scenario 2 is better than scenario 1
Acidification	-4.428	-5.77	-1.342	Scenario 2 is better than scenario 1

Table 3 comparison of scenario 2 and 3

Impacts	Scenario 2 PE	Scenario 3 PE	Difference in PE	Remarks
Global Warming	25.018	2.672	-22.346	Scenario 3 is significantly better than scenario 2
Photochemical Ozone formation Stratospheric Zone depletion	3.177	-0.007	-3.184	Scenario 3 is significantly better than scenario 2
Nutrient Enrichment	-2.128	2.359	-4.487	Scenario 2 is better
Acidification	-5.77	-1.118	-6.88	Scenario 2 is better

3.3 Life Cycle Assessment of the landfill with LFG Recovery

This scenario describes the assumed scenario of Kathmandu city where the landfill is equipped with electricity generation system. The resources consumed in this scenario were fewer than that of the actual scenario of Kathmandu. Water cooling was again a major raw material that was consumed for cooling the engines of the vehicles. 1330 kg of water was needed for cooling the engines of the vehicles. Natural gas was consumed in a lesser amount than that of Kathmandu's real scenario, i.e. only 4.782E-6 kg of gas was used per ton of waste. Similarly, other substances like Calcium Chloride, Iron, and Aluminum etc were used along with clay and soil for the liner and daily cover respectively. Due to the production of electricity almost 12 to 15 percent methane is reduced causing less Green house effect resulting in less impact on global warming than in the actual scenario.

3.4 Analysis of Life Cycle Assessment of three scenarios: Landfill without LFG recovery, Landfill with LFG recovery and Composting of Organic waste.

When all the Organic waste is composted instead of sending it to the landfill, only 2 liters of fuel is combusted per day using only 0.3 Kwh of electricity whereas 6 liters of fuel is used up for the scenario 1 and scenario 2. The electricity consumption for the landfill with electricity generation technology is highest than other scenarios due to the use of electricity for generators. The collection and transportation vehicles are very few in number, for composting, resulting in less consumption of fuel. Therefore, in the sector of energy consumption, composting the Organic matter, which covers the large content of waste i.e. ~70%, is the best alternative for Kathmandu City. According to the Life Cycle Assessment, Water is the major raw material that has been consumed in all of the three scenarios. Collection and transportation phases are the main area where water was consumed for the cooling purpose. Comparatively, less amount of water was consumed for composting scenario. Likewise, Natural gas was consumed in similar amount for the actual scenario of Kathmandu and the scenario where all the organic waste is composted. When compared between three scenarios, scenario of the Kathmandu where the waste is dumped into the landfill with electricity generation, consumed very less raw materials. Therefore, in the sector of raw material consumption, it can be analyzed that, landfill with electricity production is best for consuming less amount of raw materials. Methane is the major emission mainly dependent upon the composition of the solid waste and partially to the collection and transportation phase. Since, all the Organic waste is send for composting in scenario 3, the methane is mostly generated from the remaining waste and the collection and transportation phase. When the waste is dumped to the landfill with the energy recovery system, 14% of methane was reduced than the landfill without energy recovery hence proving to impact less on Global warming. According to the LCIA 80% of the heavy metals come from organic waste and remaining from the inorganic waste.

4. Conclusion

The results from the environmental assessment of the solid waste system in the City of Kathmandu showed that the Landfill Gas Recovery from the landfill and utilizing the Gas for Electricity production is relatively better than the current system, mainly due to the lowering of Green House Gases such as Methane, CFCs etc while the increasing in energy production from waste. The organic content of the Kathmandu city is very high, which means that more the organic matter higher the amount of methane, likewise, higher the amount of methane, more the generation of electricity. Therefore, the energy recovery system will give the city advantage from both the sides; lower the emissions of Green house gases and utilization of electricity.

References

1. M. Abu-Qudais, H.A.A. Abu-Qdais, “*Energy content of municipal solid waste in Jordan and its potential utilization*” ; Energy Conversion and Management, Volume 41, pp. 983-993, 2000.
2. M.F.M. Abushammala, N.A. Basri, A.H. Kadhum, “*Review on Landfill Gas Emission to the Atmosphere*”. Department of Civil and Structural Engineering 30, 427-436, 2009.
3. J. Acharya, S. Basnet, K. Sharma, P.S. Subedi, Y. Adhikari, “*Sisdol landfill Gas to Energy Project*”, Promotion of Renewable Energy, Energy Efficiency and Green House Gas Abatement (PREGA), CDM project Design Document, Nepal, 2006.
4. ADEME, Dechetmunicipaux/les chiffresclés, Agence de l, “*Environ. et de la Matrise de l*” (2000), EnergieAPAT-ONR (2004): Rapportoriuti 2004
5. “*Analysis of Urban Environmental Issues*”, World Bank/ ENPHO, 2007.
6. T. Astrup, H. Mosbæk, T.H. Christensen, “*Estimating long-term leaching from waste incineration air-pollution-control residues*”, Waste Management 26, 803–814, 2006.
7. M.A. Barlaz, P.O. Kaplan, S.R. Ranjithan, R. Rynk, “*Evaluating environmental impacts of solid waste management alternatives*”, Biocycle 2003 (October), 52–55, 2003.
8. M.A. Barlaz, P.O. Kaplan, S.R. Ranjithan, R. Rynk, “*Evaluating environmental impacts of solid waste management alternatives*” Biocycle 2003 (October), 52–55, 2003.
9. C.H. Benso, M.A. Barlaz, D.T. Lane, J.M. Rawe, “*Practice review of five bioreactor/recirculation landfills*”, Waste Management 27, 13-29, 2007.
10. “*A Diagnostic Report on State of Solid Waste Management in Municipalities of Nepal*”, Solid Waste Management and Resource Mobilization Centre, Lalitpur, SWMRMC, 2004.
11. Wenzel et al, “*Danish Experience with the EDIP Tool for Environmental Design of Industrial Products*”, 1997

POULTRY FAECES MANAGEMENT BY BIOCONVERSION TECHNOLOGY WITH MODIFIED GGC 2047 MODEL

S.K. Neupane¹, Ram K. Sharma², Shiva Shankar Karki³

¹Department of Civil Engineering, Advanced College of Engineering & Management, Lalitpur-1, Kathmandu, Nepal

²Department of Engineering Science and Humanities, Institute of Engineering, Central Campus, Pulchowk, Tribhuvan University, Nepal

³Department of Civil Engineering, Institute of Engineering, Central Campus, Pulchowk, Tribhuvan University, Nepal

Email Address: shreekrishna.neupane@acem.edu.np

Abstract

In this report, entitled “Poultry Faeces Management by Bioconversion Technology with Modified GGC 2047 model” focuses on various parameters relating to physico-chemical characteristics of the substrate, fertilizing value of digested poultry waste and potential to create profitability from biogas energy, thus generated and balancing the environmental aspects using poultry waste digestion. Also, biogas may be the tool of energy generation in rural areas while sanitation (waste management) in urban areas of developing countries as Nepal. Biogas production from chicken faeces could be obtained more effectively by feeding around 8.5 kg per day. It is concluded that digester could be run by around 2.5 quintal chicken faeces per month. Hence those people, who can manage this quantity of waste, can utilize bio-digester without poultry farm.

Keywords: GGC, Poultry Faeces, Fertilizing value, Biogas.

1. Introduction

Poultry faeces are directly used to fertilize farm for agriculture purpose in developing countries. This is in contrast to industrialized countries where poultry faeces are used only after giving certain degree of treatment as composting. These practices are, however, unaffordable to most urban or rural inhabitants of developing countries.

While substantial progress has been made in the field of solid waste management in developing countries over the past decades, the management and treatment of chicken droppings from poultry farm has not been addressed, either by producers or by any researchers. This is surprising as the absence or insufficiency of adequate poultry faeces management in many cities of developing countries, particularly so in low-income areas, continuously leads to serious health and environmental hazards. Chicken manure is highly sensitive to surface and groundwater as well as results in unaesthetic appearance of the area. Incineration of manure adds to the greenhouse gases in the atmosphere so it is one of the sources of environmental pollution. Currently the fertilizer values of chicken waste are not being fully utilized, resulting in loss of potential nutrients. So, proper management of chicken waste is necessary to achieve the fertilizing value and to reduce the pollution problem. A reason for this backlog in dealing with poultry faeces in urban areas is, among others, the paucity of appropriate managerial and technical measures.

Disposal of untreated poultry faeces into the farm is one of the major environmental issues in rural area. The use and improper disposal of animal wastes is one of the major sanitation problems in urban and semi-urban areas in developing countries. A number of pathogenic (disease causing) agents are also disseminated through untreated chicken manure and the economic losses accruing from these are enormous. Additionally, the fresh and semi-dried animal droppings sprayed on the farm as fertilizer is a potential health hazard to grazing animals and leaching effect into ground and surface water also poses great danger to humans.

The main focus of this study is to determine the Biogas production with different feeding rates. The specific objectives are; to study and measure the nutrient value (Total Nitrogen, Phosphorus and Potassium) also physical parameters (pH, Temperature, Moisture Content, Volatile Solids and Total Organic Carbon) of the chicken waste before and after digestion and to evaluate the performance of 4 m³ modified GGC 2047 model, fixed dome bio-digester as approved by BSP Nepal.

2. Methodology

Experimental Setup

The study was carried out in three cycles with a time period of 30 days each. Each cycle was conducted continuously and data recorded for gas production was cumulative volume. In all the cycles, *layers faeces* is only used as feedstock and frequency of feeding was 4 days. In the first cycle (cycle I) dose of feedstock was 30 kg, the second cycle (cycle II) dose of feedstock was 35 kg and in third cycle (cycle III) feedstock dose was 25 kg respectively in batch basis. To make slurry, water added to feedstock was 70 liter, 80 liter and 60 liter for first, second and third cycle respectively.

In this study, the included parameters for examinations were; measurement of temperature, pH, moisture content, total volatile solids, total organic carbon, total nitrogen, potassium, and phosphorous. In addition to this, daily biogas production and the cumulative volume was also observed. The conceptual framework of the study in each of the cycle is presented in the Fig1.

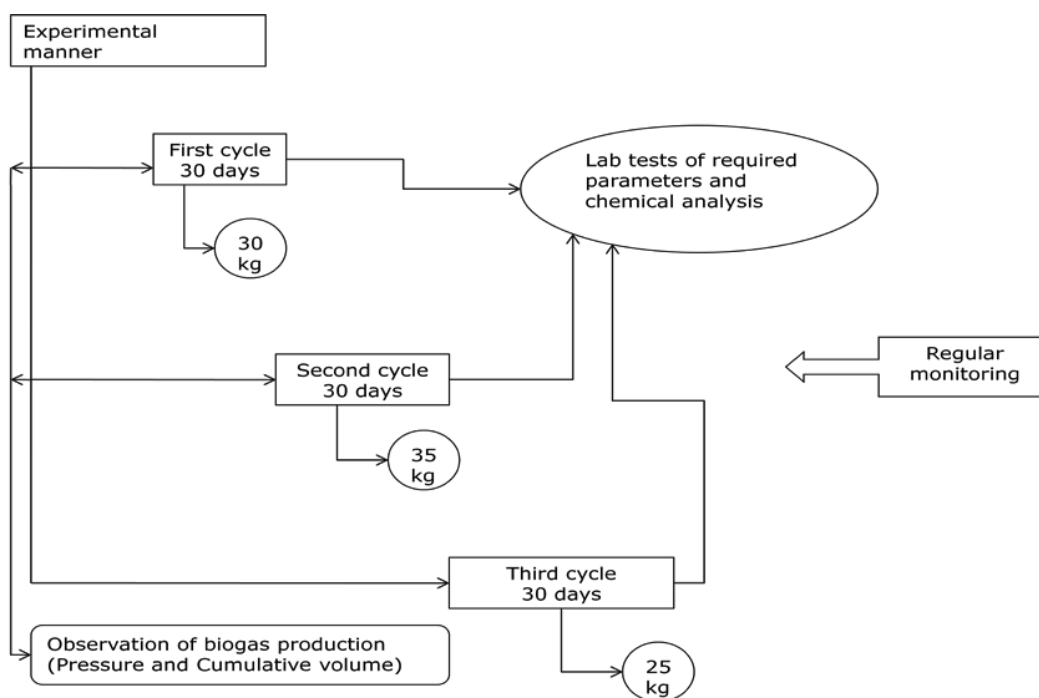


Fig1 Conceptual framework of the study

3. Result and Discussion

In each cycles, the effect on anaerobic digestion of temperature, pH, moisture content, total volatile solids, total organic carbon and total nitrogen, phosphorus and potassium content of influent and effluent were observed and analyzed. In addition to this, the biogas production in cumulative volume and dome pressure was observed and analyzed. The results obtained and their corresponding discussions of observed parameters during the study are presented in this chapter.

3.1 Variation in Temperature

Ambient temperature was observed between 25°C and 35°C where as digester temperature was between 29°C and 38°C observed in all three cycles as shown in fig 3. Reason of temperature difference is that, during the anaerobic reaction, there will be heat generation; so the reactor temperature is slightly more than ambient.

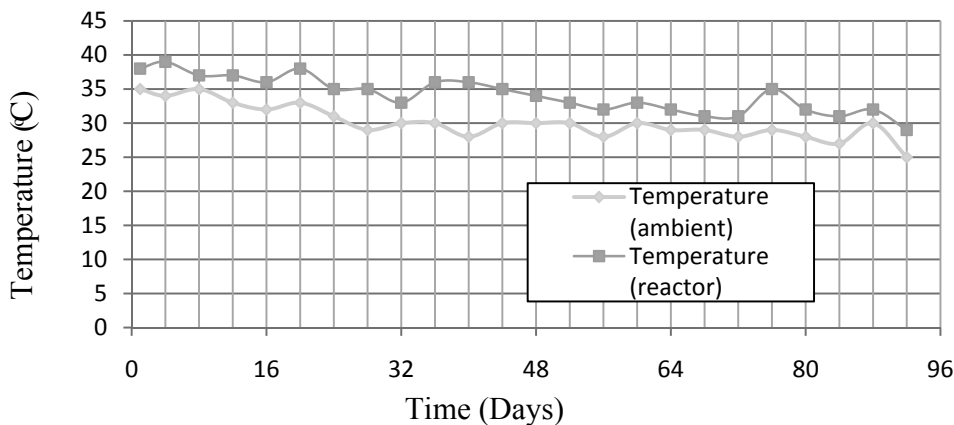


Fig 3 Variations of the temperature in the reactor and ambient

As the minimal average temperature for the methanogenesis process is above 13 degree Celsius. The ambient as well as inside reactor temperature recorded was above 25 degree Celsius. So the temperature recorded here is considered satisfactory for the methanogenesis.

3.2 Variation in pH

The variation in pH of feedstock and sludge in each cycles of each sample are shown in the Fig 4.

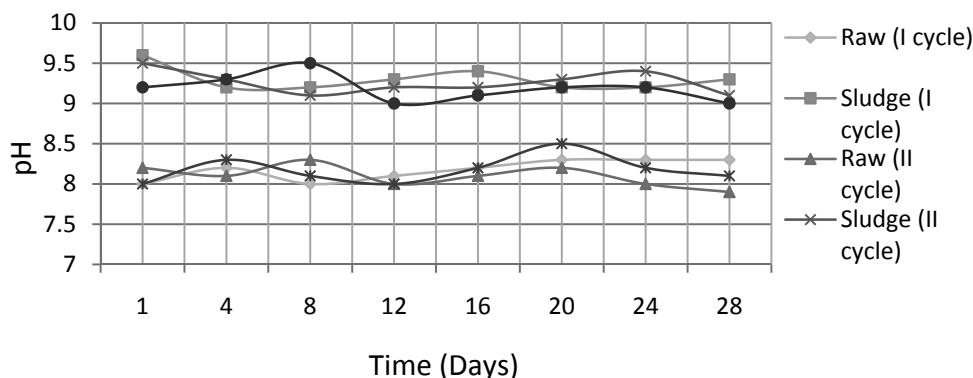


Fig 4 Variations of pH in the different cycles of each sample

In the cycle I, the pH of the fresh droppings was found to be 8 and it reached to 9.2 after digestion. Similarly in the rest of two cycles pH found was like to first cycle. In chapter 2.3.3 it was explained that the optimum biogas production is achieved when the pH value of input mixture in the digester is

at 7. Methanogenic bacteria are very sensitive to pH and do not thrive below a value of 6.5. Here the pH value obtained was above 6.5, so the methanogenesis is not presumed to be affected.

3.3 Variations in Moisture Content

The variation in moisture content of feedstock and sludge of different cycles of each samples are shown in the Fig 5.

The moisture content variation in all cycle was 75 to 90 percent in sludge where as in raw stage or material 15 to 50 percent. In all cycles the result obtained was quite similar, this is why that, the process is continuous system and feedstock fed was from same poultry farm.

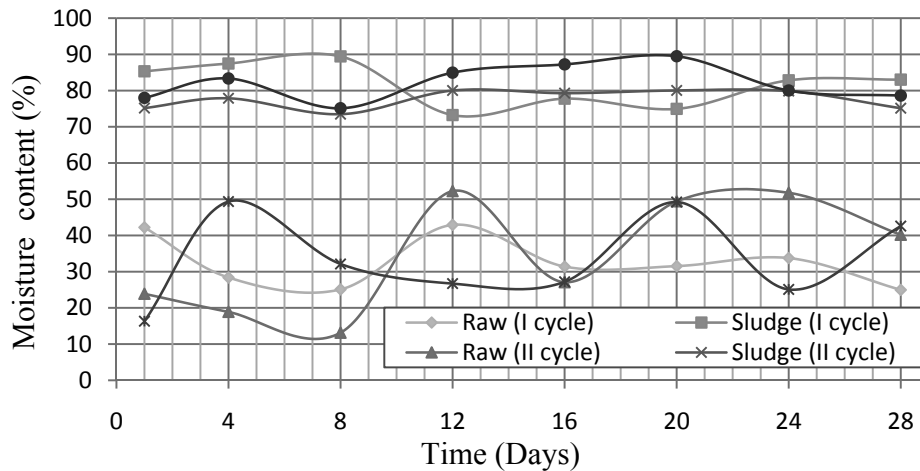


Fig 5 Variations of moisture content in the different cycles of each sample

3.4 Variations in Volatile Solids

The variation in the volatile solids in different cycles of each sample has been presented in the Fig 6.

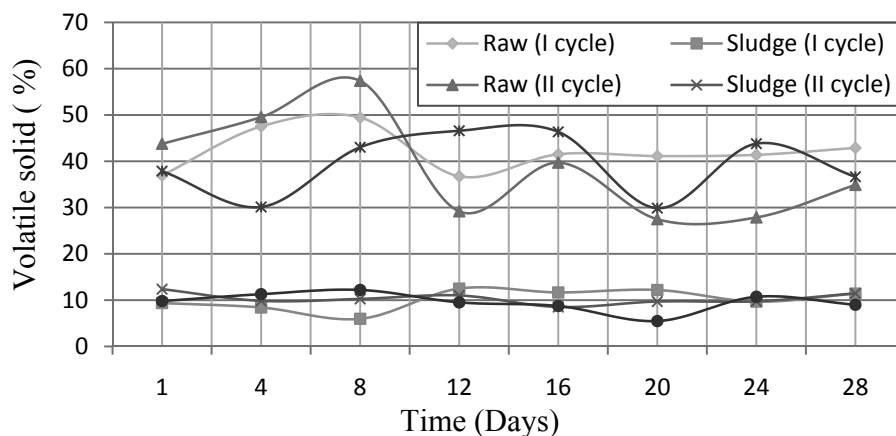


Fig 6 Variations of volatile solids in the different cycles of each sample

The raw chicken droppings containing the volatile solids of 29 to 59% were found reduced to 8 to 12% in digested sludge. The volatile solid content of the manure significantly reduced in all the cycles. The reduction of volatile solids in digestion is due to the utilization by microorganisms and for respiration and cell growth.

The volatile solids representing the organic matter were in decreasing trend throughout the experiment period. The reduction is an indication of stabilization of the fermentation process. The volatile solids in all the cycles were reduced nearly in the similar trend. It represents that the organic matter was steadily decomposed throughout the experimental period in all of the cycles.

3.5 Variations in Carbon Content

Total organic carbon was derived from the volatile solid data as per empirical formula by Gottas as stated by Bhandari (2004). It can be related by dividing volatile solids by 1.8. The change in the total organic carbon in the different cycles of each sample has been presented in the Fig 7.

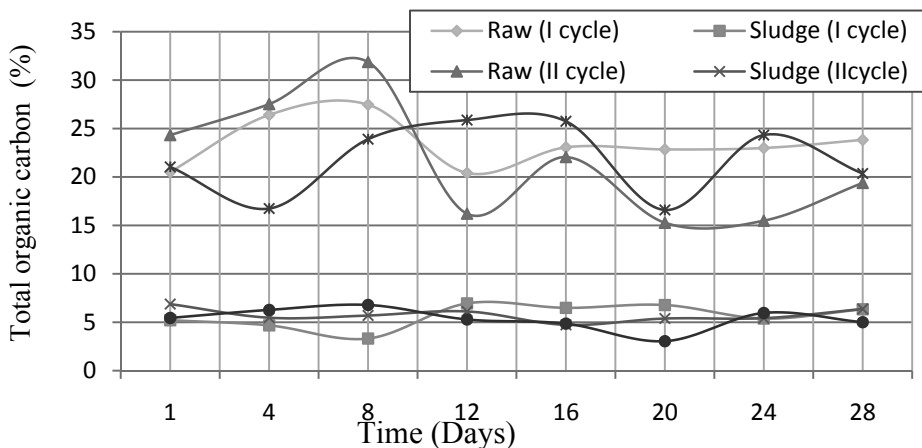


Fig 7 Variations of total organic carbon in the different cycles of each sample

In all cycles, the carbon content range of 15 to 32% in raw chicken droppings was found reduced to range of 4 to 7 % in digested sludge.

The reduction in carbon content is due to the combustion of carbon substances during the respiration and therefore represents the microbial activity in the anaerobic digestion. The reduction of carbon content was more in third cycle than other cycles. This shows a greater mineralization rate in the anaerobic digestion process due to lowest feeding rate. This indicates that the third is more efficient in the reduction of carbon content.

3.6 Variation in Nitrogen (N) Content

The changes in the total nitrogen in the different cycles are presented in the Fig 8.

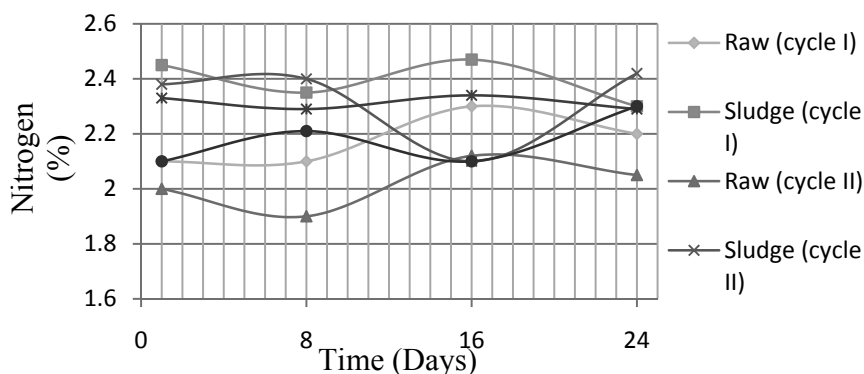


Fig 8 Variations of nitrogen in the different cycles

The percentage concentration of nitrogen is 2.01 in the raw poultry waste. In the study it was not considered the determination of $\text{NH}_4\text{-N}$ salts. So though nitrogen concentration seen to be decreased during fermentation, it is assumed that the total concentration of the ammonia compound is increased (Singh, 2004). Further, once the system becomes stable the methanogens are also capable of adapting to ammonium nitrogen concentrations in the range of 5000 to 7000 mg per liter substrate. The level of nitrogen concentration in this case is increased and the fertilizer value in terms of available nitrogen is also increased in the slurry. Also during the methanogenesis process nitrogen inhibition is presumed to be not occurred here.

3.7 Variation in Phosphorus (P_2O_5) Content

The variation of phosphorus in the different cycles is presented in the Fig 9.

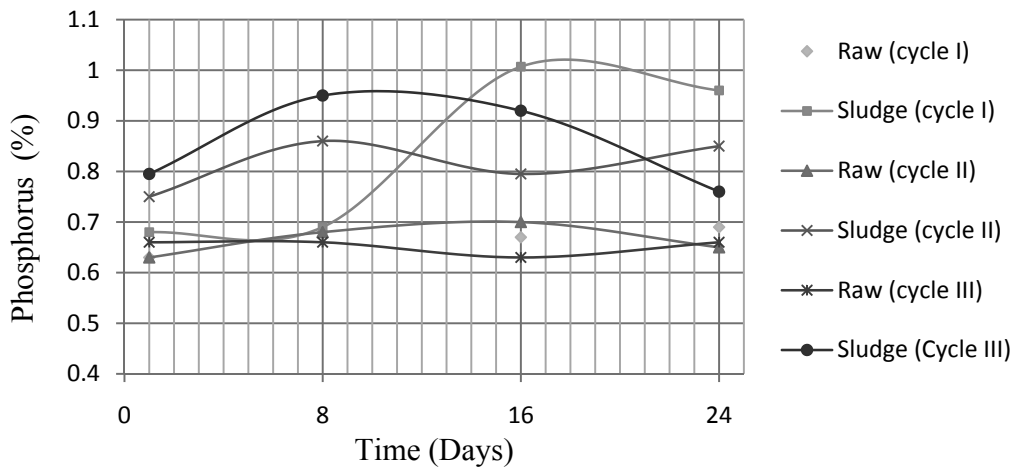


Fig 9 Variations of phosphorus (P_2O_5) in the different cycles

Phosphorus is 0.66% at the raw poultry waste and found slightly increased in digested slurry. The concentration of phosphorus has no serious inhibition in the anaerobic digestion. It has retained good level of fertilizer value of digested slurry.

3.8 Variation in Potassium (K_2O) Content

The variation of potassium in the different cycles is presented in the Fig 10.

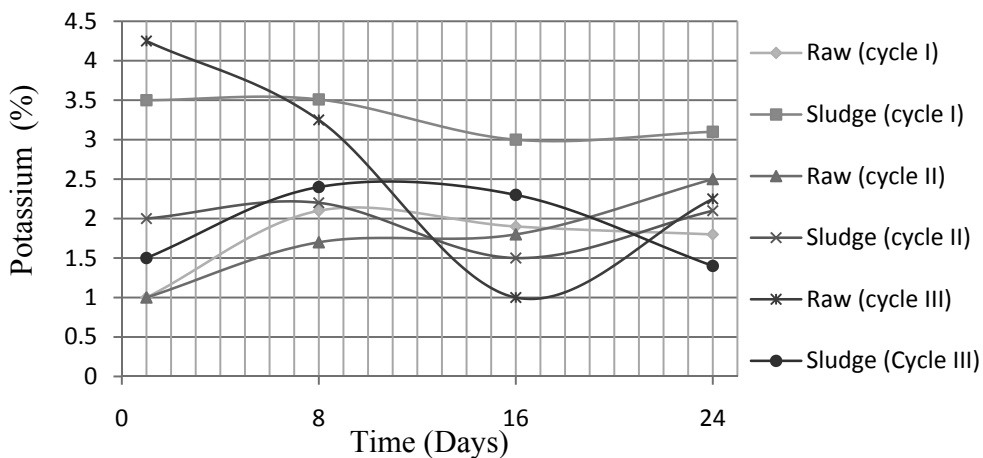


Fig 10 Variations of potassium (K_2O) in the different cycles

The initial potassium content in the raw chicken droppings was 1.01 % in cycle I and in the similar trend of rest two cycles. The potassium content of the slurry has no serious affect on the inhibition of methanogenic bacteria. However it is considered to be beneficial to the fertilizer value of the slurry.

It has been observed that all the cycles are good in terms of conservation of nutrient nitrogen, phosphorus and potassium. Overall nutrient conversion is higher in anaerobic digestion. The changes in the nutrient values during the different cycles were variable and a distinct pattern was not observed but the pattern followed is in increasing order.

3.9 Variations in Carbon to Nitrogen Ratio (C/N)

The change in the C/N ratio in the different cycles of eight days sample has been presented in the Fig 11.

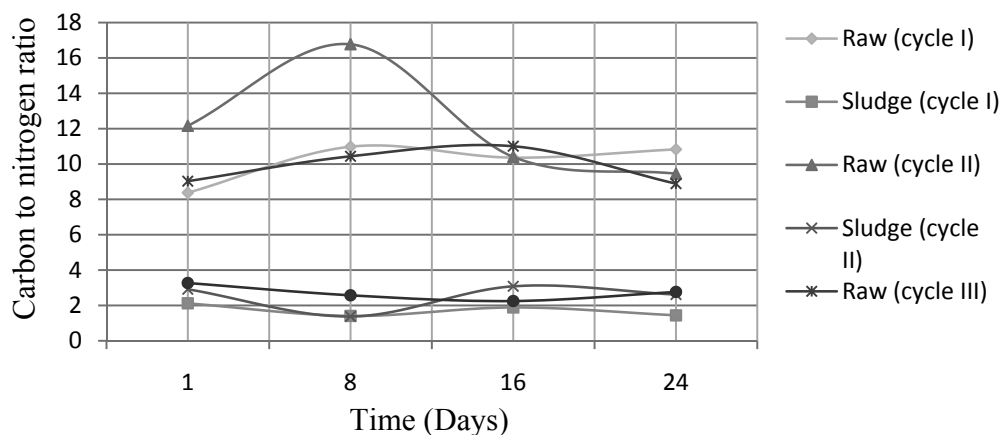


Fig 11 Variations of carbon to nitrogen ratio (C/N) in the different cycles

The initial C/N ratio in the raw chicken dropping was 10 in cycle I and its value were reduced after digestion to 3. Rest of cycles value observed was also in the similar trend.

If C/N ratio is very high, the nitrogen will be consumed rapidly by methanogens for meeting their protein requirements and will no longer react on the left over carbon content of the material. As result, gas production will be low. On the other hand, if the C/N ratio is very low; nitrogen will be librated and accumulated in the form of ammonia. Ammonia will increase the pH value of the content in the digester. At pH higher than 6.5, it will start showing toxic effect on methanogen population (FAO/CMS, 1996).

All the systems showed a decreasing trend in the C/N ratio as reported by Bansal and Kapoor (1999). The lowering of C/N ratio is due to the combustion of carbon substances during respiration. The value of C/N ratio is one of the most widely used indices do determine the slurry digestion.

3.10 Variations in Biogas Production

The gas produced is recorded in the flow meter. The gas produced which is measured in flow meter has been presented in the Fig 12.

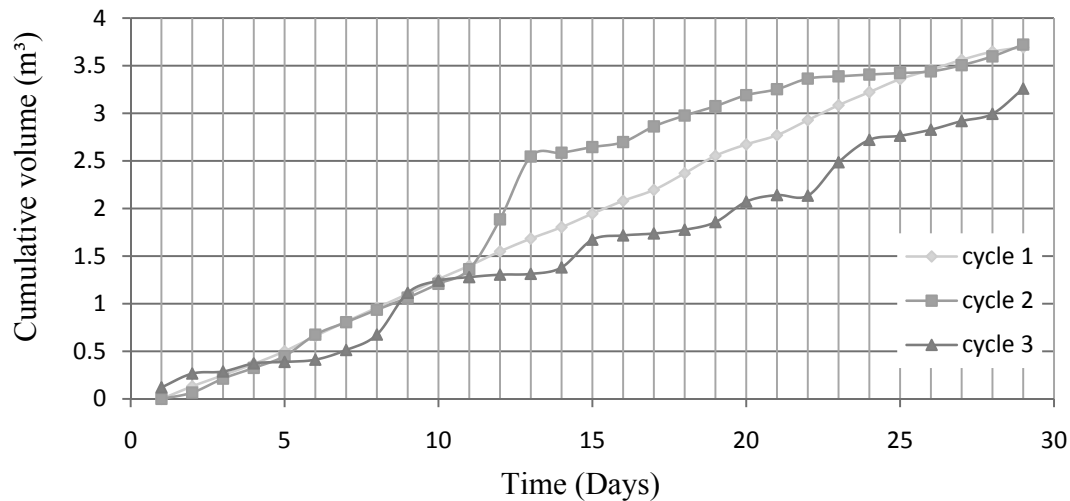


Fig 12 Variations of production of biogas in the different cycles

Higher biogas production was observed in second cycle than of other first and third cycle due to the higher feeding of poultry waste. By the observation it is known that biogas production from chicken droppings could be obtained more efficient by feeding around 8.5 kg per day. In second cycle there is more volatile solid destruction than other two cycles that is the reason of more gas generation. The biogas produced in the second cycle has greater volume among all other cycles due to higher feeding rate.

4. Conclusion

From the experiment, it was concluded that the biogas generation from chicken manure could be carried out successfully in the *layers faeces*. Based on the results obtained from the experiment and analysis of the results, the following conclusions were drawn;

1. The temperature requirement for bacteriological methane production was easily obtained in the research period. The temperature obtained in fermentation chamber was about 4°C above from ambient. It is suggested that the gas production can be increased in cold season by providing proper insulation of digester.
2. The methane producing bacteria thrive under neutral to slightly alkaline conditions. It was observed that the pH of raw chicken droppings remain in alkaline range of 8 to 8.5.
3. The moisture content obtained in chicken droppings was 15 to 50%, so that water added to prepare slurry required was relatively high to other animals dung like cow/buffalo and also the reason is that of more water requirement as higher ambient temperature observed was around 35°C. The effluent or digested sludge or slurry has moisture content range of 75 to 90%.
4. The raw chicken droppings containing the volatile solids of 29 to 59% were found reduced to 8 to 12% in digested sludge. The volatile solid content of the manure significantly reduced in all the cycles. The reduction of volatile solids in digestion is due to the utilization by microorganisms and for respiration and cell growth.
5. The carbon content range of 15 to 32% in raw chicken droppings was found reduced to range of 4 to 7 % in digested sludge. The reduction in carbon content is due to the combustion of carbon substances during the respiration and therefore represents the microbial activity in the anaerobic digestion.
6. It has been observed that all the cycles are good in terms of conservation of nutrients nitrogen, phosphorus and potassium. Overall nutrient conversion is higher in anaerobic digestion. The

changes in the nutrient values during the different cycles were variable and a distinct pattern was not observed but the pattern followed is in increasing order.

7. The initial C/N ratio in the raw chicken dropping was 10 in cycle I and its value were reduced after digestion was 3. Rest of cycle's value observed is that of similar trend. For metabolic activity, the C/N ratio of methanogenic bacteria is found to be optimized at approximately 8 to 10, here also the observed ratio remains to this range. If C/N ratio is very high, the nitrogen will be consumed rapidly by methanogens for meeting their protein requirements and will no longer react on the left over carbon content of the material. As result, gas production will be low.
8. It is recommended that biogas production from chicken droppings could be obtained more effectively by feeding around 8.5 kg per day. During the study average burning period of stove or consumption of produced gas was 2.5 hours. It is concluded that digester could be run by around 2.5 quintal chicken droppings per month hence those family who can manage this quantity waste; they can construct bio-digester without having their own poultry farm.

5. Acknowledgement

This work was supported by the BSP Nepal by providing instrument flow meter, pressure gauge and other accessories for the analysis. We would like to extend our heartfelt gratitude and sincere appreciation to Professor Dr. Bhagwan Ratna Kansakar for his encouragement and valuable suggestions till this final stage of the study.

References

1. S. Bansal and K. K. Kapoor, "*Vermicomposting of Crop Residue and Cattle Dung with Eisenia Foetida*". Bioresource Technology, 73: 95-98, 1999.
2. H. S. Bhandari, "*Survival Growth and Reproduction of Eisenia Fetida During degradation of Dried Human Feces*". MSc. Thesis No. 058/MSE/302, IOE, Pulchowk-Nepal, 2004.
3. CAMMG, "*Canada Animal Manure Management Guide*", Agriculture Canada. Ottawa, 1979
4. D. R. Cullimore, A. Maule and N. Mansuy, "*Ambient Temperature Methanogenesis from Pig Manure Waste Lagoons; Thermal Gradient Incubator Stuidies*", Agricultural Wastes, 1985.
5. FAO/CMS, Food and Agriculture Organization of The United Nations, Support for Development of National Biogas Programme (FAO/TCP/NEP/4451-T), "*Biogas Technology: A Training Manual for Extension*", Consolidated Management Services Nepal (P) Ltd, 1996.
6. ISAT/GTZ, "*Biogas Digest Volume I. Biogas Basics*", Information and Advisory Service on Appropriate Technology (ISAT/GTZ), 1999.
7. A. B. Karki and Sahayogi Dixit, N. Prakasha, "*Biogas Field book*", 1984.
8. A. B. Karki, "*Training Manual in Biogas Technology for the Trainers of Jonior Bigas Technology*", Biogas Support Programme, 2000.
9. L. Ke-Xin, and L. Nian-Guo, "*Fermentation technology for rural digesters in China*", Proceeding of Bioenergy'80, Bio-Energy Council, New York, 1980.
10. I.W. Kroodsma, Treatment of livestock manure: Air draying and composting poultry manure, In: "*Odour prevention and Control of Organic Sludge and Livestock Farming*", The Netherlands, pp. 166-174, 1986.

11. B. Lagrange, Biomethane 2: "*Principle Techniques Utilization*", EDISUD. La Calade, 13100 Aix-en-Provence, France, 1979.
12. T. H. Lane, and T. E. Bates, "*Sampling and Chemical Analysis of Manure*", In: The Manure Management Handbook, Ont, Soil and Crop Imp. Ass.. Ont. Min. of Agriculture and Food, Ont, Agriculture Collage, Canada, 1982.
13. M. S. Lund, S. S. Andersen M. Torry-Smith, "*Building of a Flexibility Bag Biogas Digester in Tanzania*", Student Report, Technical University of Denmark. Copenhagen, 1996.
14. Müller Christian, May, "*Anaerobic Digestion of Biodegradable Solid Waste in Low- and Middle-Income Countries*", Dübendorf, 2007.
15. A. Mariakulandai, and T. S. Manickam, "*Chemistry of Fertilizers and Manures*", Aaia Publication House, New Yourk, U.S.A.,1975.
16. I. Narisara, T. Supparak and M. Vissanu, "*Biogas Production from Co-Digestion of Animal wastes*", The Proceeding of the 9th APCCHE Congress abd CHEMECA 2002, Christchurch, New Zealand, 2002,
17. NBPG & CADEC, "*Biogas Sector in Nepal*" supported by BSP –Nepal, 2007.
18. L. M. Safely, "*Operating a full-scale poultry manure anaerobic digester*". Biological Wastes, 1987.
19. M. A. Sathianahan, "*Biogas Achievements and challenges*", Association of Voluntary Agencies of Rural Development, New Dehli, India,1975.
20. R. Singh, "*Production of Biogas from Poultry Waste in Kathmandu*", MSREE, IOE Pulchowk-Nepal, 2004.
21. SNV/BSP, "*Abstracts of Biogas Related Publication*" (1992-2002)
22. Standard Methods, "*Standard Methods for the Examination of Water and Wastewater*". American Public Health Association, 1989.
23. J. G. Zeikus, and M. R. Winfrey, "*Temperature Limitation of Methangenesi in Aquatic Systems*", Applied and Environmental Microbiology, 1976.

OPTIMALTRAFFIC PLANNING FOR EFFICIENT EVACUATION

S. R. Khadka

Central Department of Mathematics,

Institute of Science and Technology,

Tribhuvan University, Kathmandu, Nepal

Email Address: shreeramkhadka@gmail.com

Abstract

Efficient traffic planning during evacuation in emergency has been important issue. The planning based on research significantly improves the quality of the emergency management. In this paper, we discuss on both optimization and simulation approaches of the traffic planning. Both approaches have been extensively studied in the literature with efficient softwares.

Keywords: *Traffic planning, evacuation planning, emergency management*

1. Introduction

Emergency management deals with natural and man-made disasters with the goal of saving lives and protecting property during emergencies and disasters. The management based on research upgrades the quality. Nepal has been a vulnerable place for disasters such as earthquake, flood, land slide, explosion of glacial lakes, fire etc. The country has been suffering from such disasters like flood, land slide, fire every year and has been losing a good number of lives and property. Emergency management does not avert or eliminate the threats themselves. However, the study and prediction of the threats based on research substantially reduce the risk.

One of the most important issues in the emergency management is to plan effective transportation mode which can evacuates within a reasonable time. The traffic planning during the response phase of the emergency management has been extensively studied in the literature on both optimization as well as simulation approaches, see [6].

In this paper, we describe both optimization and simulation approaches in brief that exist in the literature.

The organization of the paper is as follows. We describe about emergency management in Section 2, evacuation planning in Section 3, traffic planning in Section 4. We give a brief report of the optimization and simulation approaches for the traffic planning. The last section concludes the paper.

2. Emergency Management

Emergency management includes prevention, planning, response and recovery (PPRR) in order to lessen the impact of disasters.

Prevention is designed to provide permanent protection from disasters though not all disasters can be prevented. The risk of loss can be lessened. It is not worthy that the Hyogo Framework has been adopted on 2005 by 168 Governments as a 10-year global plan for natural disaster risk reduction.

Preventative measures (local or international levels) are to be taken into account during the construction e.g. houses, road, hydro power etc.

Planning or mitigation focuses on preparing equipment and procedures for use when a disaster occurs. Planning measures can take many forms including the construction of shelters, efficient transportation, implementation of an emergency communication system, installation of warning devices, supply of necessary logistics, creation of back-up life-line services (e.g., power, water, sewage), and rehearsing evacuation plans.

The response phase focuses on search and rescue quickly by national or international agencies and organizations with fulfilling the basic needs of the affected population. The objective of response is to save lives and to protect property as soon as possible in an efficient manner. This takes place either of a shelter in place or an evacuation. In a shelter-in-place scenario, a population would be prepared to fend for themselves in their shelter for many days without any form of outside support. In an evacuation, a population is evacuated to a safety zone using efficient and available mode of transportation with necessary logistics. Large disasters that overwhelm local capacity require an effective coordination with efficient communication system among the local emergency management agency, national and or international organizations, volunteers and several donors.

The recovery phase starts after the immediate threat to bring the affected area and or population back to some degree of normalcy.

In this paper, we consider the planning phase focused on efficient traffic planning. This is an emerging field of research as well as implementation of developed evacuation planning procedures to a particular location. The efficient planning procedures and their effective implementation to a particular location demand a sincere and continuous group effort. We require a number of case studies, awareness program, rehearsals and implementation of an efficient and suitable procedure.

3. Evacuation Planning

Evacuation is defined as the removal of lives and/or property from the disaster zone to the safety zone as quickly as possible. Evacuation planning includes the estimation of the evacuation time, propagation time of the disaster, the potential risk, and location of the safety zone and the reorganization of the traffic routes from the disaster zone to the safety zone.

Evacuation planning depends on the disaster source (flood, explosion, hurricane, land slide etc.), the disaster zone (building, city, region or vehicle), distribution (age, gender, disability) and behavior of evacuees, safety zone and emergency facilities. The time evacuation completes is called the evacuation time. The evacuation time consists of the recognition of emergency situation time, decision time and exit time. The exit time of all the evacuees is called the clearance time of the evacuees.

The time that a lot of evacuees take from the disaster zone to the safety zone is called the exit time. The exit time depends on the availability of traffic routes, efficient traffic planning and behavior of evacuees during evacuation.

The recognition of emergency situation time and the decision time depend on behaviors and organization of the evacuators and evacuees. Thus, the exit and the clearance time have been focused for many evacuation models. Traffic planning substantially influences the exit and the clearance time.

4. Traffic Planning

The tendency of people clustering in the cities and their metropolitan areas is increasing in developing countries also. The metropolitan areas are facing serious congestion problems due to the increasing number of vehicles, which threaten to deteriorate the quality of life and increase air pollution. Rapid increase of unavoidable travel demand and less construction of new transportation facilities worsen the traffic conditions unless some innovative congestion-relief methods can be developed and implemented in time. Efficient traffic planning are concerned with the prediction of the way in which vehicles use an existing or proposed infrastructure, or with the determination of the way in which such a utilization should be done. An efficient traffic planning is seriously required when disasters occur.

The traffic planning is the reorganization of the traffic routes so that all the evacuees can reach the safety zone as soon as possible. Efficient traffic planning is required for effective evacuation of evacuees during disasters. Only the effective and efficient planning achieves the goal of saving lives and protecting property during emergencies and disasters. If no such traffic planning has been assessed in prior time basically in urban places like Kathmandu where about 4 million people live with no adequate planning, we face a great loss during the disaster due to long evacuation time and unidentified potential transportation modes and shelters. Hard real time occurs in emergency. So delay evacuation is fatal. The efficient emergency traffic planning produces high quality emergency management. The planning significantly reduces the clearance and exit time and also increases the amount of flow of evacuees during emergency response situations. The planning should be scalable for the number of evacuees being moved and the size of the transportation network. The planning should reduce risk by identifying critical locations with unusually high evacuation times through sector evaluations.

There always exists a traffic network with finite nodes and finite edges between a disaster zone and a safety zone. Usually Urban areas have complex road networks with several lanes and intersections. The population is high enough. In Urban area like Kathmandu has high population density. Evacuees extremely capacity of the street during emergency. So, high congestion occurs. The basic idea is to reorganize the traffic routing from the disaster zone to the safety zone. The disaster zone and/or safety zone may have multiple nodes. The disaster zone may be buildings, vehicles, stadiums, cities or a region. The main objective of traffic planning is prior selection of scalable traffic routes for all evacuees within a desired time.

Since disasters may occur in different places and situations there exist several evacuation models. If the evacuees be considered as homogenous flow objects, the planning is based on optimization approaches. If behavior of an evacuee is taken as a separate flow object, the planning is based on simulation.

4.1. Optimization approach

The network that exists between the disaster zone and the safety zone can be considered as a graph network with finite nodes and finite edges. A static network, in which time is not considered as an attribute, can be useful to find the shortest path i.e. a path between the disaster zone and the safety zone with minimum weight, [7].

Dynamic network, in which time is an attribute issued in each edge, has been widely used to investigate a suitable evacuation model. The seminal work of Ford and Fulkerson has begun the dynamic network for such investigations. Static network is a basis of a dynamic network. A maximum flow of evacuees is obtained converting a maximal dynamic flow network into a time expanded static flow network [8]. The dynamic flow problem sends maximum flow, based on temporally repeated flows computed by the minimum cost flow problem, of evacuees from the disaster zone to the safety

zone[22,34]. The minimum cost flow problem finds the cheapest way of sending an amount of evacuees from the disaster zone to the safety zone. A constraint in which travel time depends on the inflow of a certain point extends the dynamic network flow problem. The problem is studied with an alternative time expanded network. A pseudo polynomial solution procedure exists with the assumption of constant capacity and constant travel time in each edge. Continuous time is attributed in this case[8,19].

The network may have multiple nodes in the disaster zone and in the safety zone as well. The multiple nodes are specified in an order from high to low priority. Then the dynamic network flow problem with multiple nodes of the disaster zone is called the lexicographic maximum dynamic flow problem. There exists an approximate polynomial algorithm based on chain decomposable flow to this problem. The flow is permitted to flow along the reversed direction of the edge[22]. Chain decomposable flow means the flow decomposed into flow units with discretised travel time. The lexicographic maximum dynamic flow problem is the multi-terminal extension of the maximum dynamic flow problem. All algorithms for lex max static flow can be applied for the lex max dynamic flow converting the dynamic network into exponentially large time expanded network[14].

The minimum cost dynamic network flow problem minimizes the total cost as well as the average evacuation time. This evacuation model is investigated for building evacuation in which waiting time node is allowed[12]. The model may be useful for the case with no waiting time also. The problem can be extended to the problem with multiple nodes in the disaster and the safety zones with no waiting time[9]. A pseudo polynomial time solution exists for the problem with time dependent attributes having single node disaster and safety zone. The attributes transit time, transit cost, transit capacities, storage cost and capacities can be taken into account for the time dependent case.

The earliest arrival flow problem sends the evacuees as early as possible together with a maximum evacuees in every time period to the safety zone[11]. Such flow always exists if there is only one node of the safety zone. There may not be a maximum dynamic flow with earliest arrival case if more than one node in the safety zone occurs[9]. However, Earliest arrival flows from multiple sources to a single sink do always exist [10]. An additional constraint of flow for each node in the disaster and the safety zone is taken for the problem with more than one node in the disasters and the safety zones. Basically such a problem is modified into a dynamic flow problem with a super disaster node and a super safety node connected with each disaster node and safety node having null transit time, respectively. There exist several pseudo polynomial algorithms and an approximate polynomial algorithm for the problem. It still remains unresolved whether an exact solution procedure with polynomial time exists or not. The problem in which transit time, inflow capacity and cost depend on time has more practical importance.

The problem that minimizes the time horizon of the clearance time is another variant of the maximum dynamic network flow problem. The problem is called the quickest transshipment problem that minimizes the clearance time. The problem with a single disaster node and a single safety node case is called the quickest flow problem[5]. The quickest flow problem has been solved by polynomial and strongly polynomial solution procedures based on parametric search. The problem can be extended to the case in which the travel time depends on inflow. Several variants of the problem for example the problem with null transit time, the problem that considers rate-dependent flow and the problem with multi nodal case have been solved[23]. The problems with flow dependent travel time and load dependent travel time have been studied also[18]. The problem that allows single path with minimum clearance time is called the quickest path problem. The multi objective problem can yield an optimal solution if the evacuation time is high enough. The result holds true for the problem with multiple nodes for given evacuee capacities.

Evacuation for pedestrians from buildings based on dynamic network flow has also been extensively studied. The problem maximizes number of evacuees and evacuation time[1]. A variant of the problem avoids unnecessary obstacle during evacuation has been investigated[13]. The disaster zone may have multiple nodes. Another variant with time dependent flow uses tree structure network to evacuate from common buildings. Moreover, time dependent case updates the evacuation routes in every time period[2]. A variant of the problem evacuates through a single route. Another variant studies for the disaster caused by the flood with water depth that varies over time[4]. This minimizes the evacuation time. A cell transmission based dynamic traffic assignment model also exists in the literature [3].

The traffic planning for the disaster that occurs in a region exists in the literature. The shortest path with a minimal cost can be found[37]. A heuristic for the problem with flow that depends on travel time has been developed and improved[21]. The quickest flow with a single node of the safety zone and traffic assignment problems has solution[16]. Stochastic programming network with all possible scenarios designs a two stage programming[24]. First stage extends the capacity to the region to be evacuated and the second stage find the traffic tanssipment model. A linear dynamic traffic assignment problem with a single node of the safety zone is a basis for the regional evacuation. The upgraded model is useful for mass evacuation. The model addresses maximum flow with traffic assignment on a static network. Since the road capacity may be uncertain during evacuation due to unavoidable hurdles, the model incorporates uncertainty also. Uncertainty in road capacity as well as the number of evacuees can be incorporated.

In order to increase the road capacity during the evacuation, consideration of lane reversal or contra flow is highly applicable. The problem with more than one node in either disaster and/or safety zone that allows each edge is reversed at the initial time and the total cost is to be minimized with a given time bound is NP-complete[17,30]. Establishment of the contra flow particularly for the solution from bottle necks is useful. A heuristic based on tabu search that includes the capability of reversal of lanes has been established for a linear model based on cell transmission. Another cell transmission based model includes the level of danger of different parts in the network. Its extension includes different cell sizes. This avoids crossing conflicts. A mixed integer programming based on the cell transmission incorporates lane reversal and line addition on certain street segments but not the crossing conflicts[26]. A tabu search heuristic with Lagrangian relaxation is the solution approach for the problem with a bi-level model with capability of lane-reversal[35,36].

The traffic planning with evacuation response can be formulated in a mixed integer location routing model that incorporates the logistics[25]. The evacuation planning in a location allocation model has a genetic algorithm solution procedure. Some facilities may be damaged during the response. Such consideration has also been performed[15].

Since forecast of disaster may not always be certain, evacuation decision may be costly if disaster does not occur. A decision support model exists[31].

4.2. Simulation

Simulation approach is useful to evaluate given traffic network under different conditions. Microscopic model considers each evacuee as a separate flow object. Each evacuee is exposed to select a route step by step. The choice of route may be deterministic or random or modified random depending on the different situations. The movement pattern depends either on deterministic or probabilistic rules. There exists cellular automata simulation as well. The cellular automata study the behavior of the evacuee under various and uncertain conditions. It is particularly useful for the situations where rapid and/or random changes should occur[27].

The microscopic model simulation softwares that are widely used not only in the disaster but in the normal traffic planning situation are for example PARAMICS, CORSIM, VISSIM, EGRESS and FlightSim [20,28]. CORSIM that combines two micro-simulators NETSIM and FRESIM includes some features such as altering signals, traffic diversions, access restrictions and roadway clearance. This simulator that considers speed, queuing time and length is less effective for real world problems. However, this is effective to test the effectiveness of the contra flow. VISSIM is implemented for the comparison between the results with and without contra flow. PARAMICS simulates high risk evacuation areas. It is used for the comparison between the simultaneous and staged evacuation strategies. EGRESS and FlightSim make use of cellular automata. DOSIMIS-3 predicts the traffic evolution. The micro simulations model is expensive when the size of evacuees is large enough.

Macroscopic models have been developed for the large size case. The model is useful to analyse and simplify the situation so that one can improve the accuracy. The simulators MASSVAC for structured rural networks and NETVAC for radial evacuation from the disaster zone are popular simulators[29,32]. Other simulators for example OREMS, DYNEV and ETIS additionally incorporate advanced features.

There exist mesosimulator softwares CEMPS, Smart CAP, Smart AHS, DYNEMO that keep advantage over disadvantages of the macro and micro simulators. However, macro and micro simulators are still useful, see [28].

Simulation approach can be useful for the review of traffic generation, traffic departure times, safety zone selection, traffic route selection with clearance time and capacities and the potential hurdles along the routes. Simulation identifies the bottlenecks in the networks and estimates the evacuation time so that evacuation can be followed. The simulation models have been developed for various disasters like nuclear accidents, hurricanes, floods, wild-fires etc. Likewise, the models exist for complex buildings, cities, regions, moving vehicles too.

5. Concluding Remarks

One of the most important issues on emergency management is to plan the transportation mode during evacuation. The traffic planning can be made efficient if it is based either on optimization approach or on the simulation one. There have been several procedures depending on the situation of the evacuation. Study of the traffic network with appropriate traffic planning in populated area in Nepal like Kathmandu would be better area of research in the future.

References

1. L.G. Chalmet, R.L. Francis and P.B. Saunders, "*Network models for building evacuation*", Management Science Vol. 28, 1 (1982) 86-105.
2. L. Chen and E. Miller-Hooks, "*The building evacuation problem with shared information*", Naval Research Logistics Vol. 55 (2008) 363-376.
3. Y.C. Chiu and H. Zheng, "*Real-time mobilization decisions for multi-priority emergency response resources and evacuation groups: model formulation and solution*", Transport Research Part E: Logistics Transport Review Vol.43, 6 (2007) 710-736.
4. W. Choi, H.W.Hamacher and S. Tufekci, "*Modeling of building evacuation problems by network flows with side constraints*", European Journal of Operational Research Vol. 35 (1988)98-110.

5. Y.L. Chen and Y.H. Chin, "*The quickest path problem*", Computers and Operations Research Vol. 17 (1990), 153-161.
6. T. N. Dhamala, "*Survey on Models and Algorithms for Discrete Evacuation Planning Network Problems*", Journal of Industrial and Management Optimization , Vol. 11, 1 (2015)
7. F.R. Ford, and D.R. Fulkerson, "*Constructing maximal dynamic flows from static flows*", Operations Research Vol. 6 (1958), 419-433.
8. F.R. Ford and D.R. Fulkerson, "*Flows in networks*", Princeton University Press, Princeton, New Jersey, 1962.
9. L.K. Fleischer, "*Faster algorithms for quickest transshipment problem*", SIAM Journal on Optimization Vol. 12 (2001), 18-35.
10. L. Fleischer and M. Skutella, "*Minimum cost flows over time without intermediate storage*", SODA '03 Proceedings of the fourteenth annual ACM-SIAM symposium on Discrete algorithms, Society for Industrial and Applied Mathematics Philadelphia, 66-75, 2003.
11. D. Gale, "*Transient flows in networks*", Michigan Mathematical Journal Vol. 6(1959), 59-63.
12. H.W. Hamacher, and S.A. Tjandra, "*Mathematical modeling of evacuation problems: A state of the art*", In: M. Schreckenberger and S.D. Sharma (Eds.), Pedestrian and Evacuation Dynamics, Springer, Berlin, Heidelberg, 227-266, 2002.
13. H.W. Hamacher and S. Tufekci, "*On the use of lexicographic min cost flows in evacuation modeling*", Naval Research Logistics Vol. 34 (1987) 487-503.
14. B. Hoppe, and E.Tardos, "*The quickest transshipment problem*", Mathematics of Operations Research Vol. 25(2000), 36-62.
15. R. Huang, S. Kim and M.B.C. Menezes, "*Facility location for large-scale emergencies*", Annals of Operations Research Vol. 181(2010) 271-286.
16. N. Kamiyama, N. Katoh and A. Takizawa, "*An efficient algorithm for evacuation problems in dynamic network flows with uniform arc capacity*", Cheng S-W, Poon C (eds) Algorithmic aspects in information and management. Lecture notes in computer science, 4041 Springer, Berlin, 231-242, 2006.
17. S. Kim and S. Shekhar, "*Contraflow network reconfiguration for evacuation planning: a summary of Results*". In: Proceedings of the 13th annual ACM international workshop on geographic information systems. GIS 05. ACM, New York, 250-259, 2005.
18. E. Kohler and M. Skutella, "*Flows over time with load-dependent transit times*", SIAM Journal of Optimization, Vol. 15, 4 (2005) 1185-1202.
19. R. Koch, E. Nasrabadi, and M. Skutella, "*Continuous and discrete flows over time -A general model based on measure theory*", Mathematical Methods of Operations Research Vol. 73(2011), 301-337.
20. G. Kotusevski and K.A. Hawick, "*A review of traffic simulation software*", Technical report CSTN-095, Computer Science, Institute of Information and Mathematical Sciences, Massey University, Albany, Auckland, New Zealand, 2009.
21. Q. Lu, B. George and S. Shekhar, "*Capacity constrained routing algorithms for evacuation planning: a summary of results*", Medeiros BC, Egenhofer M, Bertino E (eds) Lecture notes in computer science, 3633 Springer, Berlin, 291-307, 2005.

22. E. Miller-Hooks and S.S. Patterson, “*On solving quickest time problems in time dependent, dynamic networks*”, *Journal of Mathematical Modeling and Algorithms* Vol. 3(2004), 39-71.
23. E. Minieka, “*Maximal, lexicographic, and dynamic network flows*”, *Operations Research* Vol, 21(1973), 517-527.
24. M. Ng and S.T. Waller, “*The evacuation optimal network design problem: model formulation and Comparison*”, *International Journal of Transportation Research* Vol. 1 (2009)111-119.
25. L. Ozdamar and W. Yi, “*A dynamic logistics coordination model for evacuation and support in disaster response activities*”, *European Journal of Operational Research* Vol.179, 3 (2007)1177-1193.
26. S.Peeta and G.Kalafatas, “*Primary emergency routes for transportation security*”. Joint transportation research program, Paper 323, 2008. <http://docs.lib.purdue.edu/jtrp/323>.
27. M.Pidd, F. de Silva and R. Eglese, “*A configurable evacuation management and planning system*”, In: *Proceedings of the Winter Simulation Conference*,1319-1323,1993.
28. P.M. Pardalos and A. Arulselvan, “*Multimodal solutions for large scale evacuations, Center for Multimodal Solutions for Congestion Mitigation*”, Department of Industrial and System Engineering, University of Florida, 2009.
29. A. Radwan, A. Hoebeika and D. Sivasailam, “*A computer simulation model for rural network evacuation under natural disaster*”, *Institute of Transportation Engineers Journal* Vol. 55(1985), 25-30.
30. S. Rebennack, A Arulselvan, L. Elefteriadou and P. Pardalos, “*Complexity analysis for maximum flow problems with arc reversals*”, *Journal of Combinatorial Optimization* Vol.19 (2010) 200-216.
31. E. Regnier, “*Public evacuation decisions and hurricane track uncertainty*”, *Management Science* Vol.54, 1 (2008) 16-28.
32. Y. Sheffi, H. Mahmassani and W. Powell, “*NETVAC: A transportation network evacuation model*”, Center for Transportation Studies, MIT, 1980.
33. S.A. Tjandra, “*Dynamic network optimization with applications to evacuation planning*”, Ph.D. thesis, University of Kaiserslautern, 1993.
34. W.L. Wilkinson, “*An algorithm for universal maximal dynamic flows in a network*”, *Operations Research*, Vol.19 (1971) 1602-1612.
35. C. Xie, D-Y. Lin and S.T. Waller, “*A dynamic evacuation network optimization problem with lane reversal and crossing elimination strategies*”, *Transport Research Part E: Logistics Transport Review* Vol.46, 3 (2010) 295-316.
36. C. Xie and M.A. “*Turnquist, Lane-based evacuation network optimization: an integrated Lagrangian relaxation and tabu search approach*”, *Transport Research Part C Emergency Technique* Vol.19, 1 (2011) 40-63.
37. T. Yamada, “*A network flows approach to a city emergency evacuation planning*”, *International Journal of System Science* Vol. 27, 10 (1996) 931-936.

INTRUSION DETECTION SYSTEM USING BACK PROPAGATION ALGORITHM AND COMPARE ITS PERFORMANCE WITH SELF ORGANIZING MAP

Subarna Shakya¹, Bisho Raj Kaphle²

¹Department of Electronics and Computer Engineering

Central Campus, Pulchowk, Lalitpur

Email Address: drss@ioe.edu.np

² Kathmandu Engineering College

Email Address: bishorajkafle@gmail.com

Abstract

In recent years, internet and computers have been utilized by many people all over the world in several fields. On the other hand, network intrusion and information safety problems are ramifications of using internet. In this thesis it propose a new learning methodology towards developing a novel intrusion detection system (IDS) by back propagation neural networks (BPN) and self organizing map (SOM) and compare the performance between them. The main function of Intrusion Detection System is to protect the resources from threats. It analyzes and predicts the behaviors of users, and then these behaviors will be considered an attack or a normal behavior. The proposed method can significantly reduce the training time required. Additionally, the training results are good. It provides a powerful tool to help supervisors and unsupervisors analyze, model and understand the complex attack behavior of electronic crime.

Keywords: *Intrusion Detection, Neural Network, Back Propagation Neural Network, Intrusion Attacks, Self Organizing Map*

1. Introduction

The problem of protecting information has existed since information has been managed. However, as technology advances and information management systems become more and more powerful, the problem of enforcing information security also becomes more critical. The enlargement of this electronic environment comes with a corresponding growth of electronic crime where the computer is used either as a tool to commit the crime or as a target of the crime [1].

In past years, numerous computers are hacked because they do not consider the necessary of precautions to protect against network attacks. The failure to secure their systems puts many companies and organizations at a much greater risk of loss. Usually, a single attack can cost millions of dollars in potential revenue. Moreover, that's just the beginning. The damages of attacks include not only loss of intellectual property and liability for compromised customer data (the time/money spent to recover from the attack) but also customer confidence and market advantage. There is a need to enhance the security of computers and networks for protecting the critical infrastructure from threats. Accompanied by the rise of electronic crime, the design of safe-guarding information infrastructure such as the intrusion detection system (IDS) for preventing and detecting incidents becomes increasingly challenging. The intrusion detector learning task is to build a predictive model (i.e. a classifier) capable of distinguishing between

bad intrusions and normal connections. Recently, an increasing amount of research has been conducted on applying neural networks to detect intrusions. An artificial neural network consists of a collection of processing elements that are highly interconnected. Give a set of inputs and a set of desired outputs, the transformation from input to output is determined by the weights associated with the interconnections among processing elements. There are two general methods of detecting intrusions into computer and network systems, namely Anomaly detection and Signature recognition.

Anomaly detection techniques establish a profile of the subject's normal behavior (norm profile), compare the observed behavior of the subject with its norm profile, and signal intrusions when the subject's observed behavior differs significantly from its norm profile. Signature recognition techniques recognize signatures of known attacks, match the observed behavior with those known signatures, and signal intrusions when there is a match [2].

Neural network is an universal classifier and with the proper choosing of its architecture it can solve any, even very complicated, classification task [3].

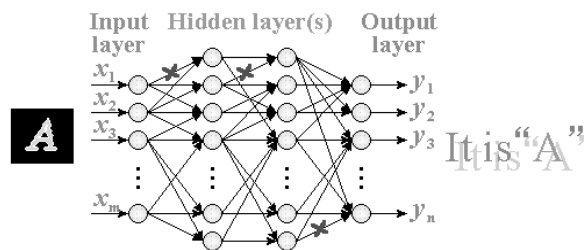


Fig 1 Multilayer Perceptron^[1]

Here above figure 1.2 shows the input layer, hidden layer(s) and output layer of Multilayer Perceptron (MLP).

Attacks can be gathered in four main categories:

- 1) **Denial of Service Attack (DoS)**: is an attack in which the attacker makes some computing or memory resource too busy or too full to handle legitimate requests, or denies legitimate users access to a machine.
- 2) **User to Root Attack (U2R)**: is a class of exploit in which the attacker starts out with access to a normal user account on the system (perhaps gained by sniffing passwords, a dictionary attack, or social engineering) and is able to exploit some vulnerability to gain root access to the system.
- 3) **Remote to Local Attack (R2L)**: occurs when an attacker who has the ability to send packets to a machine over a network but who does not have an account on that machine exploits some vulnerability to gain local access as a user of that machine.
- 4) **Probing Attack**: Attacker tries to gain information about the target host [2].

Activation Function:

Multilayer perceptron networks typically use sigmoid transfer functions in the hidden layers. These functions are often called "squashing" functions, because they compress an infinite input range into a finite output range.

The bipolar sigmoid function: $f(x) = -1 + 2 / [1 + e^{-x}]$

which has derivative of: $f'(x) = 0.5 * [1 + f(x)] * [1 - f(x)]$

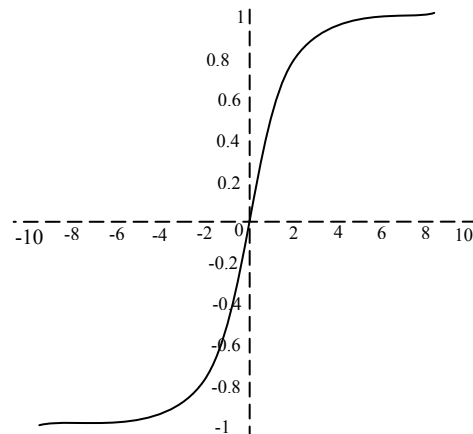


Fig 2 Bipolar Sigmoid Function

2. Literature Review

At first the concept of intrusion detection system was suggested by Anderson (1980) [1]. He applied statistic method to analyze user's behavior and to detect those attackers who accessed system in an illegal manner. In [2] proposed a prototype of IDES (intrusion detection expert system) in 1987, subsequently, the idea of intrusion detection system was known progressively, and paper was regarded as significant landmark in this area. In [4] the author proposed a data mining framework for constructing intrusion detection models. The key idea is to apply data mining programs namely, classification, meta-learning, association rules, and frequent episodes to audit data for computing misuse and anomaly detection models that accurately capture the actual behavior (i.e., patterns) of intrusions and normal activities. Although, proposed detection model can detect a high percentage of old and new PROBING and U2R attacks, it missed a large number of new DOS and R2L attacks. Reference [5] is mostly focused on data mining techniques that are being used for such purposes, and then presented a new idea on how data mining can aid IDSs by utilizing biclustering as a tool to analyze network traffic and enhance IDSs. Reference [6] proposed a new weighted support vector clustering algorithm and applied it to the anomaly detection problem. Experimental results show that mentioned method achieves high detection rate with low false alarm rate. Intrusion detection attacks are segmented into two groups,

- Host-based attacks [3-5] and
- Network-based attacks [6, 7].

Intruders attack these systems by transmitting huge amounts of network traffic, utilizing familiar faults in networking services, overloading network hosts, etc. Detection of these kinds of attacks uses network traffic data (i.e., tcpdump) to look at traffic addressed to the machines being monitored.

3. Research Methodology

Back Propagation Algorithm

The back propagation algorithm is a quite essential one of the neural network. The algorithm is the training or learning algorithm rather than the network itself. The network used is generally of the simple type shown in figure 3.1, and in the examples up until now. The network operates in exactly the same way as the others have seen. Now, let's consider what Back Propagation is and how to use it. A Back

Propagation network learns by example. You give the algorithm examples of what you want the network to do and it changes the network's weights so that, when training is finished, it will give you the required output for a particular input. Back Propagation networks are ideal for simple Pattern Recognition and Mapping Tasks⁴. As just mentioned, to train the network you need to give it examples of what you want the output you want (called the Target) for a particular input as shown in Figure 3.1.

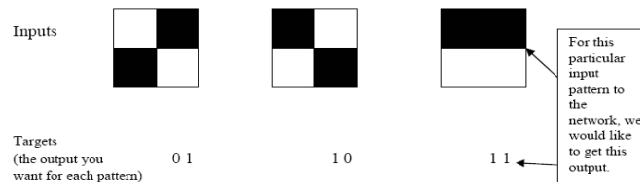


Fig 3.1 A Back Propagation Training Set.

So, if the first pattern to the network, we would like the output to be 0 1 as shown in figure 3.1 (a black pixel is represented by 1 and a white by 0 as in the previous examples). The input and its corresponding target are called a Training Pair.

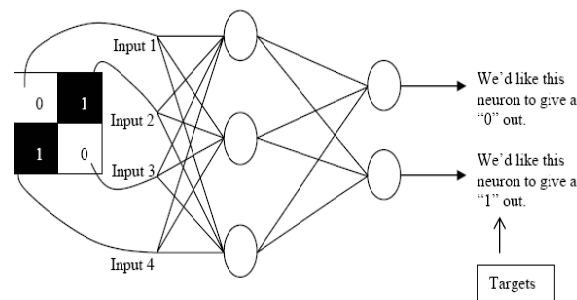


Fig 3.2 Applying a Training Pair to a Network

Once the network is trained, it will provide the desired output for any of the input patterns. Let's now look at how the training works. The network is first initialized by setting up all its weights to be small random numbers – say between -1 and $+1$. Next, the input pattern is applied and the output calculated (this is called the forward pass). The calculation gives an output which is completely different to what you want (the Target), since all the weights are random. Then calculate the Error of each neuron, which is essentially: $\text{Target} - \text{Actual Output}$ (i.e. what you want – What you actually get). This error is then used mathematically to change the weights in such a way that the error will get smaller. In other words, the Output of each neuron will get closer to its Target (this part is called the reverse pass). The process is repeated again and again until the error is minimal. Let's do an example with an actual network to see how the process works. Just look at one connection initially, between a neuron in the output layer and one in the hidden layer, figure 3.2.

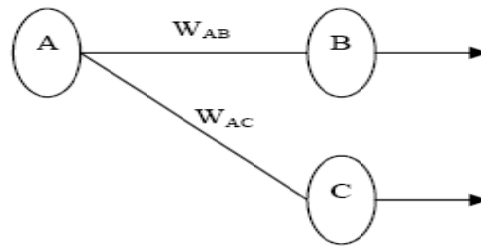


Fig 3.3 A Single Connection Learning in a Back Propagation network.

The connection interested in is between neuron A (a hidden layer neuron) and neuron B (an output neuron) and has the weight W_{AB} . The diagram also shows another connection, between neuron A and C, but we'll return to that later. The algorithm works like this:

1. First apply the inputs to the network and work out the output – remember this initial output could be anything, as the initial weights were random numbers.
2. Next work out the error for neuron B. The error is what you want – What you actually get, in other words: $Error_B = Output_B (1 - Output_B) (Target_B - Output_B)$ The “Output (1-Output)” term is necessary in the equation because of the Sigmoid Function – if we were only using a threshold neuron it would just be $(Target - Output)$.
3. Change the weight. Let W_{+AB} be the new (trained) weight and W_{AB} be the initial weight. $W_{+AB} = W_{AB} + (Error_B \times Output_A)$ Notice that it is the output of the connecting neuron (neuron A) we use (not B). We update all the weights in the output layer in this way.
4. Calculate the Errors for the hidden layer neurons. Unlike the output layer we can't calculate these directly (because we don't have a Target), so we Back Propagate them from the output layer (hence the name of the algorithm). This is done by taking the Errors from the output neurons and running them back through the weights to get the hidden layer errors. For example if neuron A is connected as shown to B and C then we take the errors from B and C to generate an error for A. $Error_A = Output_A (1 - Output_A) (Error_B W_{AB} + Error_C W_{AC})$ Again, the factor “Output (1 - Output)” is present because of the sigmoid squashing function.
5. Having obtained the Error for the hidden layer neurons now proceed as in stage 3 to change the hidden layer weights. By repeating this method we can train a network of any number of layers. W_{+} represents the new, recalculated weight, whereas W (without the superscript) represents the old weight. Reverse process is done in the same way. Hence the attackers are calculated.

Self-Organizing Map

The Self-Organizing Map [9] is a neural network model for analyzing and visualizing high dimensional data. It belongs to the category of competitive learning network. The SOM defines a mapping from high dimensional input data space onto a regular two-dimensional array of neurons. In designed architecture is input vector with six input values and output is realized to 2 dimension space. Every neuron i of the map is associated with an n -dimensional reference vector.

$$M_i [M_1 \dots \dots \dots M_n]^T \dots \dots \dots (3.1)$$

Where, n denotes the dimension of the input vectors. The reference vectors together form a codebook. The neurons of the map are connected to adjacent neurons by a neighborhood relation, which dictates the

topology, or the structure, of the map. Adjacent neurons belong to the neighborhood N_i of the neuron i . In the SOM algorithm, the topology and the number of neurons remain fixed from the beginning. The number of neurons determines the granularity of the mapping, which has an effect on the accuracy and generalization of the SOM. During the training phase, the SOM forms elastic net that is formed by input data. The algorithm controls the net so that it strives to approximate the density of the data. The reference vectors in the codebook drift to the areas where the density of the input data is high. Eventually, only few codebook vectors lie in areas where the input data is sparse. The learning process of the SOM goes as follows:

1. One sample vector x is randomly drawn from the input data set and its similarity (distance) to the codebook vectors is computed by using Euclidean distance measure:

$$\|x - m_c\| = \min\{\|x - m_i\|\} \dots \dots \dots (3.2)$$

2. After the BMU has been found, the codebook vectors are updated. The BMU itself as well as its topological neighbors are moved closer to the input vector in the input space i.e. the input vector attracts them. The magnitude of the attraction is governed by the learning rate. As the learning proceeds and new input vectors are given to the map, the learning rate gradually decreases to zero according to the specified learning rate function type. Along with the Intrusion Detection System, Using Self Organizing Map learning rate, the neighborhood radius decreases as well. The update rule for the reference vector of unit i is the following:

$$m_i(t + 1) = m_i(t) + \alpha(t)[(x(t) - m_i(t))], I \in N_c(t)$$

$$m_i(t + 1) = m_i(t), I \in N_c(t) \dots \dots \dots (3.3)$$

3. The steps 1 and 2 together constitute a single training step and they are repeated until the training ends. The number of training steps must be fixed prior to training the SOM because the rate of convergence in the neighborhood function and the learning rate are calculated accordingly.

Mapping Precision

The mapping precision measure describes how accurately the neurons respond to the given data set. If the reference vector of the BMU calculated for a given testing vector x_i is exactly the same x_i , the error in precision is then 0. Normally, the number of data vectors exceeds the number of neurons and the precision error is thus always different from 0. A common measure that calculates the precision of the mapping is the average quantization error over the entire data set:

$$E_q = \frac{1}{N} \sum_{i=1}^N \|x_i + m_c\| \dots \dots \dots (3.4)$$

Topology Preservation

The topology preservation measure describes how well the SOM preserves the topology of the studied data set. Unlike the mapping precision measure, it considers the structure of the map. For a strangely twisted map, the topographic error is big even if the mapping precision error is small. A simple method for calculating the topographic error:

$$E_q = \frac{1}{N} \sum_{i=1}^N u(x_x) \dots \dots \dots (3.5)$$

Where $u(x_x)$ is 1 if the first and second BMUs of x_k are not next to each other. Otherwise $u(x_x)$ is 0.

SOM Implementation to Intrusion Detection System

The goal of the proposed architecture is to investigate effectiveness of application a neural network SOM figure.3.5 at modeling user behavioral patterns so they can distinguish between normal and abnormal behavior. In order to model user behavior identified and isolated the system logs that were required as sources of information for the networks. These logs being common log data provided the required user activity information from where system derived the following behavioral characteristics which typifies users on the system:

- User activity times - The time at which a user is normally active.
- User login hosts - The set of hosts from which a user normally logs in from.
- User foreign hosts - The set of hosts which a user normally accesses via commands on the system (FTP hosts).
- Command set - The set of commands which a user normally uses.
- CPU usage - The typical CPU usage patterns of a user.
- Memory usage – The typical usage of memory for a user.

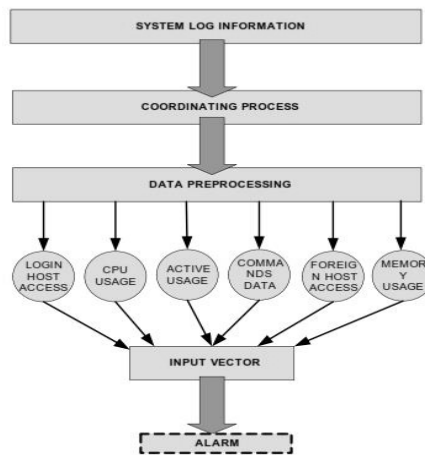


Fig 3.4 Structure of an Automated User Behavior Anomaly Detection System

Figure 3.5 illustrates how a complete system for the detection of user behavioral anomalies is structured. The coordination process is responsible for channeling system information to the neural networks. Each of the behavioral characteristics are both modeled by a SOM network, as well as checked by a limited static rule filter for easy breaches of security. Data acquired from the system logs is required to filter through input data preprocessor. The input to the neural network Fig. 3.5 represents data vector consisting from data controlled on the monitored system. Before input vector processing it is needed to normalize input data. The input to neural network is data vector, which consists from six properties representing User activity times, User login hosts, User foreign hosts, Command set CPU usage and Memory Usage. According to large numbers of variations of this data it is necessary to normalize every input vector to be

value in range of values [-1, 1]. This range comes out from the previous applications of neural network to system IDS realized within research activity on the Department of Computers and Informatics in Kosice. This normalization is more suitable for implementation in proposed SOM network. The architecture uses normalization given by:

$$nv[i] = \frac{v[i]}{\sqrt{\sum_k^n v[k]^2}} \dots \dots \dots (3.6)$$

Where $nv[i]$ is the normalized value of feature (i), $v[i]$ is the feature value of i , and K is the number of features in a vector. The processing realized by the SOM network consequently produces results for every user characteristic gives as input to the SOM network. Expected network reply is the value close to-for user, which behavior does not divert from normal behavior. If the value for given user exceeds specified threshold value obtained through the SOM network representing its intrusion behavior denotes raising alarm. If the output value of network is above specified threshold value, alarm is raised. It is necessary to remark that basic request for this detection mechanism is to setup threshold value to specific system whereby make it possible to adapt sensitivity directly to computer system.

4. Data Analysis

Input Dataset Analysis

Under the sponsorship of Defense Advanced Research Projects Agency (DARPA) and Air Force Research Laboratory (AFRL), the MIT Lincoln laboratory has established a network and captured the packets of different attack types and distributed the data sets for the evaluation of researches in computer network intrusion detection systems. The KDDCup99 data set is a subset of the DARPA benchmark data set [9]. Each KDDCup99 training connection record contains 41 features and is labeled as either normal or an attack, with exactly one specific attack type. This dataset will be taken as training data for performing the proposed research work. The result thus obtained will be compared with the rest of test data set. One of the reasons for choosing this data set is that the data set is standard. Another reason is that it is difficult to get another data set which contains so rich a variety of attacks.

Feature Extraction: For each network connection in the data set, the following three key groups of features for detecting intrusions will be extracted.

- **Basic features:** This group summarizes all the features that can be extracted from a TCP/IP connection. Some of the basic features in the KDDCup99 data sets are protocol type, service, src_bytes and dst_bytes.
- **Content features:** These features are purely based on the contents in the data portion of the data packet.
- **Traffic features:** This group comprises features that are computed with respect to a 2 Sec. time window and it is divided into two groups: same host features and same service features. Some of the traffic features are counted, error_rate, error_rate and srv_error_rate.

Instance Labeling: After extracting KDDCup99 features from each record, the instances are labeled based on the characteristics of traffic as Normal, Dos, Probe, R2L and U2R.

Pre Processing

The data set will be preprocessed so that it may be able to give it as an input to our proposed system. This data set consists of numeric and symbolic features and will be converted in numeric form so that it can be

given as inputs to our MLP network. Now this modified data set will be used as training and testing of the multi layer perceptron. Table 4.1 below shows the feature columns name and type of 10% KDDCup 99 dataset. Table 0.1:KDD feature columns name and type [9]

The following tables represent the data feature columns before and after transformation.

Table 1 Feature Column Before Transformation

0, tcp, http, SF, 181, 5450, 0, 0, 0, 0, 0, 1, 0, 0, 0, 0, 0, 0, 0, 0, 0, 8, 8, 0.00, 0.00, 0.00, 0.00, 1.00, 0.00, 0.00, 9, 9, 1.00, 0.00, 0.11, 0.00, 0.00, 0.00, 0.00, 0.00, normal.

Table 2 Feature Column After Transformation

0, 1, 20, 10, 181, 5450, 0, 0, 0, 0, 0, 1, 0, 0, 0, 0, 0, 0, 0, 0, 8, 8, 0.00, 0.00, 0.00, 0.00, 1.00, 0.00, 0.00, 9, 9, 1.00, 0.00, 0.11, 0.00, 0.00, 0.00, 0.00, 0.00, 1, 0, 0, 0, 0.

Training and Testing of MLP

The input dataset is divided into 3 subsets. The first subset is the training set, which is used for computing the gradient and updating the network weights and biases. The second subset is the validation set. The error on the validation set is monitored during the training process. The validation error normally decreases during the initial phase of training, as does the training set error. However, when the network begins to over-fit the data, the error on the validation set typically begins to rise. When the validation error increases for a specified number of iterations (`net.trainParam.max_fail`), the training is stopped, and the weights and biases at the minimum of the validation error are returned. The test set error is not used during training, but it is used to compare different models (MathWorks Matlab Help, 2013).

In this thesis, 80% data from the input dataset are used for training, 10% for validation and 10% for testing of the MLP to analyze the performance of various back propagation algorithms.

5. Performance Parameters

Mean Square Error, Total CPU Time of Converge and Accuracy will be the performance parameters to compare various back propagation algorithms.

Following parameters will be calculated while training and testing of MLP.

- **True Positive (TP):** Situation in which a signature is fired properly when an attack is detected and an alarm is generated.
- **False Positive (FP):** Situation in which normal traffic causes the signature to raise an alarm.
- **True Negative (TN):** Situation in which normal traffic does not cause the signature to raise an alarm.
- **False Negative (FN):** Situation in which a signature is not fired when an attack is detected.
- **Attack Detection Rate (ADR):** The detection rate is defined as the number of intrusion instances detected by the system (True Positive) divided by the total number of intrusion instances present in the test set.

Attack Detection Rate (ADR) = (Total detected attacks / Total attacks) * 100 %

- **False Alarm Rate (FAR):** It is the ratio between the total number of misclassified instances and the total number of normal connections present in the data set.

False Alarm Rate (FAR) = (Total misclassified instances / Total normal instances) * 100 %

- **Recall Rate:** Recall rate measures the proportion of actual positives which are correctly identified.

Recall Rate = $TP / (TP + FN)$

- **Precision Rate:** Precision rate is the ratio of true positives to combined true and false positives.

Precision Rate = $TP / (TP + FP)$

6. Simulation Result

6.1 Determining Hidden Layer Neurons in Scale Conjugate Gradient (SCG):

The Multilayer Perception is trained to find the number of hidden layer neurons using the following parameters:

Number of input data = 494021

Number of input layer neurons = 41

Number of output layer neurons = 5

Change in weight for second derivative approximation (σ) = $5.0e-5$

Parameter for regulating the indefiniteness of the Hessian(λ)= $5.0e-7$

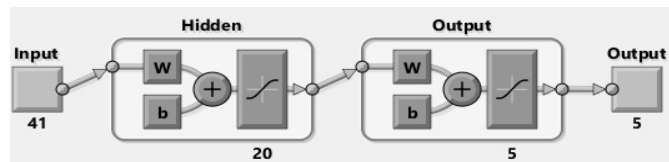


Fig 6.1 MLP Architecture of Back Propagation of 20 hidden neuron layer.

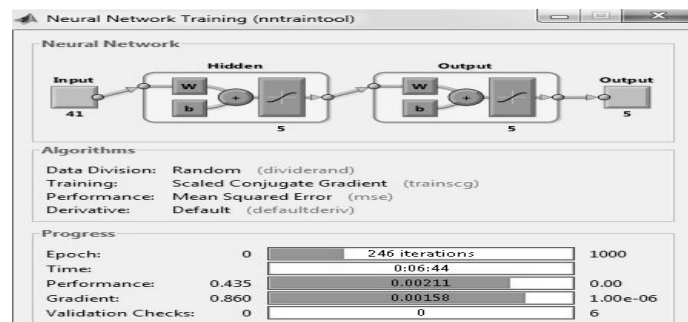


Fig 6.2 Performance of MLP with 5 neurons in hidden layer.

6.2 Performance Assessment of Scale Conjugate Gradient (SCG) Back Propagation Algorithms

Simulation is done to analyze the performance of Scaled Conjugate Gradient. The Multilayer Perceptron was trained with SCG algorithm by using following parameters.

Change in weight for second derivative approximation (σ) = 5.0e-5

Parameter for regulating the indefiniteness of the Hessian (λ) = 5.0e-7

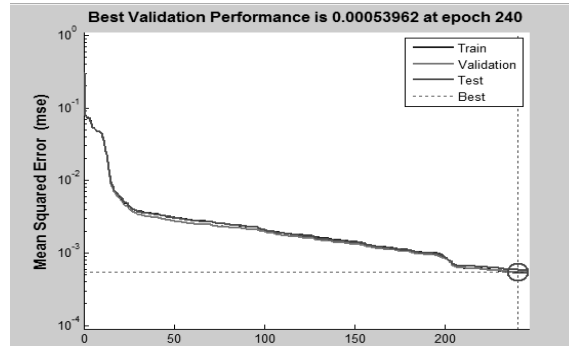


Fig. 6.3 Performance of SCG Algorithm

Table 6.1 Evaluation Results for each Attack Classes (SCG)

Attack	TP	FP	FN	Recall	Precision
DoS	391407	35	42	99.99%	99.99%
U2R	0	0	32	0%	0%
R2L	915	106	189	82.88%	89.61%
Probe	3898	30	200	95.12%	99.23%
Total	396220	171	463	98.88%	99.95%

6.3 Determining Hidden Layer Neurons in Self Organizing Map

The Multilayer Perception is trained to find the number of hidden layer neurons using the following parameters:

Number of input data = 14020

Number of input layer neurons = 41

Number of output layer neurons = 5 and 10

Simulation is done to analyze the performance of Self Organizing Map in terms of different number of hidden layer, epoch and iteration time required.

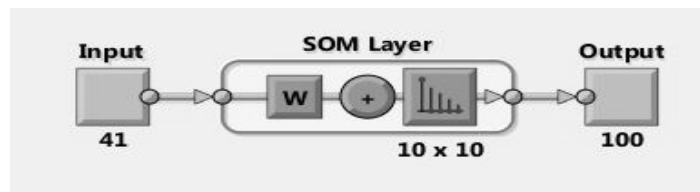


Fig 6.4 SOM Network of 10 hidden neuron layer

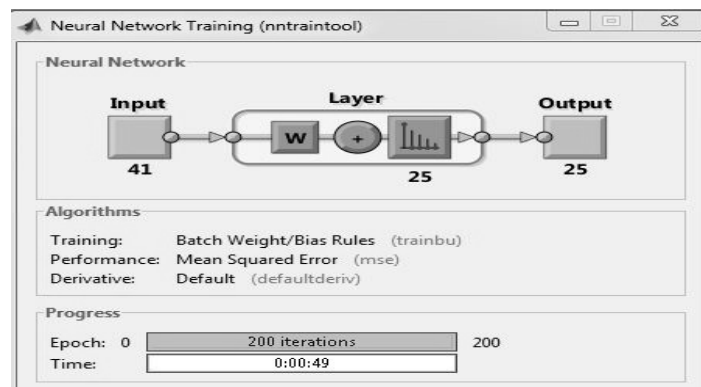


Fig 6.5 Performance of SOM with 5 neurons in hidden layer.

7. Conclusion

At present, security inside the network communication is of a major concern. Intrusion detection system tries to identify security attacks of intruders by investigating several data records observed in processes on the network. From simulation result using Matlab tool and java programming code we suggest that the performance like iteration completion time of SOM (Self Organizing Map is far better than BP (Back Propagation) algorithm.

References

1. S. Mukkamala, G. Janoski and A. Sung, "Intrusion detection using neural networks and support vector machines", Proceedings of International Joint Conference on Neural Networks (IJCNN '02), Vol. 2, Pp. 1702–1707, 2002.
2. Snehal A. Mulay, P.R. Devale and G.V. Garje, "Intrusion Detection System using Support Vector Machine and Decision Tree", International Journal of Computer Applications, Vol. 3, No. 3, Pp. 40-43, 2010.
3. D. Anderson, T. Frivold and A. Valdes, "Next generation intrusion detection expert system (NIDES): a summary", Technical Report SRI-CSL-95-07. Computer Science Laboratory, SRI International, Menlo Park, CA, 1995.
4. S. Axelsson, "Research in intrusion detection systems: a survey", Technical Report TR 98-17 (revised in 1999). Chalmers University of Technology, Goteborg, Sweden, 1999.
5. S. Freeman, A. Bivens, J. Branch and B. Szymanski, "Host-based intrusion detection using user signatures", Proceedings of the Research Conference. RPI, Troy, NY, 2002.
6. K. Ilgun, R.A. Kemmerer and P.A. Porras, "State transition analysis: A rule-based intrusion detection approach", IEEE Trans. Software Eng, Vol. 21, No. 3, Pp. 181–199, 1995.
7. D. Marchette, "A statistical method for profiling network traffic", Proceedings of the First USENIX Workshop on Intrusion Detection and Network Monitoring, Santa Clara, CA, Pp. 119–128, 1999.
8. Chan, L. W. and Fall side, F., "An adaptive training algorithm for back propagation networks", Computer Speech and Language, Vol. 2, page 205-218,1987
9. KDD Cup 1999 dataset. Available on: <http://kdd.ics.uci.edu/databases/kddcup99/kddcup99.html>

Journal of Advanced College of Engineering and Management

Guidelines to Authors

AIM & SCOPE

The journal of Advanced College of Engineering and Management (jacem) is a refereed journal to serve the interests of professionals, academics and research organizations working in the field of applied sciences and engineering. Publication of journals regarding the achievements and problems in the field of science and engineering work in context of Nepal is yet to go long way for an established tradition.

The scope of the journal includes all the disciplines of applied science and engineering. The paper in the journal will be in English.

GUIDELINES TO AUTHORS

1. Article(s) should be original in nature and have not been published elsewhere.
2. The length of manuscripts should not, in general, exceed 10 pages.
3. If the copyrighted material is used, the author should obtain the necessary copyright release and submit it along with the manuscript.
4. Manuscript should be print in A4 size paper with 1" margin on top and bottom and 1.25" on left and 0.75" on right.
5. The manuscript must be in Time New Roman text font of font size 11. Adjust the line spacing to accommodate 45 lines in the pages. Number all pages starting with the title page.
6. The first page must contain the title of the paper, author's full name(s), affiliation(s), position(s), mailing address, phone number and email address.
7. The paper should include the following major sections in addition to the main body of the text.
 - a) **Introduction:** Describe the motivation and purpose of the research.
 - b) **Literature Review:** Describe the previous research works done related to your research.
 - c) **Methodology:** Provide sufficient information to allow readers to repeat the work.
 - d) **Result and discussion:** Discuss and analysis the outcomes of the research work.
 - e) **Conclusions:** State conclusions precisely without elaboration.

Contents

		1-10
1.	Best Fit Void Filling Segmentation Based Algorithm in Optical Burst Switching Networks. <i>A.K. Rauniyar, A.S. Mandloi</i>	
2.	Improvement of Complexity and Performance of Least Square Based Channel Estimation in MIMO System. <i>Ananda Kumar Sah, Dr. Arun Kumar Timalsina</i>	11-24
3.	Post Construction Effectiveness of Kathmandu-Naubise Alternative Road <i>Anjana Bhatta</i>	25-33
4.	Open Channel Surges. <i>Bharat Raj Pandey</i>	35-43
5.	A One-Dimensional Bio-Heat Transfer Equation with Galerkin FEM in Cylindrical Living Tissue. <i>Hem Raj Pandey</i>	45-50
6.	Fuzzy Clustering Based Blind Adaptive OFDM System. <i>Krishna Sundar Twayan, Prof. Shashidhar Ram Joshi</i>	51-58
7.	Some Classical Sequence Spaces and Their Topological Structures. <i>Dr. Narayan Prasad Pahari</i>	59-65
8.	Optimal Materialized View Management in Distributed Environment Using Random Walk Approach. <i>Purushottam Bagale, Prof. Shashidhar Ram Joshi</i>	67-73
9.	Earthwork Planning and Visualisation of Time-Location Information in Road Construction Projects. <i>R. K. Shah</i>	75-84
10.	3D Modeling of the First Trifurcation Made in Nepal. <i>Radha Krishan Mallik, Paras Poudel</i>	85-96

11. Life Cycle Assessment of Municipal Solid Waste Management System in Kathmandu Nepal. 97-106
Ramesh Ranabhat
12. Poultry Faeces Management by Bioconversion Technology with Modified GGC 2047 Model. 107-117
S. K. Neupane, Ram K. Sharma, Shiva Shankar Karki
13. Optimal Traffic Planning for Efficient Evacuation. 119-126
S. R. Khadka
14. Intrusion Detection System Using Back Propagation Algorithm and Compare it's Performance with Self Organizing Map. 127-138
Prof. Dr. Subarna Shakya, Er. Bisho Raj Kaphale



**Journal of Advanced College of
Engineering and Management**

Vol. 1, 2015



